

THE UNIVERSITY OF ASTON IN BIRMINGHAM

"INDUCTIVELY COUPLED PLASMA ATOMIC
EMISSION SPECTROSCOPY
FOR THE ANALYSIS OF TRACE ELEMENTS IN
BORON MATERIALS"

by

Peter Hulmston

For the degree of Doctor of Philosophy

Submitted May 1986

"INDUCTIVELY COUPLED PLASMA ATOMIC
EMISSION SPECTROSCOPY
FOR THE ANALYSIS OF TRACE ELEMENTS IN
BORON MATERIALS"

Peter Hulmston

Submitted May 1986

For the degree of Doctor of Philosophy

SUMMARY

An investigation into the application of inductively coupled plasma atomic emission spectroscopy (ICP/AES) to the quantitative determination of trace level multi-element impurities in boron materials has been undertaken. Two ICP-Spectroscopic systems were developed and applied. An ICP-Spectrograph system, which uses photographic detection and computer controlled microdensitometry for plate evaluation, provided wide element coverage and is well suited to dealing with complex emission spectra. The ICP-Scanning monochromator system, which is equipped with photoelectric detection, gave the better sensitivity and precision. Combined, the two systems provided useful detection limits (typically ≤ 1 ppm), good accuracy and precision for 50 elements.

In order to apply ICP/AES to cases where the sample quantity was limited a recirculating nebuliser was developed and tested. A $\times 10$ improvement in efficiency over conventional methods of nebulisation was achieved without any deterioration in sensitivity or precision. A microprocessor controlled version provided a suitable approach to routine analysis and a detailed study into the nebulisation characteristics showed that the nebuliser was free from the instabilities apparent in other designs of closed system nebulisers.

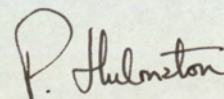
Sample introduction by hydride generation was investigated and provided ng/ml detection limits for several elements which were not sufficiently sensitive by pneumatic nebulisation.

A comparison of ICP/AES, neutron activation analysis and spark source mass spectrometry showed that only by using all three techniques could the full requirements be met. ICP-Mass spectrometry and X-ray fluorescence have been examined and preliminary assessments indicated that both techniques have considerable potential for boron analyses.

Keywords ICP/AES. Trace Element Analysis Boron.

DECLARATION

The work described in this thesis, apart from the neutron activation analysis and spark source mass spectrometry, was carried out by the author between 1980 and 1986. It has been done independently by the undersigned and has not been submitted for any other degree.

A handwritten signature in cursive script, appearing to read 'P. Hulmston'.

P Hulmston

ACKNOWLEDGEMENTS

I wish to express my gratitude to Dr. E. R. Clark, of the University of Aston in Birmingham, and Dr. J. A. Davies, of the Ministry of Defence, for their kindness, advice and valuable assistance throughout this research. I am deeply indebted for their help and useful guidance.

Special mention should also be made of my employer, the Ministry of Defence, who gave me help and financial support.

CONTENTS

SUMMARY	(i)
DECLARATION	(ii)
ACKNOWLEDGEMENTS	(iii)
LIST OF CONTENTS	(iv)
LIST OF TABLES	(x)
LIST OF FIGURES	(xiii)

CHAPTER 1

Page No.

1. INTRODUCTION

1.1 The Basic Principles of Spectrochemical Analysis	1
---	---

CHAPTER 2

2. OPERATIONAL ASPECTS OF THE ARGON RADIOFREQUENCY INDUCTIVELY COUPLED PLASMA	11
--	----

CHAPTER 3

3. SAMPLE INTRODUCTION	18
3.1 Nebulisers and Spray Chambers	18
3.2 Hydride Generation	26
3.3 Electrothermal Vaporization	28
3.4 Carbon Rod Injection	28
3.5 Laser Ablation	31

CHAPTER 4

4.	SPECTROMETERS	33
----	---------------	----

CHAPTER 5

5.	DEVELOPMENT OF AN ICP-SPECTROGRAPHIC SYSTEM	44
	5.1 Instrumentation	45
	5.2 Spectral Line Identification and Measurement	52
	5.3 Application to Boron Materials	62
	5.4 Results	64
	5.5 Discussion	69
	5.6 Conclusions	69

CHAPTER 6

6.	DEVELOPMENT OF A MICROCOMPUTER CONTROLLED SCANNING MONOCHROMATOR ICP SYSTEM	74
6.1	Instrumentation	75
6.2	Software Development	79
6.2.1	Procedure	79
6.2.2	Spectral Line Identification and Measurement	81
6.2.3	Determination of Single Wavelengths	82
6.2.4	Spectrometer Wavelength Calibration	82
6.3	Assessment of Instrumental Performance	84
6.4	Results and Discussion	85
6.5	Conclusions	92

CHAPTER 7

7.	COMPARISON OF SPECTROGRAPHIC AND SCANNING MONOCHROMATOR SYSTEMS	93
7.1	Experimental	93
7.2	Results and Discussion	94
7.3	Conclusions	99

CHAPTER 8

8.	DEVELOPMENT OF A RECIRCULATING PNEUMATIC NEBULISER FOR SMALL SAMPLE VOLUMES	102
8.1	Design Requirements	103
8.2	Prototype Recirculating Nebuliser	104
8.2.1	Performance	107
8.2.2	Appraisal of the Prototype Recirculating Nebuliser	109
8.3	Development of a Microcomputer Controlled Version	110
8.4	Nebulisation Characteristics of a Recirculating Nebuliser	114
8.4.1	Results and Discussion	115
8.5	Conclusions	124

CHAPTER 9

9.	HYDRIDE GENERATION FOR SENSITIVE DETERMINATION OF SELECTIVE ELEMENTS IN BORON CARBIDE	126
9.1	Instrumentation	127
9.2	Experimental	127
9.3	Results and Discussion	129
9.4	Conclusions	131

CHAPTER 10

10.	A COMPARISON OF ICP/AES AND OTHER MULTI-ELEMENT TECHNIQUES	134
10.1	Inductively Coupled Plasma Atomic Emission Spectroscopy	134
10.2	Spark Source Mass Spectroscopy	138
10.3	Neutron Activation Analysis	138
10.4	Comparison of Results	143
10.5	Wavelength Dispersive X-ray Fluorescence	150
10.5.1	Experimental	150
10.5.2	Results and Discussion	156
10.5.3	Conclusions on XRF Method	165
10.6	Inductively Coupled Plasma Mass Spectrometry	167
10.6.1	Experimental	167
10.6.2	Results and Discussion	169
10.6.3	Conclusions on ICP/MS Method	173

CHAPTER 11

11.	CONCLUSIONS	177
	REFERENCES	180

TABLES

5.1	Conditions used with ICP-Spectrograph System	49
5.3	SA1 and SA3 Photographic Plate Processing Conditions	49
5.3	Performance of Method	66
5.4	Precision	68
5.5	Analysis of Simulated Samples	70
5.6	Comparative Analysis of Boron Sample R23	71
6.1	Conditions for Scanning Monochromator System	78
6.2	Mechanical Performance	86
6.3	Detection Limits	89
6.4	Precision	90
6.5	Analysis of Boron Sample R23	91
7.1	Comparison of Mechanical Performance	97
7.2	Comparison of Sensitivities	98
7.3	Comparison of Precision	100
7.4	Analysis of Boron Sample R23	101
8.1	A Comparison of Detection Limits and Stability Achieved by Conventional and Recirculating Nebulisers	108
8.2	Comparison of Detection Limits using a Microprocessor Controlled Version	116
8.3	Comparison of Precision for Five Replicate Analysis on a Multi-element Standard Solution	116
8.4	Concentration of Cu in a Sample Solution after each Nebulisation	120

9.1	Optimum Conditions for Hydride Generation and Comparison of Detection Limits	130
9.2	Results from Analysis on Boron Carbide Sample BC1	132
10.1	ICP/AES Results for BC1	135
10.2	ICP/AES Results for BC2	136
10.3	ICP/AES Results for BC3	137
10.4	Operating Conditions for SSMS	139
10.5	SSMS Results for BC1	140
10.6	SSMS Results for BC2	141
10.7	SSMS Results for BC3	142
10.8	ENAA Results for BC1	144
10.9	ENAA Results for BC2	145
10.10	ENAA Results for BC3	146
10.11	General Appraisal of Multi-element Techniques Currently used for Boron Analysis	149
10.12	Crystals used in the Philips 1400 XRF Instrument	151
10.13	Philips 1400 Instrument Conditions used	152
10.14	Comparison of XRF Results with Results Obtained by Other Techniques: Using Boron Carbide Control Materials as Standards	158
10.15	Comparison of XRF Results with Results Obtained by Other Techniques: Using Synthetic Standards	161
10.16	Precision on Five Replicate Determinations on BC3	162
10.17	Limits of Detection	166
10.18	ICP/MS Instrumental Conditions	170
10.19	ICP/MS Detection Limits for Trace Elements in Boron	174
10.20	ICP/MS Semi-Quantitative Analysis Results for BC2	175
10.21	ICP/MS Semi-Quantitative Analysis Results for BC3	176

FIGURES

1.1	Principles of Atomic Emission	5
1.2	Basic Layout of a Spectrograph	7
1.3	Photograph of a DC Arc Source	9
2.1	Fassel Demountable ICP Torch	12
2.2	Schematic Diagram of an ICP Torch in Operation	13
2.3	Photograph of an ICP with Boric Acid Spraying	16
3.1	Meinhard Concentric Nebuliser	20
3.2	Cross-Flow Pneumatic Nebuliser	21
3.3	Ultrasonic Nebuliser System	23
3.4	V-Groove Babington Nebuliser	25
3.5	Spray Chamber Fitted with Nebuliser	27
3.6	Photograph of an Electrothermal Vaporizer Device	29
3.7	Direct Sample Injection from a Graphite Rod	30
3.8	ICP-Laser Microprobe System	32
4.1	Diagrammatic Representations of Dispersion and Resolution	35
4.2	Schematic Diagram of a Photomultiplier Tube	39
4.3	Schematic Diagram of a Polychromator	40
4.4	Schematic Diagram of a Scanning Monochromator	42
4.5	Schematic Diagram of an EBERT Spectrograph	43

5.1	Optical Configuration of the ICP-Spectrograph System	46
5.2	Photograph of the ICP-Spectrograph System	47
5.3	Photograph of the PDP11-Microdensitometer System	50
5.4	Schematic Diagram of Joyce Loebel 3CS Microdensitometer	51
5.5	Plots of H+D, Seidel and L Transform	57
5.6	Emulsion Calibration for Kodak SA1: SLOPE/WAVELENGTH	58
5.7	Emulsion Calibration for Kodak SA1: f/WAVELENGTH	59
5.8	Emulsion Calibration for Kodak SA3: SLOPE/WAVELENGTH	60
5.9	Emulsion Calibration for Kodak SA3: f/WAVELENGTH	61
6.1	Schematic Diagram of the Computer Controlled Scanning Monochromator System	76
6.2	Photograph of ICP-Scanning Monochromator System	77
6.3	Plot of Wavelength Calibration	83
6.4	Diagram of SPEX 1802 Wavelength Drive Mechanism	88
7.1	Spectral Scans of Ti Solution using Spectrographic and Scanning Monochromator Systems	95

8.1	Diagram of the Prototype Recirculating Nebuliser	105
8.2	Diagram Showing the Valve and Argon By-Pass Systems of the Recirculating Nebuliser	106
8.3	Photograph of the Microprocessor Controlled Recirculating Nebuliser	111
8.4	Schematic Diagram of the Nebulising Unit	112
8.5	Signal and Temperature Variation Plots for Nebulising under Ambient Conditions	119
8.6	Signal and Temperature Variation Plots for Nebulising under Various Conditions	121
8.7	Plot Showing Change in Nebulisation Efficiency with Temperature	123
9.1	Schematic Diagram of the Hydride Generator	128
10.1	Calibration Plots Obtained for Ca and Fe During Preliminary Studies in XRF	154
10.2	Calibration Plots for Fe and Ti using Control Materials	157
10.3	Calibration Plots for Pb using Synthetic Standards	160
10.4	Plots Showing Pb Absorption Interferences	163
10.5	Plots Showing Si Enhancement Interference on Al	164
10.6	Schematic Diagram of ICP/MS System	168
10.7	ICP/MS Spectrum of a Boric Acid Blank Solution	171
10.8	ICP/MS Spectrum of Boron Carbide Sample BC3	172

CHAPTER 1

1. INTRODUCTION

It is well known that the presence of impurities, often at trace levels, can alter significantly the chemical and physical properties of materials. Consequently much effort has been devoted over many years to the development and improvement of methods for such work to the extent that several instrumental multi-element techniques now exist eg spark source mass spectrometry (SSMS), inductively coupled plasma atomic emission spectroscopy (ICP/AES), neutron activation analysis (NAA) and X-ray fluorescence (XRF). These techniques, either individually or in a complementary manner are used for the characterisation of a wide range of materials in biological, geological, manufacturing and electronic industries, and also in research and development programmes. The extent of element characterisation can vary widely from a single specific element determination to a comprehensive analysis, often requiring 60 to 70 elements. The latter situation is often found in the micro-electronics and nuclear industries.

Boron and various boron compounds are used extensively in the nuclear industry, e.g in control systems in fission reactors. In such an application the presence of impurity elements can be detrimental to the reactor's performance. Consequently trace element characterisation of boron materials requires as many elements as possible to be determined quantitatively

to ppm levels. This has been the subject of much research and methods based on NAA, SSMS, XRF and AES using a DC arc source have been reported (1). Each of these is influenced to various extents by the interference effects of the matrix and impurity elements present. SSMS provides high sensitivity and covers a wide range of elements but has poor accuracy unless representative standards are used. The preparation of synthetic standards having a sufficiently fine dispersion of impurities for good replicate sampling and excitation, with a micro-spark, is extremely difficult. Thermal neutron activation methods are limited by the strong self absorption capacity of ^{10}B (3840 barns) but this can be overcome by using the epithermal region of a neutron spectrum (ENAA) as opposed to the more conventional thermal region. However, ENAA has poor limits of detection for some elements, e.g Ca, Sr, Y, Ba, Nb, Fe, Pb, Tl and Bi. Although boron and related compounds are ideal matrices in XRF studies, this technique did not have the required sensitivity and was initially not considered further at the outset of this work. AES provides an attractive alternative tool but the performance is governed considerably by the choice of excitation source. Although DC arc sources have been used for powdered boron samples the validity of comparing mixed powdered standards with samples is questionable and it is common experience that the physical form and the sample preparation can influence the results. Furthermore, boron produces a band spectrum in the DC arc source that extends over much of the spectrum thereby decreasing the sensitivity of the method for other elements. During the last two decades the radio-

frequency argon/argon inductively coupled plasma (ICP) has superseded, to a certain extent, DC arc and spark sources. The high stability and low spectral background of low powered argon plasmas gives the ICP an improvement in both sensitivity and precision over that obtained by arc or spark sources. Consequently the ICP source is an attractive alternative in emission spectroscopy.

At the outset of this work (1980) a review was made of available commercial ICP/AES instrumentation and from which it was concluded that no system having the required optical performance was available. Consequently it was decided to develop systems using spectrometers of known desired performance. An ICP-Spectrograph and an ICP-Scanning monochromator system were developed and applied to trace element determination in boron materials. This thesis describes the construction and application of these two systems and associated methodology.

1.2 The Basic Principles of Spectrochemical Analysis

An atom consists of a nucleus of positively charged protons, neutrons which have no charge and a nebulous system of orbiting electrons. Radiation occurs when there is an electron transition from a discrete high to low energy level. If radiation is to be emitted by an atom, an equal amount of energy must be absorbed. This, in spectroscopic sources, is the kinetic energy of gas particles driven to motion by a high temperature, or by charged particles travelling through the potential field of an

electric discharge or through the magnetic fields produced by an induction coil. Initially outer shell electrons are excited. Depending on the magnitude of the absorbed energy, these electrons are excited to higher energy levels (Fig. 1.1a). The atom reverts to its ground state through a series of quantised levels, emitting the absorbed energy as radiation, (Fig. 1.1b). These quantised states represent levels of energy, the difference between any two being the radiation energy. As these differences are discrete and fixed the radiation energy is also fixed, i.e. monochromatic. If the electron has been raised to a higher level but is still within the electrostatic field of the nucleus, the atom is said to be excited. If the electron has been driven completely out of the electrostatic field, the atom is said to be ionized. An ionized atom, with the absorption of sufficient energy, then forms a second system of energy levels, completely different from the excited system of the neutral atom.

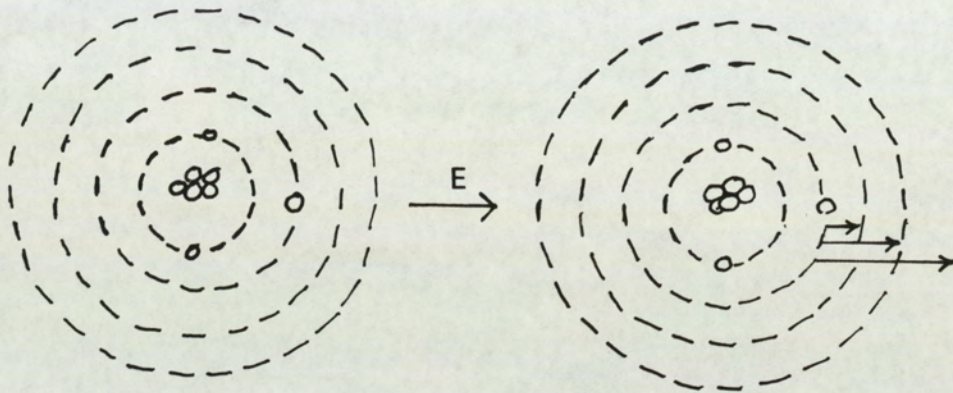
The emission spectrum of an element consists of a number of lines, varying from a few for elements such as B and Al, to thousands for others such as the rare-earth elements. The wavelengths are fixed, invariant characteristics of a specific element. This characteristic makes AES valuable in chemical analysis, because identifying the spectrum identifies the element unequivocally. Quantification can be achieved by measuring the spectral lines and referring them to concentrations or weights of the unknown elements.

PRINCIPLES OF ATOMIC EMISSION

FIG. I.IA

Normal Ground State Atom

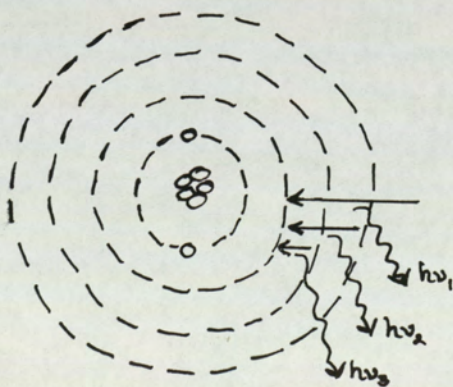
Excitation of Ground State Atom



Thermal excitation of electrons in ground state atoms to higher energy orbitals.

FIG. I.IB

Relaxation of Excited Atom



On returning to their original groundstate orbitals, the electrons emit quanta of energy in the form of photons.

A more detailed account of the origin and characteristics of emission spectra are given elsewhere (2).

The principal instrumentation for quantitative work are of one of two forms depending on the method used for recording the spectrum. If photographic detection is used it is called a "spectrograph", if the "detector" is a photo-multiplier tube it is called a "spectrometer".

In construction the spectrograph is a special type of camera, (Fig. 1.2). The light from the source illuminates a slit which is the entrance aperture of the camera. The slit is imaged, by a lens, on to a spherical mirror, which in turn, focusses the image on to a photographic plate held in a removable plate holder. Between the slit and plate is the dispersing medium, which can be either a glass or quartz prism, or a diffraction grating. The spectra are measured using a densitometer. The spectrometer is similar to the spectrograph but the plate holder is replaced by a photo-multiplier tube and the grating is mounted on a rotating carriage so that spectral scanning can be achieved. This more modern instrument is referred to as a "scanning monochromator". A more detailed description of spectroscopic instrumentation is given in Chapter 4.

Until recently the sources most commonly used were either the graphite DC arc or spark. The sample, usually a dry, non-conducting powder, is charged into a cavity drilled in the end of a graphite rod. This makes the lower electrode of an arc, with

BASIC LAYOUT OF A SPECTROGRAPH

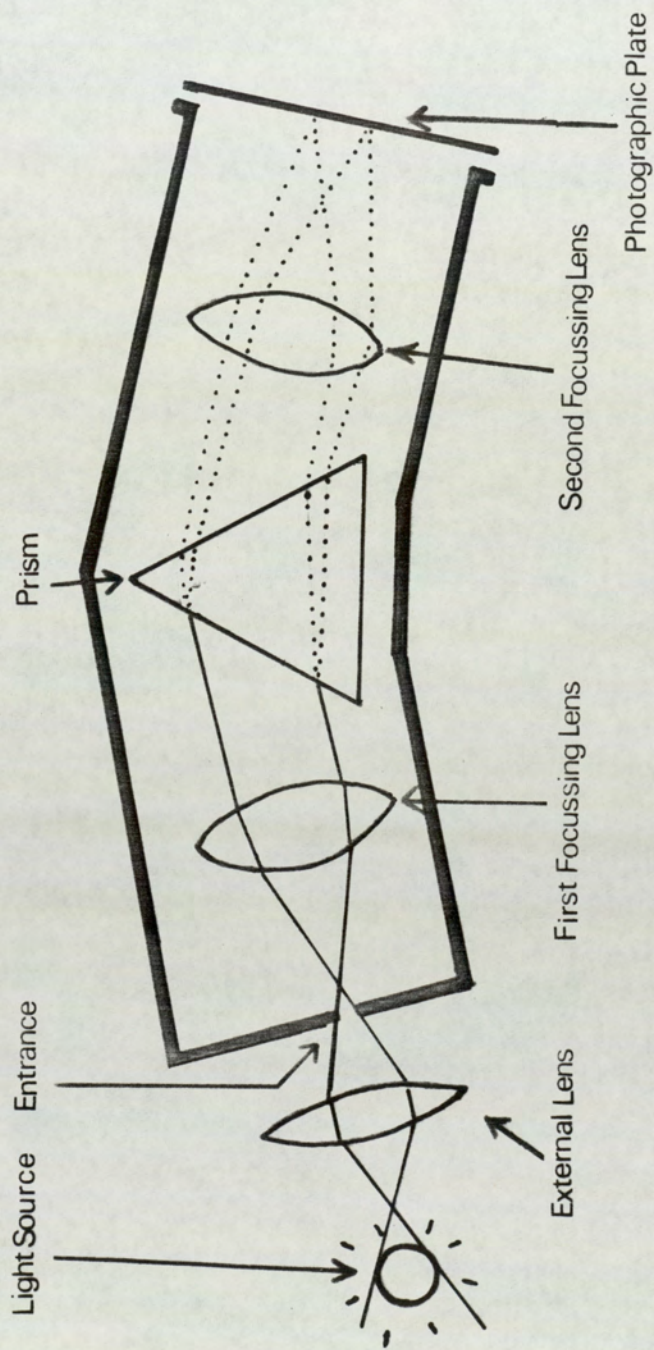


FIG.1.2

a similar graphite rod placed concentrically a few mm away as the opposite electrode. The power supply is a direct current of about 1 to 5A at 250V. The arc is initiated by a spark and then allowed to burn until the sample is consumed. The high temperature generated volatilizes electrode material and sample with sufficient ionization of the vapour to sustain the flow of current across the gap, (Fig. 1.3). Spectral emission occurs between the electrode gap. The best way of differentiating between the spark and arc is that the former is intermittent and the latter is continuous. The spark is not suitable for non-conducting materials but with metals it is very effective in producing an excited vapour and has been widely used.

The excitation source most commonly used in AES was the DC carbon arc (3). Its main advantages are: (i) the simplicity with which solid samples can be handled, (ii) the small risk of contamination and (iii) high detection power. Its disadvantages are: (i) the poor precision and accuracy and (ii) the fact that solutions cannot be analysed directly. Because of the poor precision and accuracy, DC arc methods are semi-quantitative.

The ICP has been available as an emission source for atomic spectroscopy for nearly twenty years. The early work by Reed (4), Greenfield (5), Wendt and Fassel (6) used high power, low frequency sources of the type commonly used for inductive heating. The advent of compact low power high frequency sources in 1974 led to a widening interest in the ICP and they have been used extensively in chemical analysis. Reviews by Greenfield (7)

FIG. 1.3

DC CARBON ARC



and Barnes (8) provide comprehensive surveys of the literature. It provides an improvement in precision and sensitivity over that obtained by arc or spark sources (9) and its advantageous multi-element capability has been widely reported (10, 11). In this technique the sample is injected into the plasma, usually as an aerosol from nebulised sample solutions, and the emission is viewed in the tail-flame of the plasma. The plasma is stable, runs with a constant sample feed, is a high temperature but low background source, provides a long residence time for excited atoms and it requires no high purity support electrodes. These attributes combine to provide a multi-element analytical technique which is sensitive, precise and accurate.

CHAPTER 2

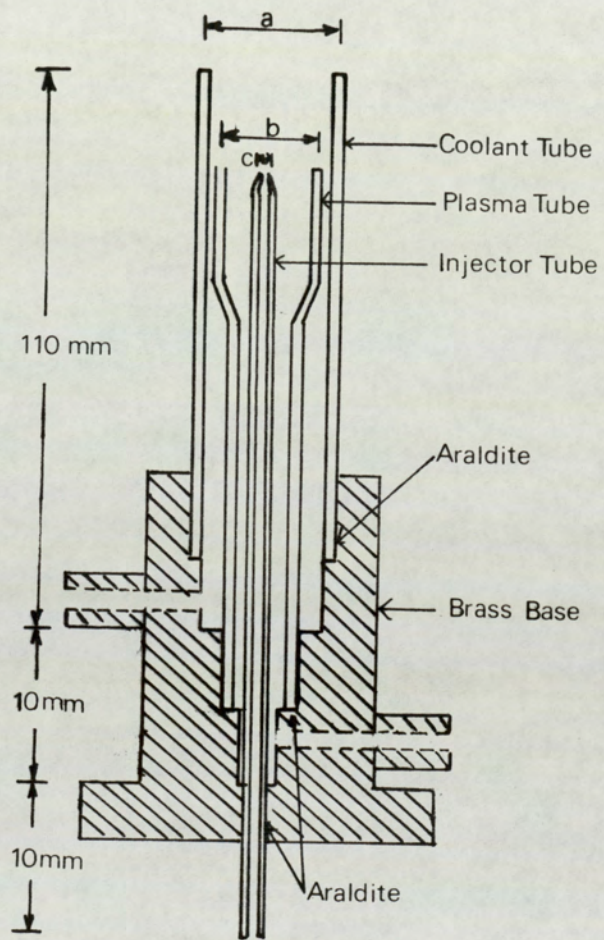
OPERATIONAL ASPECTS OF THE ARGON RADIOFREQUENCY INDUCTIVELY COUPLED PLASMA EMISSION SOURCE

Greenfield et al (5), in 1964, were the first to introduce analytical samples into a plasma discharge and they subsequently designed an ICP torch specifically for spectroscopic use. However, the high argon consumption (100 l/min) and power requirements (up to 8 kW) precluded its universal application. Fassel et al (6), in 1965, designed a smaller torch which gave a similar analytical performance but was more economical, operating with less gas (16 l/min) and at a lower power (1 to 2 kW). A sub-sequent modification has included demountable versions which are of practical advantage as damaged silica tubes can be replaced quickly and economically. Fig. 2.1 shows the design of a demountable torch which is similar to the Fassel design but with the silica tubes held in position by a brass base and araldite.

Fig. 2.2 shows schematically the operation of an ICP torch, the argon flow patterns and the magnetic fields which are induced by radiofrequency currents flowing through the work coil. For plasma initiation, the argon is partially ionized by a Tesla coil discharge and the liberated electrons and ions are accelerated on each half cycle of the oscillating magnetic field.

FIG. 2.1

THE DEMOUNTABLE TORCH

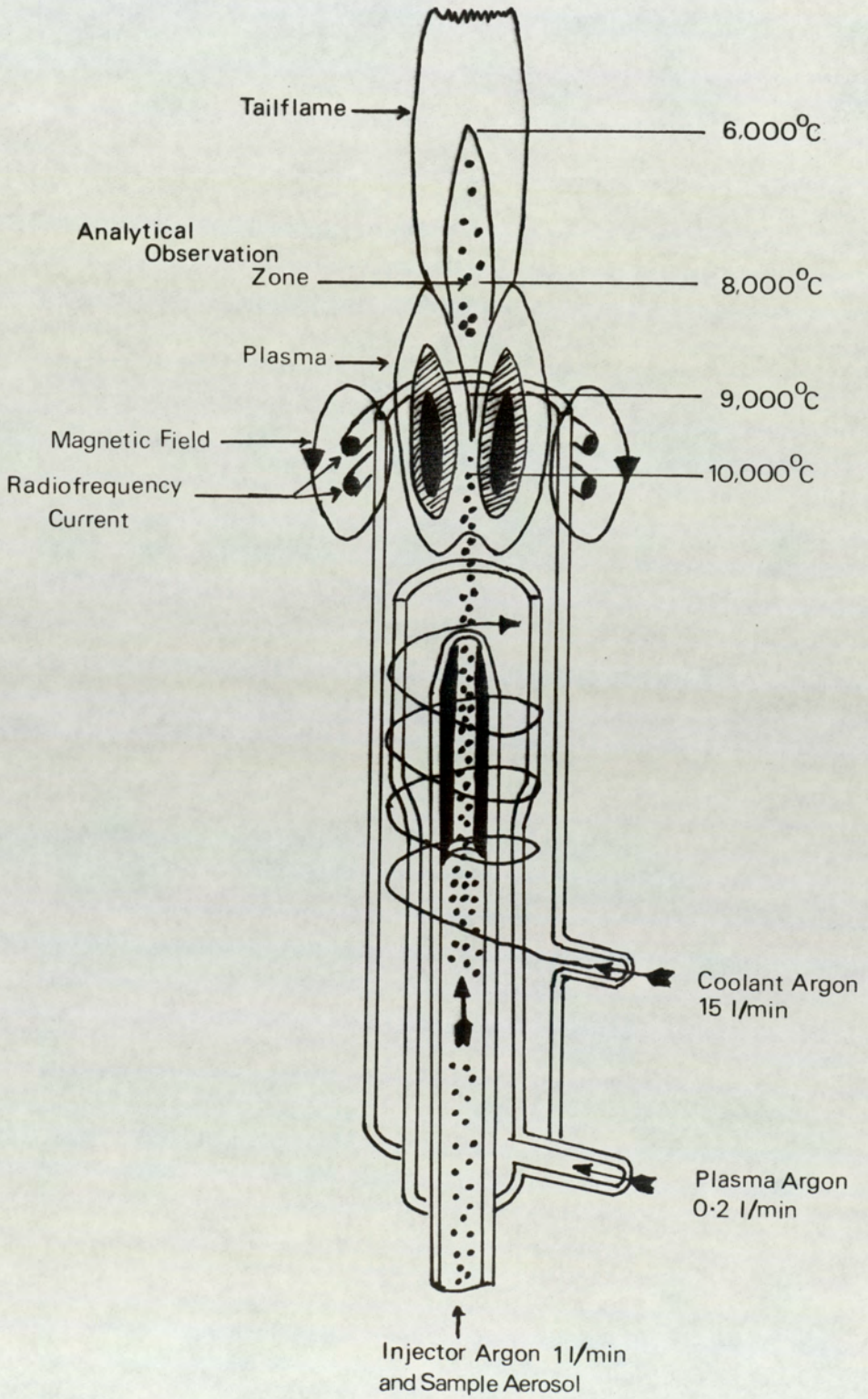


Silica Tube Dimensions.

- (a) 18 mm I.D
- (b) 14 mm I.D
- (c) 2 mm I.D

FIG. 2.2

ICP TORCH



The accelerated ions and electrons flow in close annular paths (eddy currents) inside the silica tube, and resistance to their flow causes Joule heating and hence additional ionization occurs. These steps lead to the almost instantaneous formation of a stable plasma of extended dimensions. The shape of the plasma is important. If one gas flow is used so that the sample is mixed with the gas in which the plasma is formed, emission from the sample occurs throughout the whole volume of the discharge resulting in poor sensitivity. Also, the presence of sample atoms in the part of the discharge where most of the electrical energy is dissipated causes a change in the electrical properties thereby changing the power density and hence the stability of the plasma. The introduction of a second argon gas stream, called the coolant, flowing tangentially around the plasma gas stream flattens the base of the spheroidal discharge. This enables a third argon stream containing the sample aerosol to be injected up the axis of the plasma which causes a long narrow, well defined central channel to emerge in the fireball. The tail-flame, which is the part used for spectroscopic observation, contains the analyte atoms that are heated up as they pass through the central channel. The region of the tail-flame observed for analytical work is normally a 2 to 5 mm vertical window viewed at a height 12 to 20 mm above the coil.

For sensitivity a high excitation temperature is required in order to excite the maximum number of atoms of both low and high excitation potentials. A high kinetic temperature is desirable in order to dissociate molecules with the advantage of suppressing band spectra and reducing matrix effects.

The analytical benefits of the ICP source arise from both the high kinetic and electrical temperature of the source, and from the unique method of heating the sample. As sample is introduced along the central channel radiative heating volatilizes and atomizes the sample. Only when a point some distance above the coil is reached does the temperature profile resemble other spectroscopic sources. The temperature which analyte species reach depends not only on the plasma temperature but also on their residence time, which is proportional to the length of the tunnel. When the sample species reach the observation zone they have experienced temperatures ranging from 5,000 to 10,000 °C for 2 ms. These are approximately twice those found in nitrous oxide-acetylene flames, the hottest combustion flames used in atomic absorption spectroscopy.

Fig. 2.3 illustrates the ICP source with boric acid spraying and gives a good indication of what conditions are experienced in the plasma by the analyte. At the hottest point, at the plasma base, a distinct blue plume is visible within the central channel. This emission is from the B doublet atomic lines at 249 nm which indicates that the sample aerosol is completely vaporized and atomized. Only much higher up in the plasma tail-flame are there any signs of the green emission from BO molecular species which are formed by recombination. This molecular band spectrum, which extends from 300 to 500 nm, gives rise to the highly complex emission spectra for B observed in a DC arc.

FIG. 2.3

ICP SOURCE WITH BORIC ACID SPRAYING



An RF generator maintains a constant high frequency alternating current within the work coil thereby inducing an oscillating magnetic field which provides kinetic energy to the charged species within the plasma. RF generators generally use piezo-electric crystals to regulate the frequency of current (generally 27 MHz). Provision of the power levels (1 to 2 kW) is obtained using vacuum tube valves in the amplifier circuit. Exciter circuits also employ triode valves but solid state exciter circuits are becoming available commercially. Good stability is necessary where precisions of 1% RSD are required. Thus, power stability of better than $\pm 0.005\%$ (12) is desirable and modern generators provide this. The work coil functions in a similar manner to an aerial and optimum coupling of the RF to the plasma is achieved by including a phase and frequency matching unit in the aerial circuit. The waste heat generated in the coil is dissipated by water cooling. A full treatise on radiofrequency generators is documented elsewhere (13).

CHAPTER 3

SAMPLE INTRODUCTION

This chapter reviews methods of sample introduction and those which are potentially most useful for application to trace multi-element boron analysis will be identified and considered for development.

In order to obtain optimum sensitivity and accuracy the sample material must be completely dissociated and atomized in the plasma. Thus the sample is introduced as finely dispersed as possible, such as a liquid aerosol, vapour, gas, or a cloud of microscopic particles of the solid material.

3.1 Nebulisers and Spray Chambers

Samples are generally introduced into the ICP source as a fine aerosol suspended in the injector argon gas stream. The required aerosol is produced using pneumatic nebulisers, in which the sample liquid is drawn up and dispersed into fine droplets by means of the low pressure generated by a very fast gas stream passing through a small orifice.

ICP sources require an injector flow of 0.5 to 1 l/min. This sharply contrasts with the much higher gas flows of nebulisers used in atomic absorption spectroscopy which typically

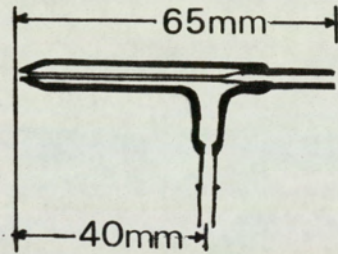
use 10 l/min. Consequently, ICP nebulisers are smaller, and the engineering tolerances more critical. Liquid uptake rate and the proportion of liquid transferred to the plasma determine sensitivity. Standards and sample solutions must be matched as much as possible with respect to surface tension, viscosity and density.

Several types of pneumatic nebulisers are available; the most commonly used being the glass Meinhard concentric type (14), shown in Fig. 3.1. Gas pressure applied at the side port produces a venturi effect at the orifice positioned coaxially with the internal capillary. Liquid flowing outward to the capillary edge is sheared by the gas stream and propelled as an aerosol. A major limitation of this design occurs when spraying solutions containing >0.5% dissolved solids. The gas flow characteristics change and sensitivity is degraded. This is caused by "salting up", a process whereby dried solute from the test solution partly constricts the annular gas orifice. It can be partially overcome by humidifying the argon injector gas thereby inhibiting evaporation of the solution droplets near the orifice.

Cross-flow nebulisers are also used increasingly. Among the early models was the Knisely design (15), shown in Fig. 3.2, which had adjustable capillaries. An advantage of the cross-flow nebulisers is that they are less prone to "salting-up" and solutions up to 2% dissolved solids can be nebulised for long periods without drift. As with the concentric

FIG.3.1

MEINHARD CONCENTRIC NEBULISER



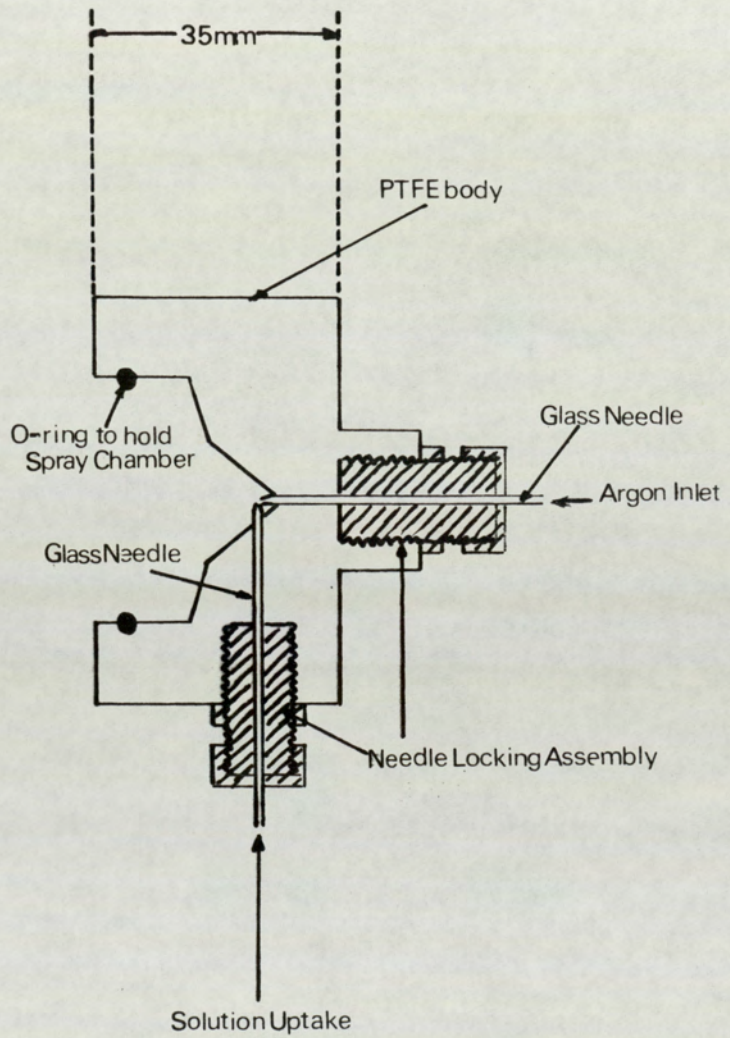
Geometry of a Meinhard nebuliser. The material is borosilicate glass.



The tip of a Meinhard showing the narrow (10-35 μ m) annular gap for the gas flow.

FIG. 3.2

CROSS-FLOW PNEUMATIC NEBULISER

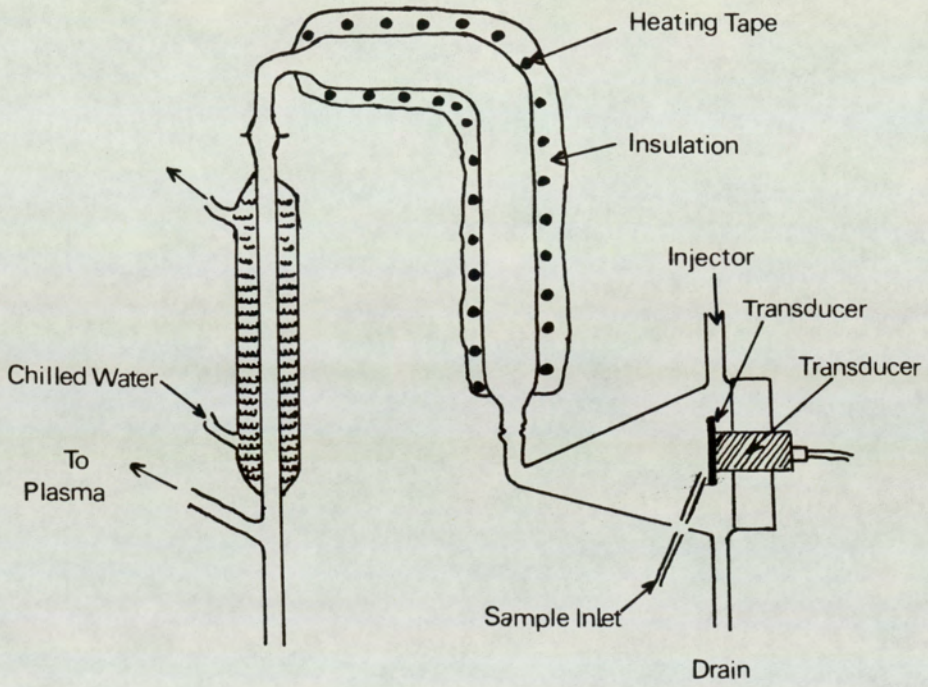


nebulisers, cross-flow nebulisers are self-priming and self-actuating, i.e solutions are drawn up by the low pressure generated by the injector gas. Both types of pneumatic nebuliser were used in this work.

Ultrasonics can be used to nebulise solutions (16, 17). In these the solution is agitated using a transducer operating in the MHz frequency range. This is shown diagrammatically in Fig. 3.3. An aerosol containing a high proportion of droplets smaller than 10 μm continuously breaks away from the surface of the liquid, providing nebulisation of high efficiency. Delivery rate to the plasma can exceed that achieved by pneumatic nebulisation by a factor of X20, thereby leading to lower detection limits. However, two serious factors limit its potential. The greater quantities of water which are injected cool the plasma excessively such that limits are only marginally (X20) improved. To reduce the quantity of water entering the plasma desolvation of the aerosol is used. Although this gives an improvement in detection limits (X10) this does lead to further restrictions when analysing solutions comprising of >0.1% dissolved solids. Significant quantities of analyte are also removed from the injector argon gas stream by a deposition process and the extent to which this deposition occurs depends strongly on the element composition of the sample. Thus, detection limits are determined by the level of interference effects experienced during the desolvation process (18, 19). For this reason, the method was not used.

FIG.3.3

ULTRASONIC NEBULISER SYSTEM

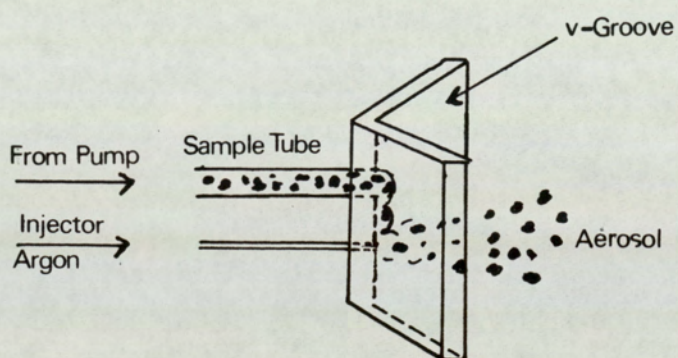


A further type of nebuliser was developed by Babington (20). In this a film of solution is passed over a very narrow orifice in a glass sphere or v-groove (Fig. 3.4). The argon gas stream emerges from the orifice and ruptures the solution film to form a fine aerosol. As there are no sample needles to block, this nebuliser can be used for solutions with high salt content or slurries. According to Ebdon (21) slurry nebulisation offers a practical means of continuous introduction of solid material. In this, fine powdered sample (particle size $<30 \mu\text{m}$) is slurried with water, up to a 1:10 ratio, and is rapidly pumped to a Babington nebuliser. Calibration is carried out by mixing aqueous standards with the pure sample matrix or with sample materials containing known concentrations of the sought elements. However, nebulisation efficiency is influenced by the particle size of the sample and as the boron samples investigated in this study are known to vary in particle size distribution poor accuracy can be expected. Hence, this method was not used.

Sensitivity is very dependent on the particle size of droplets entering the plasma and directly spraying sample into the base of the source using a nebuliser causes plasma instability and possible extinction. Best results are obtained using a sample aerosol containing droplets $<10 \mu\text{m}$ but this particle size range constitutes $<2\%$ of the total solution sprayed. Hence, separation of the fine aerosol from the total solution spray is required. This is achieved using a spray chamber. The type most commonly used is the Scott (22) double-pass spray chamber shown in Fig. 3.5. The separation of aerosol droplets is achieved by forcing the injector gas to

FIG.3.4

V-GROOVE BABINGTON NEBULISER



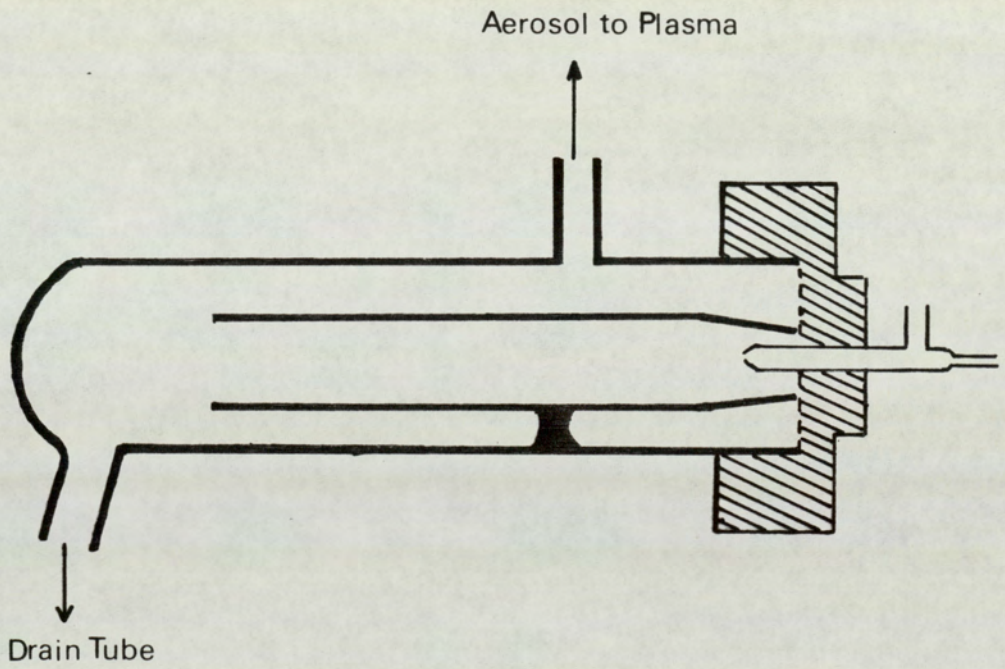
change direction sharply. The smaller droplets follow the gas flow, but the larger droplets, because of their higher momentum, impinge on the chamber walls. Excess liquid is drained away. As the drained solution constitutes 98% of the sample an important area of development should be directed to improving efficiency. This is particularly important when sample conservation needs to be considered. Hence, a part of this thesis will be devoted to the development of a recirculating nebuliser.

3.2 Hydride Generation

In principle, the introduction of sample in the gas phase is an ideal technique for ICP/AES and has been used in flame atomic absorption for many years (23). It involves mixing solutions of analyte with acidified NaBH_4 , and transporting the volatile reaction products to the source. Thompson et al (24) developed a generator specifically for the ICP source. Stable plasma conditions were obtained using a continuous flow system in which the rate of production of H_2 is constant and the RF generator was tuned exactly to the impedance of the plasma. A number of commercial designs are now available. The method has direct application to the determination of low levels of specific trace elements in boron materials and will therefore be studied in detail.

FIG.3.5

SPRAY CHAMBER FITTED WITH NEBULISER



3.3 Electrothermal Vaporization

Electrothermal vaporization of samples (~10 mg) into the ICP source was developed by Kirkbright et al (25). In this the sample is placed on to a resistively heated carbon rod. After desolvation and carbonisation of organic material at ~700°C, the temperature is rapidly raised to ~3000°C. The sample is vaporized and carried by an argon injector gas stream from the vaporizing chamber through a length of tubing to the plasma. The device is illustrated in Fig. 3.6. In the absence of any matrix element, detection limits ≤ 10 ng/ml can be obtained using a commercial graphite rod atomiser. These are generally 1 to 2 orders of magnitude better than those obtained by pneumatic nebulisation. The major disadvantage of this method originates from other chemical reactions taking place during the stages of vaporization. At high temperatures refractory elements such as W, Zr, Hf, Ti, and U tend to form involatile carbides on the rod. The other disadvantage is that the method is not continuous and therefore only single elements can be determined when using a scanning monochromator. In general, the method has limited application to boron materials.

3.4 Carbon Rod Injection

In direct sample injection from a carbon rod, 5 μ l of sample are placed on the tip of a carbon rod, which is then raised axially to a position (1 mm) just below the base of the plasma. This is shown schematically in Fig. 3.7. Under zero injector gas flow rate the sample material is heated and

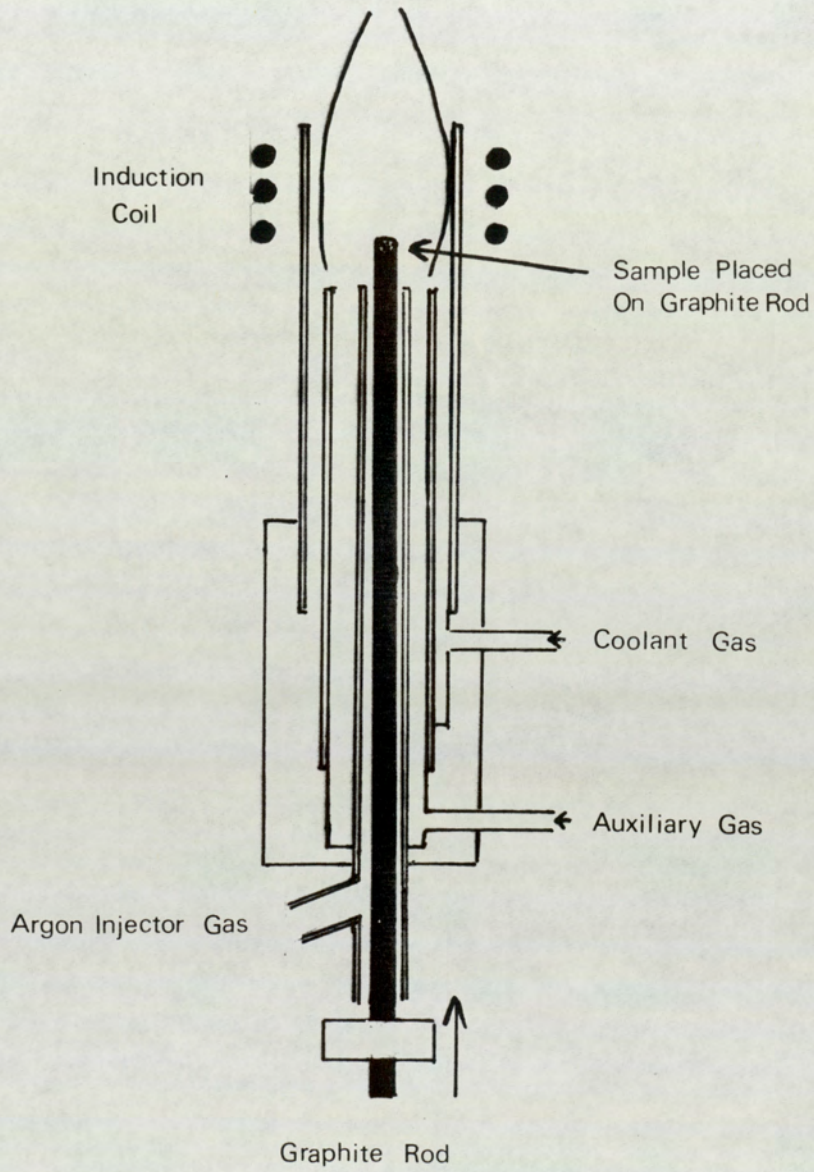
FIG. 3.6

ELECTROTHERMAL VAPORIZER



FIG.3.7

DIRECT SAMPLE INJECTION FROM A GRAPHITE ROD



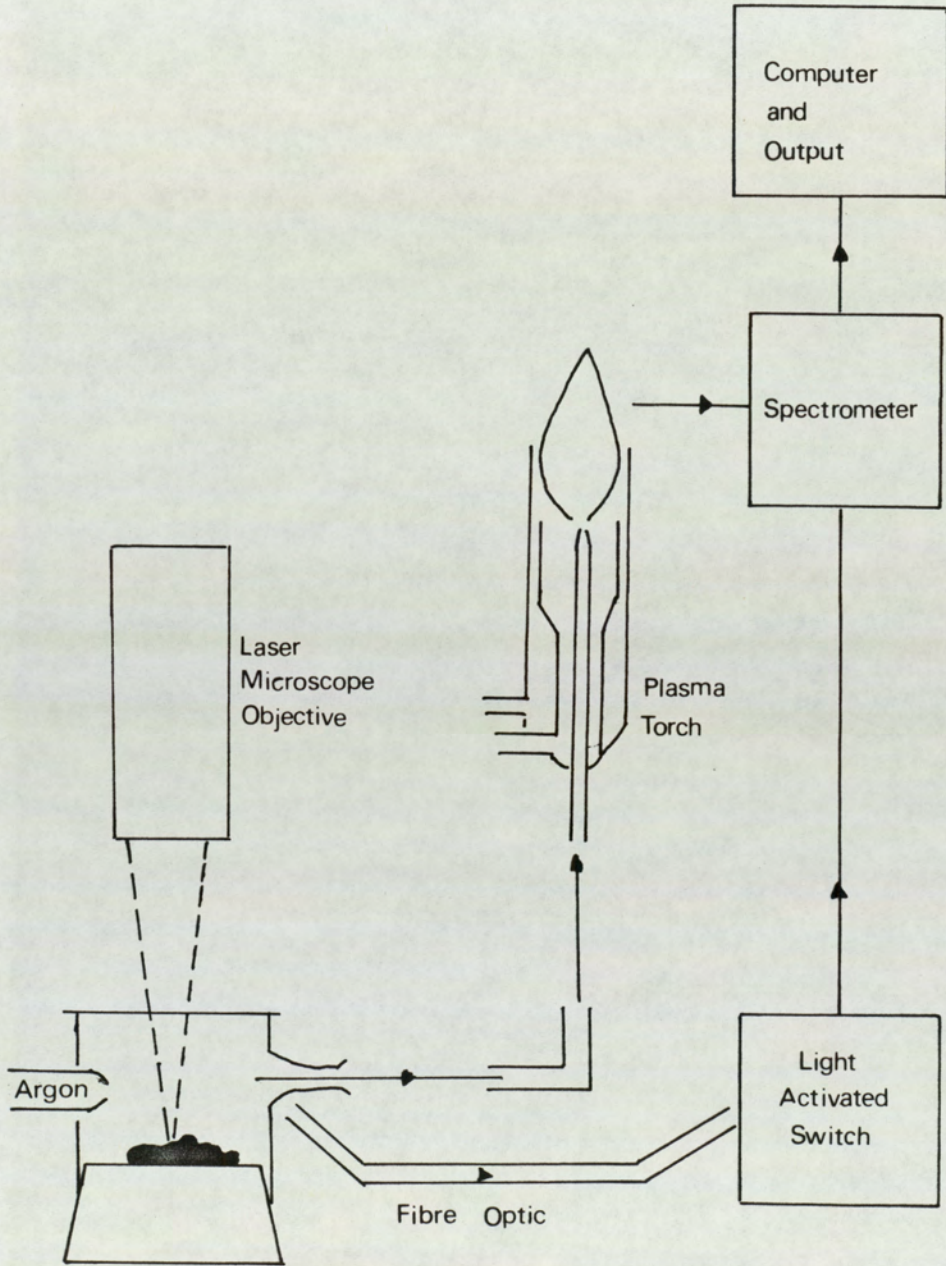
volatilized into the plasma. Detection limits for U, Zr and Ti are in the 1 to 2 ng/ml range (26). Difficulties occur when samples with complex matrices are volatilized instead of the pure analyte solutions used hitherto. Many of the selective volatility problems found in DC spectroscopy are encountered although the effects of the matrix on the excitation in the ICP source will be much less of a problem than in arc sources. This technique was not considered further.

3.5 Laser Ablation

Lasers can be used to ablate material off the surface of the sample into the injector gas stream of a plasma (27). A schematic diagram of a laser-microprobe ICP system is shown in Fig. 3.8. As very high temperatures (~5000°C) are reached refractory materials are readily sampled and analysed. Calibration is normally carried out using certified standard reference materials. The method has potential for the analysis of intractable materials, and microsampling as in the case of individual grains of rock or investigating inhomogeneity in materials. However, during operation only a small quantity (200 µg) is removed from the surface of the sample. Consequently precision and accuracy are strongly dependent on sample homogeneity and therefore this method is not suitable for bulk analysis.

FIG.3.8

LASER-MICROPROBE ICP SYSTEM



CHAPTER 4

SPECTROMETERS

A spectrometer consists of four principle components:

- (i) A dispersing device such as a prism or a diffraction grating which disperses light at different angles according to wavelength.
- (ii) An optical system of mirrors and lenses for focussing the light.
- (iii) An entrance aperture, usually a rectangular slit, whose images, formed by the optical system in light of different wavelengths, are the observed spectral lines.
- (iv) A detector to record the image of the spectral lines.

The important parameters in assessing the performance of spectrometers are dispersion, resolution, stray-light characteristics, wavelength range and detection range.

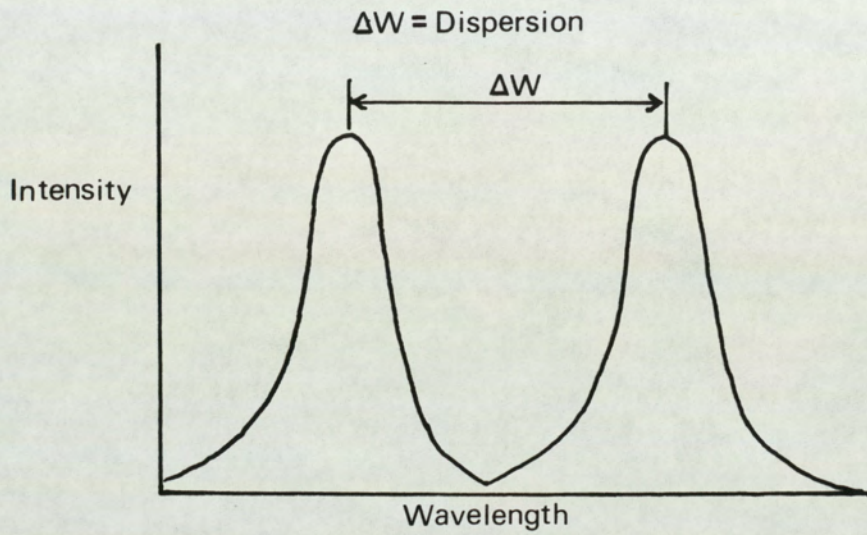
In simple terms, by considering two emission peaks, the distance separating the peak height positions is a measure of the dispersion (nm/mm). Resolution refers to the total separation of the peak profiles such that at the point where the emission intensity from one peak has no significant effect on the

measurement of the second, the peaks are said to be totally resolved. The closest relative wavelength position at which an emission peak can approach an analyte peak, but does not influence its measurement, is a measure of an instrument's resolving power. Practically, resolution is expressed as the full width at half maximum (FWHM). Dispersion and resolution are defined diagrammatically in Fig. 4.1, and are related to the focal length of the spectrometer and to the type and quality of the dispersing device. To cover the prominent wavelengths of most elements a spectral range of 200 to 500 nm is required. In order to benefit from the large linear calibration range of ICP emission a recording system capable of providing a 10^6 detection range is required. Of the last two points, with few exceptions commercial spectroscopic instrumentation is designed to meet these requirements. However, optical performances (resolution and dispersion) vary greatly (0.01 to 0.03 FWHM and 0.4 to 1.0 nm/mm) and careful consideration of the analytical requirements is essential. Where highly complex spectra are to be evaluated quantitatively only instruments offering the best optical performance can be considered.

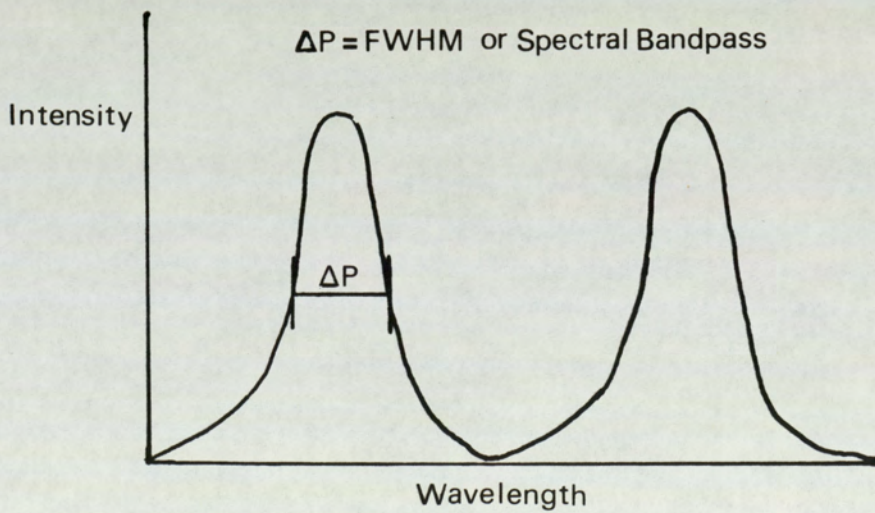
The theoretical aspects of refraction and diffraction by prisms and gratings are discussed thoroughly elsewhere (28). Spectrometers employing prism dispersion devices such as the MEDIUM and LITTROW spectrographs (29), are generally optically inferior to those employing diffraction gratings such as the EBERT design.

FIG. 4.1

(A) DISPERSION



(B) RESOLUTION: TWO TOTALLY RESOLVED PEAKS



Essentially a diffraction grating consists of a series of grooves cut at regular intervals on a reflecting surface such as glass coated with aluminium. The grooves must be cut extremely accurately with a spacing that is of the same order of magnitude as the wavelength of radiation to be dispersed. Resolution is related to the total number of grooves on a grating and dispersion is related to the number density, (grooves/mm). Typical groove densities commercially available are 1200, 2400 and 3600 grooves/mm.

Since in most instruments the detected image is a replica of the slit, and the spectral purity is a function of the slit characteristics, it is essential that the slit is of exceptional quality. If it has a slight indentation or a dust particle this will show in the spectrogram. The dust particle will appear as a white streak, and the indentation as a black streak. The width of the slit partly determines the resolution and intensity of the line. A slit which is too wide produces a wider line without an increase in intensity. With an infinitely narrow slit, the slit image is a simple diffraction pattern in which the intensity of the central maximum is zero. As the slit is opened, the intensity of the central maximum rises rapidly at first, and then more slowly. The slit which gives an optimum resolution and intensity is therefore determined experimentally. Slit widths of 10 to 30 μm are typical. A more detailed treatise on spectrometer slits is given elsewhere (30).

The emission from a spectroscopic source is transmitted to the spectrometer by means of external optics which usually consist of a system of focussing lenses and masks. Their function is to illuminate the spectrometer entrance slit with light from only the portion of the source which gives optimum signal to background response. This is achieved by either focussing the spectral source image on the slit, or by using a mask. External optic configurations for instrumentation developed will be given in Chapters 5 and 6. Internal optics may, in addition to the dispersing device, be focussing lenses and mirrors.

A spectrographic plate is a flat glass plate on to which a thin gelatin emulsion containing microscopic particles of silver halide is evenly coated. The production of a photographic image is dependent on the formation of a latent silver halide image by a photochemical action, reduction of the latent image by a developer to yield the metallic silver image, and the removal, by a solvent, of the uneffected silver halide. The important physical characteristics are, contrast, speed, useful range of exposure, and spectral sensitivity. They are dependent on the size of the silver halide crystals in the emulsion. Both detection range and sensitivity increase with crystal size. However, the ability to discriminate close neighbouring lines deteriorates with increasing grain size. Hence, an emulsion which gives a compromise of all these effects is normally used in spectrographic work. All photographic emulsions display sensitivity towards ultraviolet light. Gelatin begins to absorb

wavelengths shorter than 280 nm and the loss in photographic sensitivity below 250 nm results in poor detection limits for a number of elements which have their most prominent spectral lines in this region of the spectrum. As the wavelength of light increases emulsion sensitivity increases until a wavelength above 500 nm is reached when once again the emulsion sensitivity deteriorates.

The principle device used for photo-electric detection is the photo-multiplier tube. Fig. 4.2 shows the arrangement of electrodes in a typical multiplier phototube. Generally, a tube has 10 electrodes and usually operates at 1 to 1.6 kV. The first electrode is the photoemission cathode, from whose surface electrons are released when struck by photons. These, in turn, are accelerated toward the next dynode, which is 100 V more positive than the second. With each stage current amplification occurs. The overall amplification factor may be of the order of 10^6 .

There are numerous types of spectrometer but for simplicity they will be considered as three distinct groups, namely polychromators, scanning monochromators and spectrographs.

Polychromators consist essentially of a lens, a slit, a concave diffraction grating and a series of secondary, or exit slits to isolate the resolved spectral lines. A typical arrangement is shown schematically in Fig. 4.3. The dispersed

FIG 4.2

SCHEMATIC DIAGRAM OF PHOTOMULTIPLIER TUBE

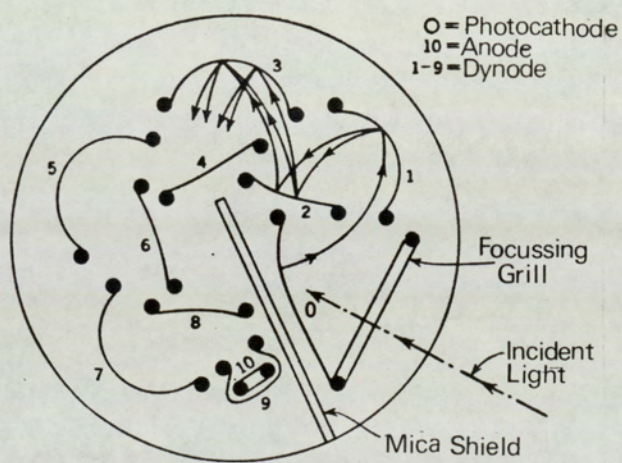
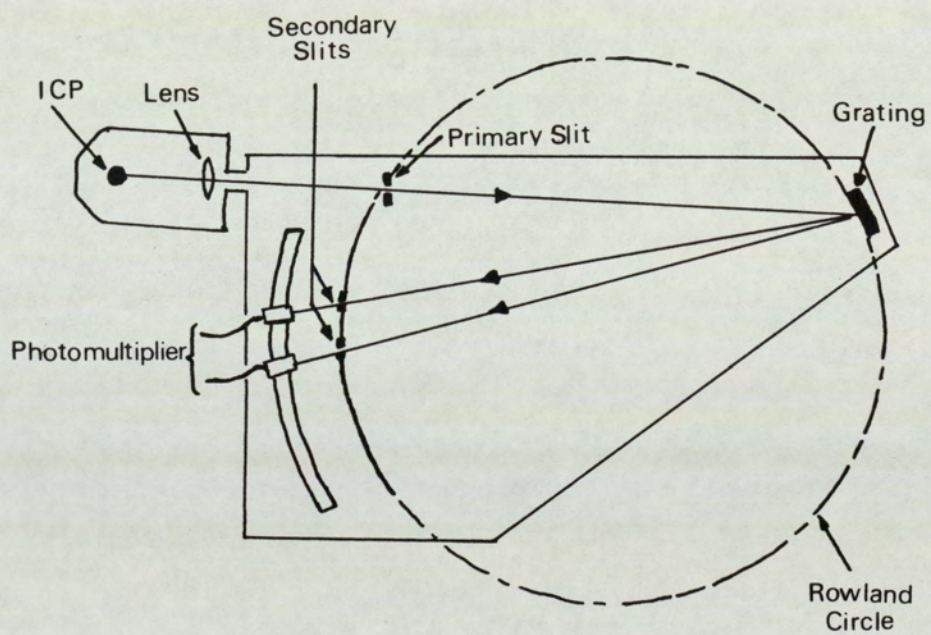


FIG.4.3

SCHEMATIC DIAGRAM OF A POLYCHROMATOR



wavelengths are measured by photomultiplier tubes. The components are mounted in a light tight box. Spectral lines are measured simultaneously.

A typical arrangement of a scanning monochromator is shown in Fig. 4.4. Light entering the monochromator through the entrance slit, is reflected from a concave mirror as parallel light before falling on to the grating. The light is dispersed and reflected on to a second concave mirror which focusses the light on to the exit slit. The wavelength of light falling on the exit slit is dependent on the angle of the grating. A single photomultiplier tube detects the light. Scanning monochromators are increasing in popularity, due mainly to their low cost, but more importantly because of the free choice of spectral lines available. They provide the necessary flexibility to deal with difficult matrices, unusual analytes, and as both prominent and less intense lines can be used a wider concentration range can be measured.

As with a polychromator, a spectrograph employs a static dispersing device and the entire spectral range is recorded simultaneously during a single exposure using a photographic plate. A schematic diagram of the 3.4 metre focal length EBERT spectrograph is given in Fig. 4.5.

FIG.4.4

SCHEMATIC DIAGRAM OF A
SCANNING MONOCHROMATOR

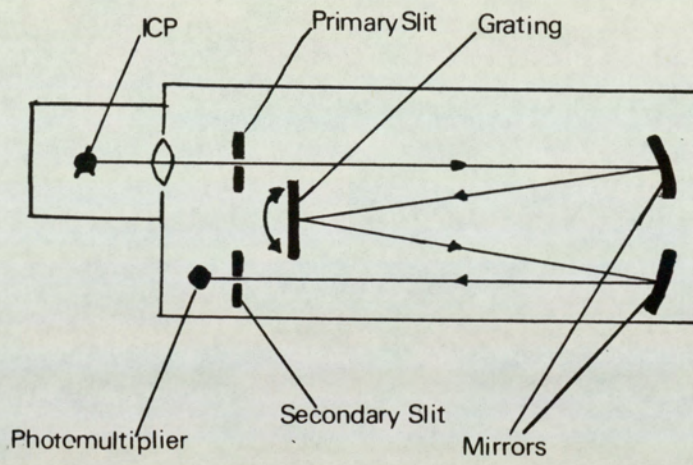
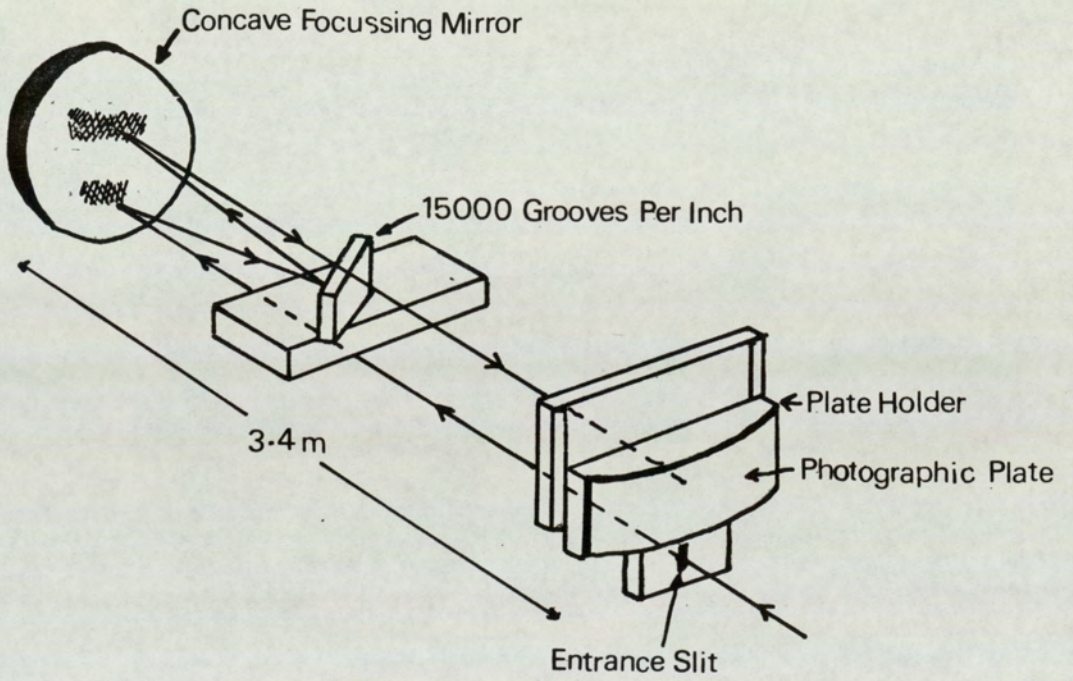


FIG.4.5

EBERT SPECTROGRAPH



CHAPTER 5

DEVELOPMENT OF AN ICP-SPECTROGRAPH SYSTEM

Previous to the advent of photo-electric detectors spectrographs were widely used. However, commercial ICP systems predominantly use photo-electric detection. Although the good precision and high sensitivity of photo-electric detection cannot be equalled by photographic detection, the important advantages offered by the latter technique are mainly over looked. The advantages of using photographic detection with a spectrograph of relatively good optical performance are; (i) wide element coverage, (ii) the capability of handling complex emission spectra, (iii) economy of sample since all elements are recorded simultaneously and (iv) provision of a permanent record for future reference. When the measurement of optical density of spectral lines on a photographic plate and the conversion of optical density to relative intensity are carried out using a computer controlled microdensitometer, the method has application to routine quantitative analysis. These attributes provide a technique well suited to trace multi-element analysis of boron materials and on this basis a system was designed and constructed. A commercial ICP source unit was purchased and used with an existing grating spectrograph. The system was applied to the determination of trace element impurities in boron materials.

5.1 Instrumentation

The RF generator (Model 120-27 supplied by International Plasma Corporation, Hayward, California) consists of a crystal controlled oscillator and an air cooled power amplifier. The oscillating frequency is 27.12 MHz and the power output is adjustable up to a maximum of 2.4 kW. A 2 turn water cooled coil having a 28 mm internal diameter was made from a 5 mm external diameter copper tubing. A demountable plasma torch was used. Pure argon (>99.9%) was introduced into the coolant tube at 15 l/min. The introduction of argon into the plasma tube was found to cause signal suppression and therefore argon was only supplied to the plasma tube during flushing of the torch and for ignition of the plasma.

A pneumatic cross-flow nebuliser Model TN-1 (Plasma-Therm Inc Kresson N5) and a double pass glass spray chamber were used. For an argon flow of 1 l/min the solution uptake is 3.0 ml/min.

Spectra were recorded using a 3.4 metre focal length EBERT spectrograph (Jarrel-Ash Co.) having a dispersion of 0.5 nm/mm. Optics external to the spectrograph consist of a 15 cm focal length condensing lens focussing on to a mask which allows emission from the plasma in the region 20 to 25 mm above the work coil to be aligned on the spectrograph slit by a 14 cm focal length cylindrical lens. The optical configuration is shown schematically in Fig. 5.1 and the system is illustrated in

OPTICAL CONFIGURATION OF ICP

FIG.5.1

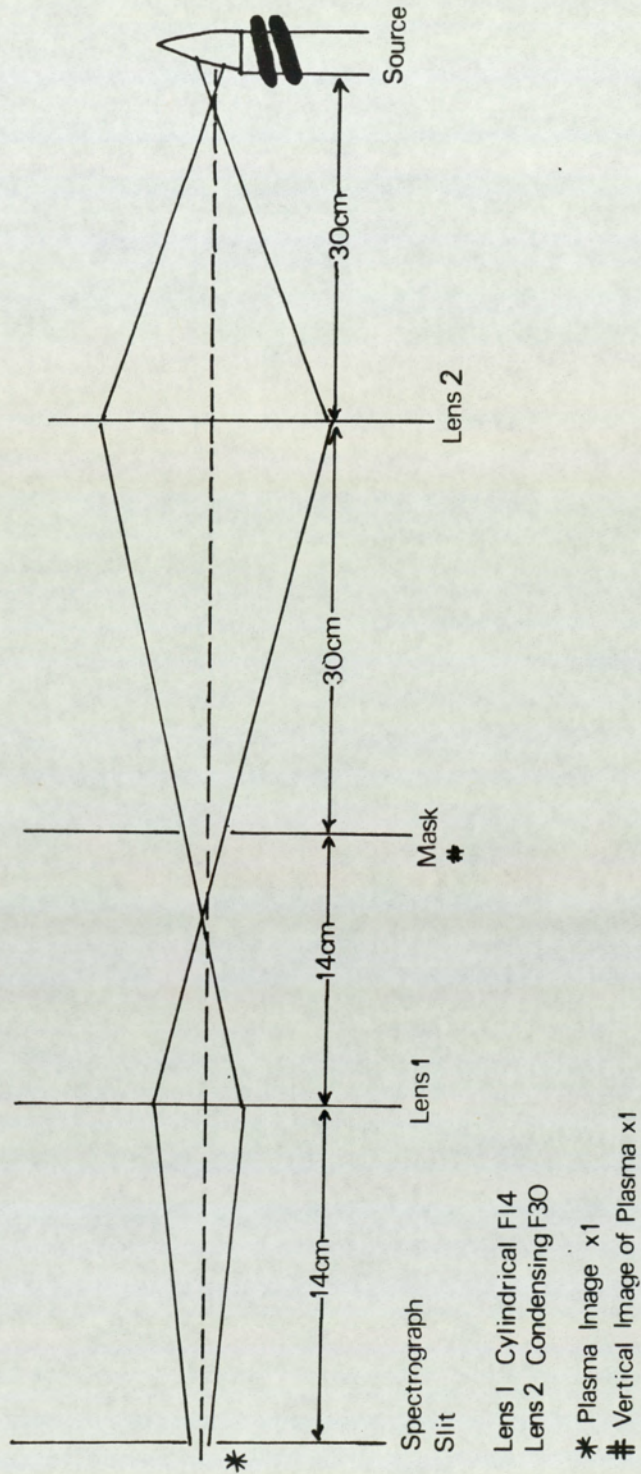


FIG. 5.2

ICP/EBERT 3-4M SPECTROGRAPH SYSTEM



Fig. 5.2. Details of spectrograph conditions used are given in Table 5.1. Two types of photographic plate were used, namely, Eastman Kodak Spectrum Analysis No. 1 for the wavelength range 200 to 350 nm and Spectrum analysis No. 3 for 350 to 500 nm. Plate processing conditions are given in Table 5.2.

The plate reading instrumentation consisted of a Model 3CS autodensitometer (Joyce Loebel Ltd), a DEC PDP 11/10 computer and interface, and is shown in Fig. 5.3. The 3CS is a double beam instrument with the intensity of the light passing through the plate being compared with light passing through a linear optical wedge (Fig. 5.4). A servo system drives the optical wedge to maintain balance between the two beams, and a potentiometer connected to the wedge generates an analogue signal which is a measure of the optical density of the plate. A magnified image of the plate is projected on to the jaws of the slit, and this image may be scanned across the slit by movement of the plate. The slit is adjustable in height and width so that the area of the plate being measured can be controlled.

The carriage holding the plate can be moved in both X and Y directions by incremental motors. The increment in the X direction may be varied by changes in gearing but was set at 2.5 μm per step, while the Y increment was fixed at 5 μm per step. The maximum scanning speeds are 1.0 mm/s in the X direction and 0.45 mm/s in the Y direction. Mechanical counters show the position of the plate at any time and manual controls enable the plate to be moved in both directions, either step-wise or continuously. Micro-switches limit the travel of the carriage and the optical wedge.

TABLE 5.1

SPECTROGRAPH CONDITIONS

Grating	15000 grooves/inch blazed at 300 nm
Grating angle	5.85°
Wavelength range	220 to 460 nm
Dispersion	0.5 nm/mm
Slit width	20 μ m
Slit height	2 mm

TABLE 5.2

SA1 AND SA3 PHOTOGRAPHIC PLATE PROCESSING CONDITIONS

Developer	Kodak D19
Developing time	4 min
Developing temperature	20°C
Fixer	20% Perfix with 5% "S" type hardener (May and Baker)
Fixing time	4 min
Fixing temperature	20°C
Washing time	15 min

FIG. 5.3

GENERAL VIEW OF MICRODENSITOMETER SYSTEM

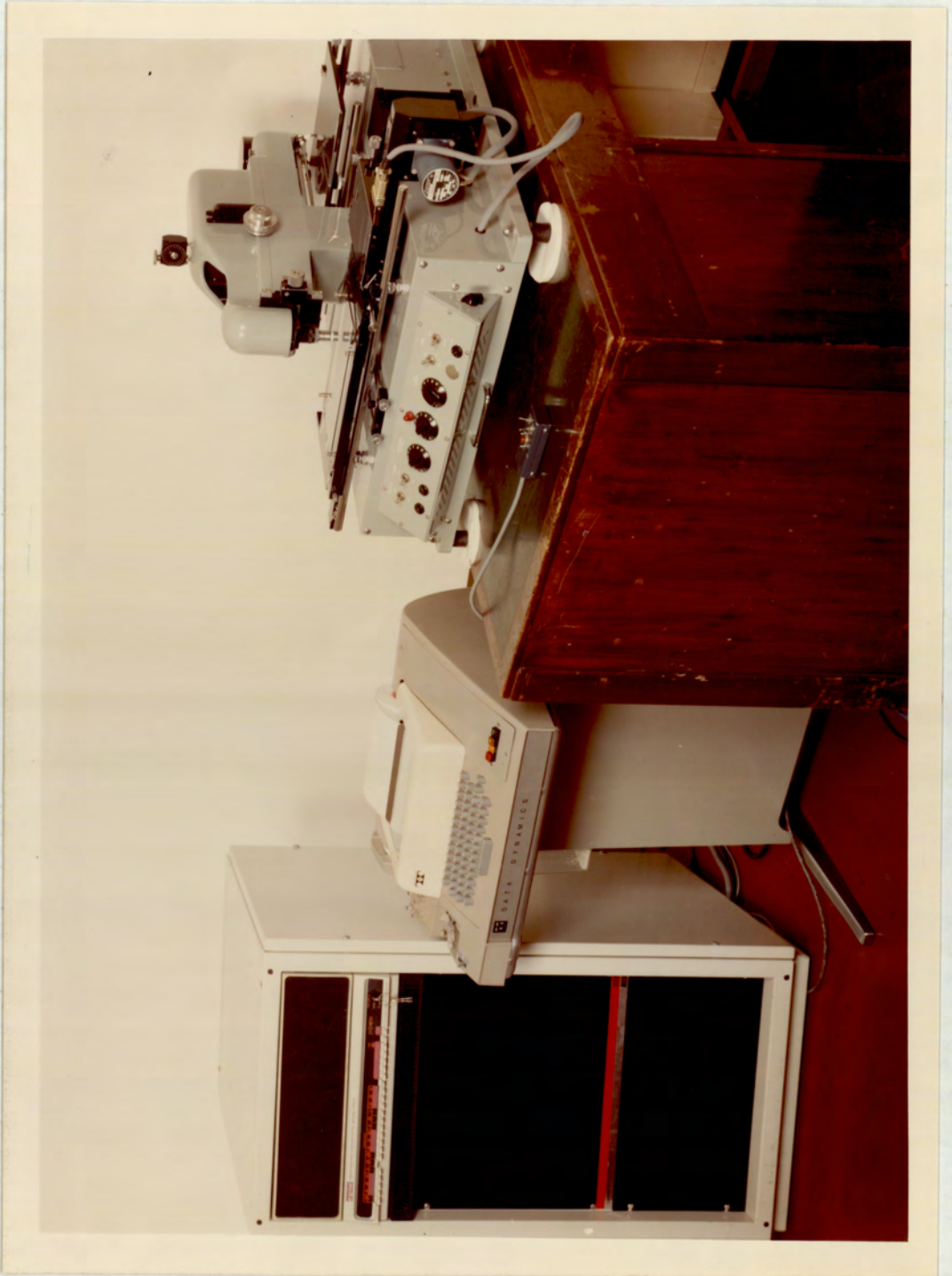
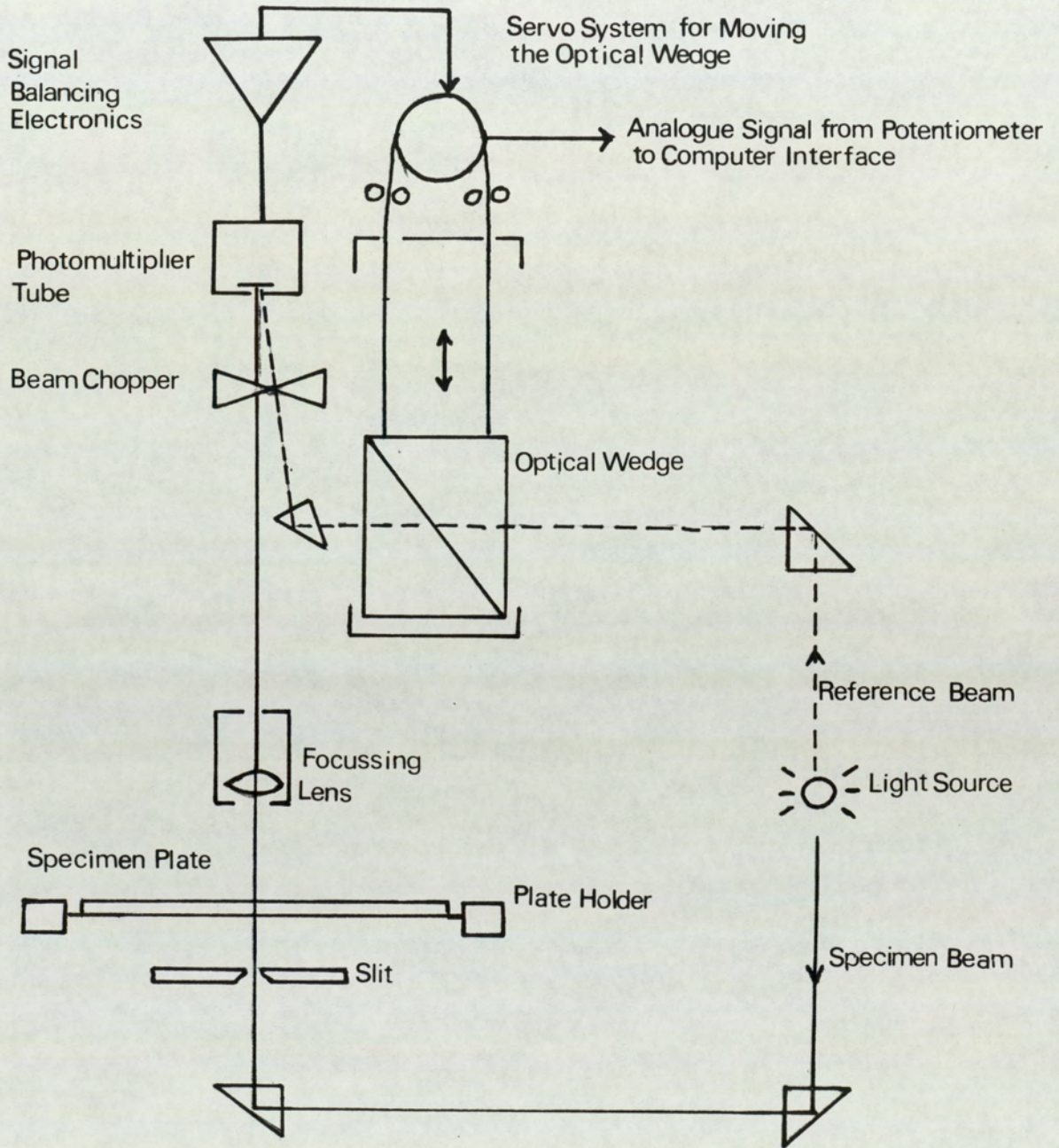


FIG.5.4

JOYCE LOEBL 3CS MICRODENSITOMETER
SCHEMATIC



The interface consisted of a DEC DR-11C interface with a Joyce Loebel designed interface board. The interface input register receives information from the microdensitometer giving the wedge position, the state of the limit switches and an indication that the wedge or plate carriages are stationary or moving. The output register sends signals to the incremental motors to control the direction of movement of the plate carriage. The interrupt register controls whether interrupt signals, given by the microdensitometer when the plate carriage or wedge cease to move or the limit switches are activated. Interrupt signals cause the computer to suspend its current task to process the interrupt. The PDP 11/10 computer has 16,392 (16K) 16 bit words of memory. I/O is via an ASR-35 teletype which can also generate signals to the computer.

5.2 Spectral Line Identification and Measurement

Comprehensive plate reading programs specifically written (31) for optical emission spectra were used. The programs are written in PDP-11 machine language and stored on paper tape and loaded into the computer by the teletype tape reader.

Control programs allow the microdensitometer to move to the area of the plate containing the line of interest and to step-scan across this area recording the optical density at each step. For an impurity element the optical densities for 96 steps, centred about the estimated position of the line, are recorded while for an internal standard line 128 readings are

taken. The wider search limits for the internal standard line are needed because there is no fiducial line from which its position can be measured and there is frequently some lateral shift between spectra due to variations in the spectrograph racking mechanism. A search was then made of the data to find the approximate position of the line peak using the following criteria for a maximum:

$$R_n - R_{(n \pm m)} > P$$

where R_n is the value of the n th reading, $m = 7$, $P = 0.013$ O.D. for an impurity line and $P = 0.05$ O.D. for an internal standard line. The search for a maximum commences at the middle of the set of data and extends away from the centre alternatively to higher and lower wavelengths until the above criteria are satisfied or until the boundary of the data is reached. When a maximum is identified the 14 readings either side of the approximate line centre are smoothed using a 7 point quadratic convolution (32). If a maximum exists a parabola is fitted to the seven points centred on the maximum. The co-ordinates of this parabola give the line position and the value of the line maximum. The background under the line is measured as the mean of the eight consecutive readings within the set of data points giving the lowest total.

When the optical density of an image on a photographic plate is plotted against the logarithm of the light intensity causing the image, the well known Hutler and Driffield curve is obtained (33). This curve is linear only in the optical density

range 0.5 to 1.5 O.D, and normally a graphical representation is necessary for computation below 0.5 O.D. because of the curvature of the line. For computer calculation it is necessary to find a mathematical treatment which linearises the H + D curve. One such approach uses the Seidel transformation i.e

$$S = \log (10^D - 1)$$

where D is the optical density. If S is plotted against the logarithm of the intensity the linear portion of the curve is maintained, but the curvature at low optical densities is reversed. The L-transform gives a combination of optical density and Seidel value which is linear over the whole of the optical density range. Thus

$$L = (1-f) D + f S$$

where f is the linearising factor which is computed using an iterative procedure. Since a plot of L against log intensity is linear and in practice the intensities are relative and not absolute, the slope (K) of the plot and the optical densities are sufficient to allow the intensities to be calculated. The emulsion calibration coefficients f and K are dependent on the type of photographic emulsion and the wavelength of light. Plate emulsion calibrations were obtained using a seven step rotating sector positioned at the spectrograph slit, thus permitting the exposure time to be varied by a factor of two at each step. For emulsion calibration it is necessary to have an evenly illuminated slit of 15 mm height and as this could not be provided by the EBERT spectrograph a MEDIUM spectrograph was used. An important characteristic of photographic detection is reciprocity and its failure (34). Reciprocity infers that the

line blackening produced by a source of light for a fixed exposure time should be reproduced by a second source which gives half the intensity when an exposure twice as long has been taken, and vice versa. Technical data supplied by Kodak (35) show that under the experimental conditions used, reciprocity is maintained. Another source of error in photographic reading is the "intermittency effect" and occurs when two exposures of equal intensity, one continuous and the other delivered in installments, do not lead to the same image density. Pierce and Nachtrieb (36) found no evidence for the intermittency effect for the Eastman Kodak SA1 and SA3 plates for sector speeds varying from 100 to 1800 rpm. As the rotating sectors used in this work operate at 1400 rpm then, intermittency is not expected to be a problem.

Initially, a high pressure Xenon arc was used to provide a continuum calibration source enabling many optical density readings to be taken from the microdensitometer for a given wavelength. However, although this method proved convenient it was inaccurate. The optical densities taken from an ICP specimen plate are from a line spectrum source and not a continuum source. The response of photographic emulsions, to continuum and line sources give different characteristics particularly in the case of high contrast plates such as SA1. In addition to changes in the emulsion response, both the chemical processes used in the development of the plate and the actual readings taken by the microdensitometer were found to vary according to whether continuum or line spectra were being

examined. This was also observed by Heltai and Zimmer (37). Consequently, in preference to using a continuum spectrum, a line spectrum as produced by a DC arc source using steel bolts as electrodes was used for emulsion calibration.

The optical density and Seidel values were calculated from the microdensitometer readings from each step and an iterative method was used to find the value of f which gave the best fit to a straight line for the plot of L against the logarithm of the intensity.

Fig. 5.5 shows typical calibration plots of H and D , Seidel and L curves which were obtained for a Kodak SA1 plate at 300 nm. The response for SA1 and SA3 plates for slope and f factor with respect to wavelength are shown in Fig. 5.6 to 5.9. The most accurate method of calculating intensities is to represent the relationship between wavelength and emulsion calibration factors as two polynomial equations from which the appropriate factors could be interpolated. However, due to the limited memory space available in the computer a more simple approach was used. The spectrum for a single plate was divided into seven regions, each with its own emulsion calibration data. As the contrast of the plate increases at increasing wavelength the wavelength range for such a region decreases in order to ensure representative calibration.

Before starting to measure a plate, the program requires a set of instructions to define its task. Each impurity element is defined by its chemical symbol and its distance in mm

FIG.5.5

PLOTS OF H+D CURVE SEIDEL AND
L TRANSFORM

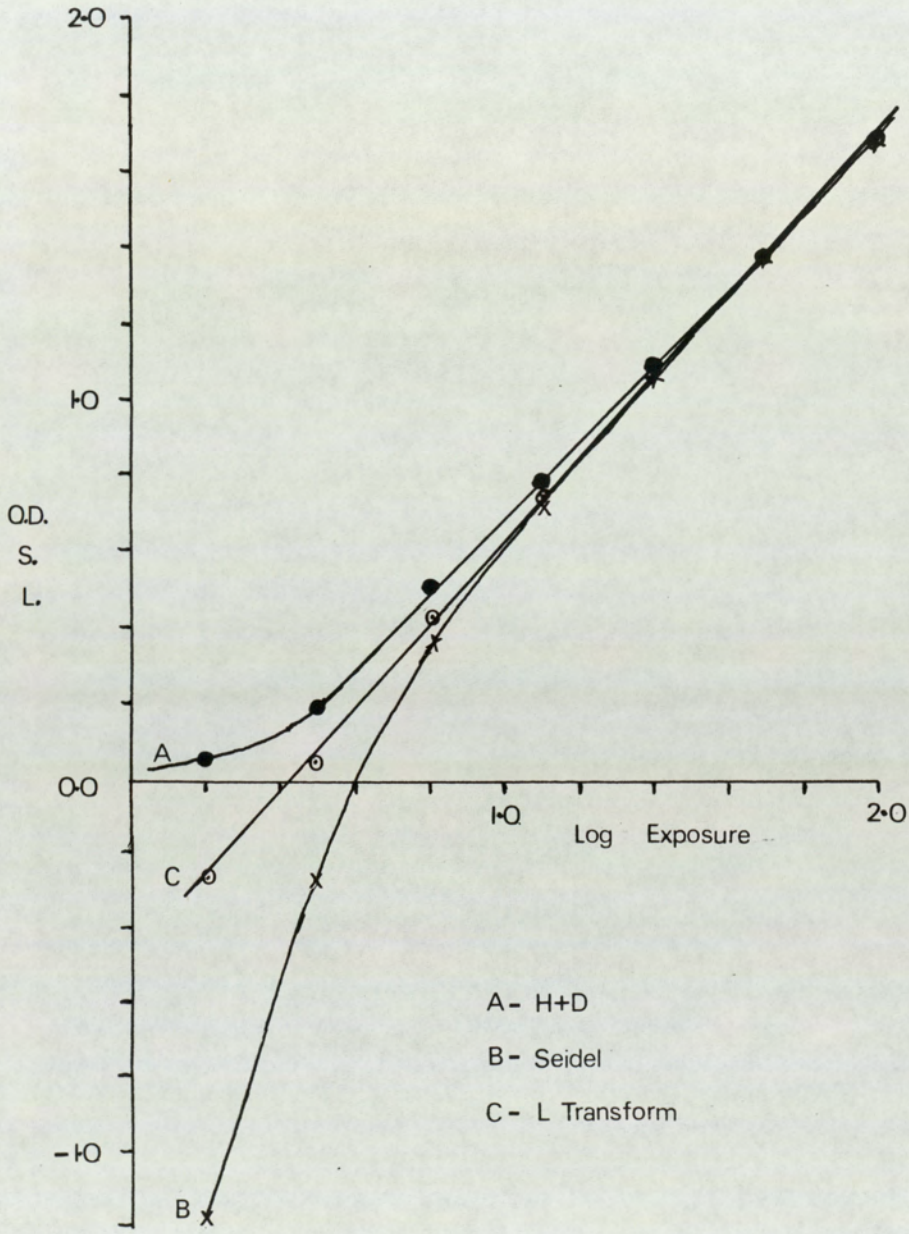


FIG. 5.6

EMULSION CALIBRATION FOR KODAK SA1

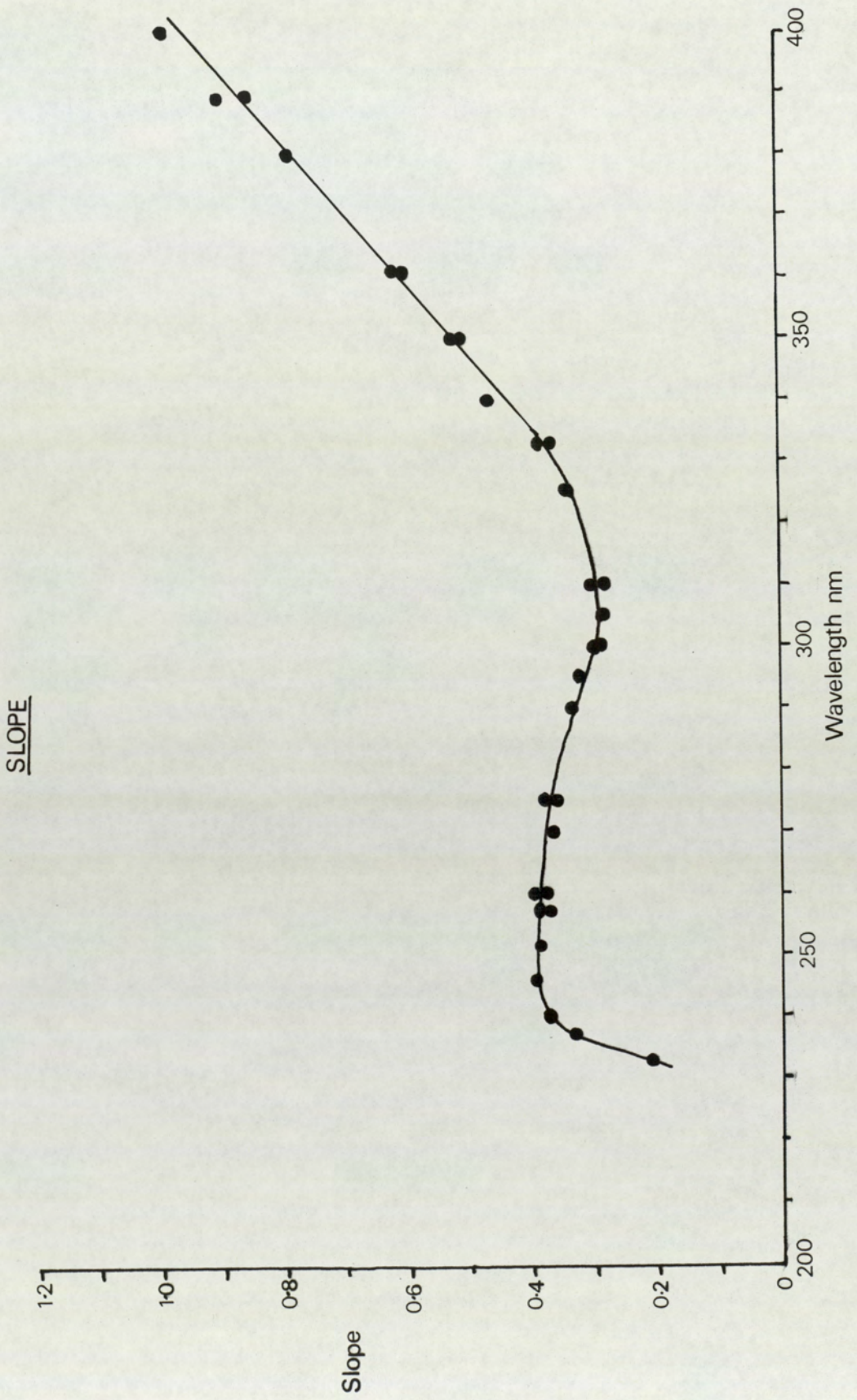


FIG. 5.7

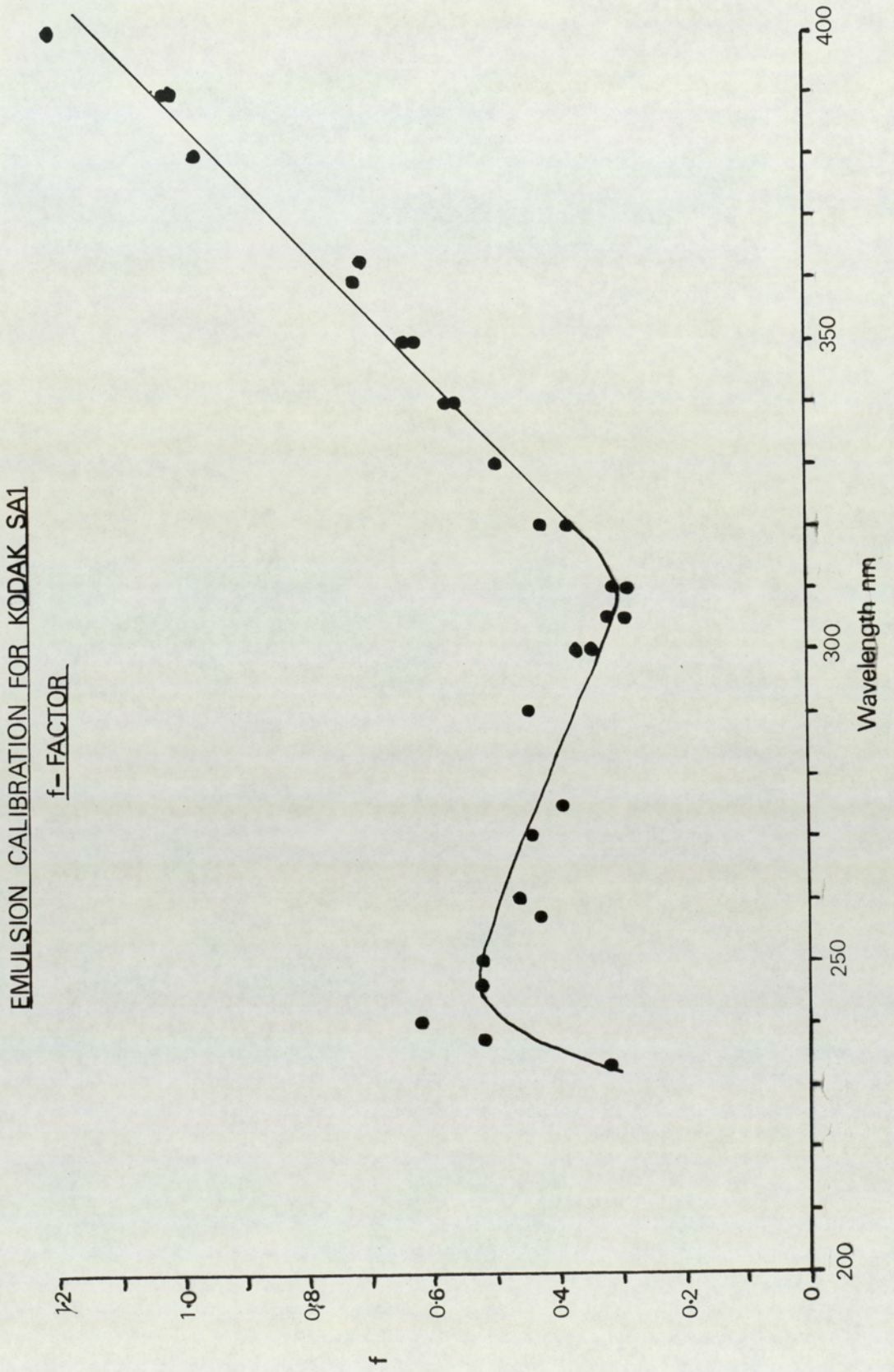


FIG.5.8

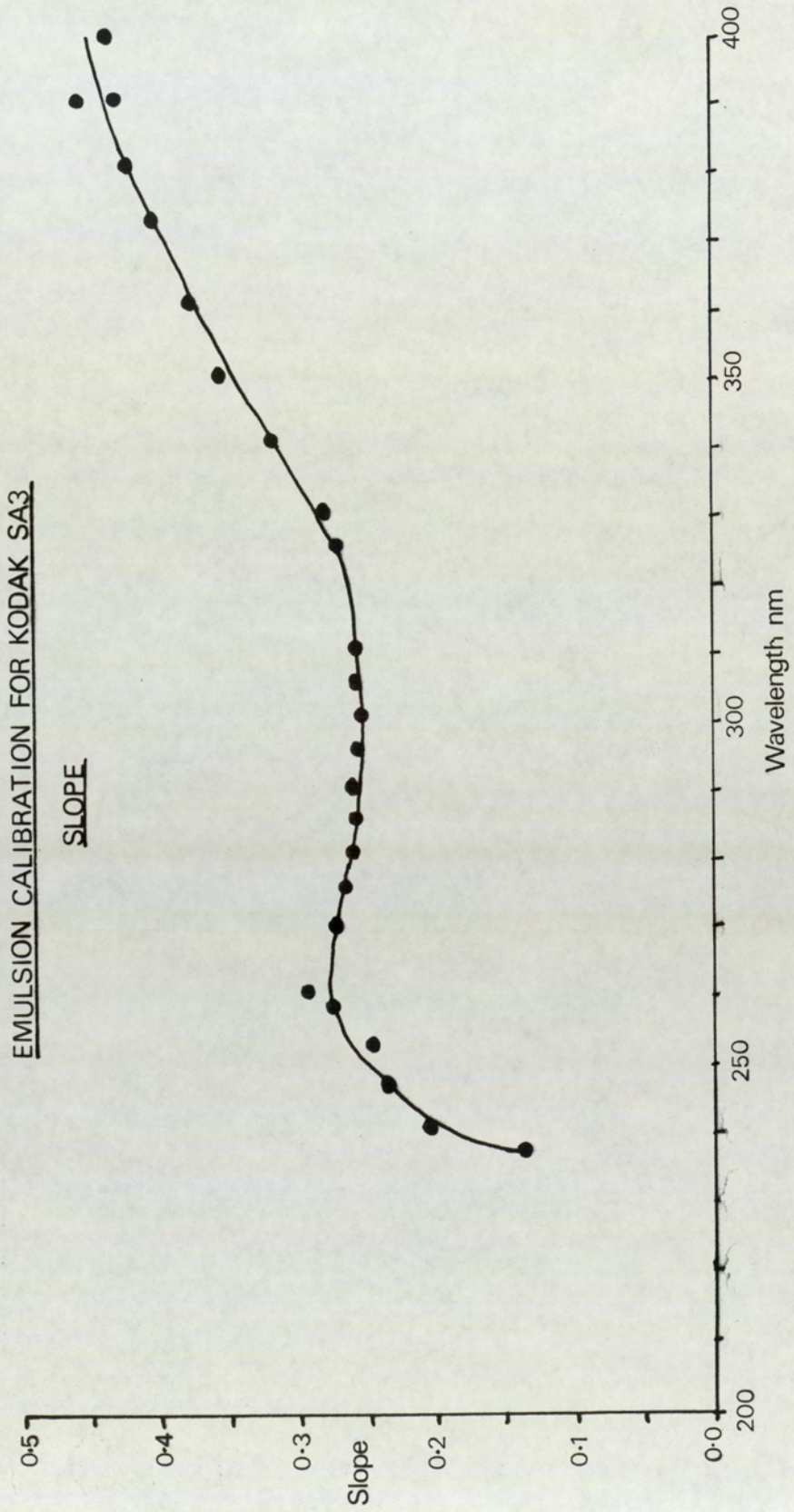
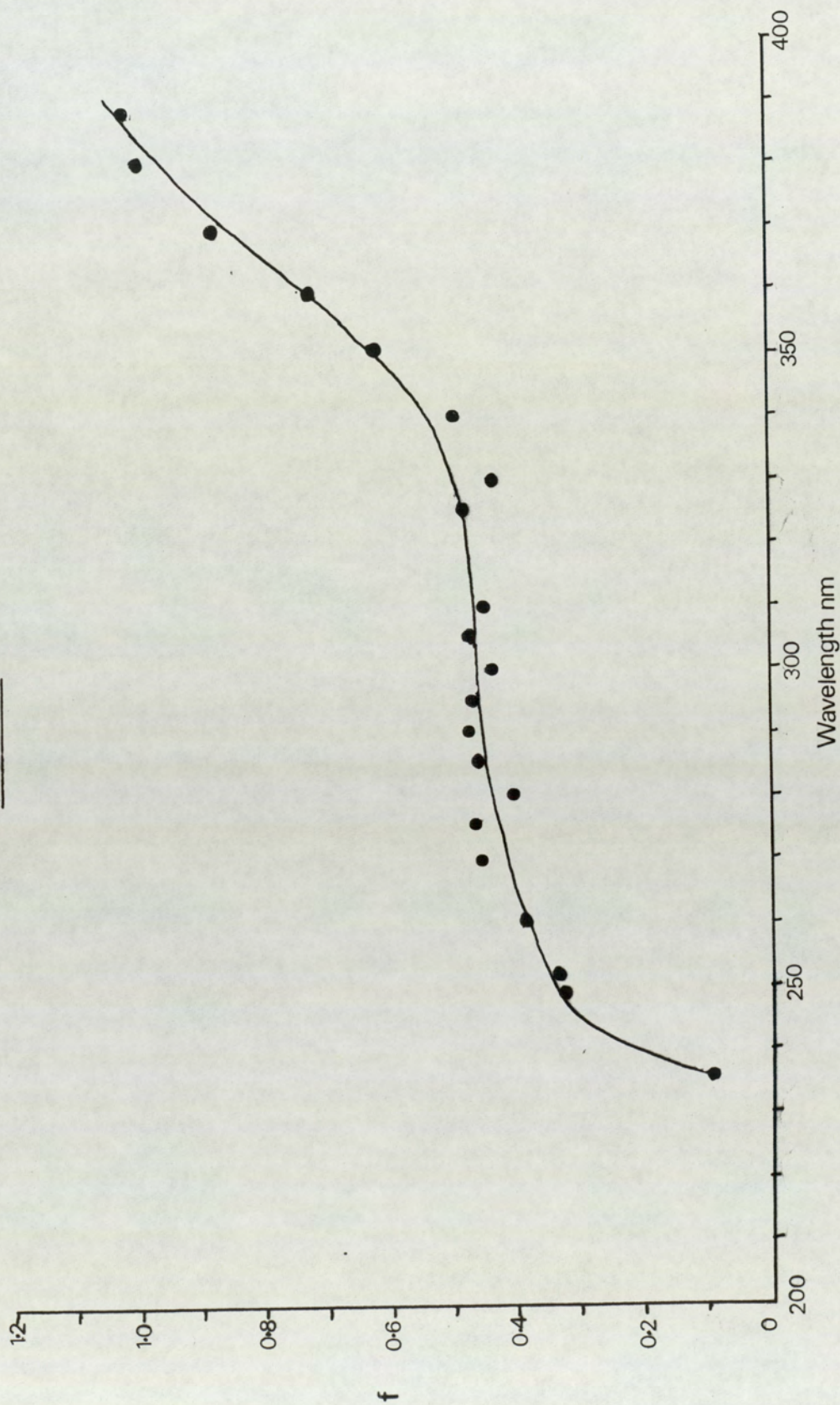


FIG.5.9

EMULSION CALIBRATION FOR KODAK SA3

f-FACTOR



from the associated internal standard line. A standard spectrum is defined by the concentration in the standard and by its vertical distance from the previous spectrum. A sample spectrum is defined by a four character title, which must begin with a non-numeric character, and the distance in mm from the previous spectrum. Once the instructions have been fed into the computer and the first internal standard line in the first spectrum has been centred on the microdensitometer slit the measurement is started. When the computer has stored the intensity ratios and concentrations for each element in each standard spectrum, calibration equations are calculated using a least squares fit to the equation:

$$\log R = A \log C + B$$

where R is the intensity ratio at the concentration C and A and B are constants. These coefficients are printed for each impurity line together with a value for the blank in the standards if a significant line is found in the blank spectra. The microdensitometer then commences to scan sample spectra and having determined the intensity ratio for each impurity it converts these to concentrations using the calibration equations. The calculated concentrations are printed together with the intensities and positions of the line peaks.

5.3 Application to Boron Materials

Boron solutions can be prepared by oxidation of boron powder to boric acid (H_3BO_3) using concentrated HNO_3 . Since the

solubility of H_3BO_3 is 0.0635 g/ml the maximum concentration of boron in solution which can be prepared by dilution is 1%. To obtain a more concentrated solution (i.e 7% B) H_3BO_3 was converted to the more soluble borofluoric acid (HBF_4) by addition of concentrated HF. HF ('ARISTAR' grade) has a maximum concentration of 40% and this limits the maximum boron concentration in solution to 7%. Since matrix interference effects are considered to be less in the ICP than in other sources, initial trace element determinations were carried out with the boron still present. However preliminary measurements showed that the boron oxide band spectrum was still sufficient to give unacceptably high limits of detection. Also HF attack on the torch injection tube results in large Si, Fe, Al, Mg and Ca blanks. Consequently it was necessary to remove the boron before analysis. This was achieved by volatilizing the boron trifluoride BF_3 from the HBF_4 solutions.

A boron sample (particle size 38 to 75 μm), identified as R23, and known to contain 5 to 100 ppm of several impurities, was selected for method development. Three 2.00 g samples were weighed into clean 150 ml conical flasks and 15 ml of distilled HNO_3 ('ARISTAR' grade) were added dropwise to each flask. After the vigorous reaction had subsided the flasks were transferred to a hot plate and heated under reflux for three hours. The H_3BO_3 formed was transferred to clean Pt crucibles by washing with deionized water. 40% (w/v) HF was added in sufficient quantity to dissolve all the H_3BO_3 . The crucibles were then transferred to a hot plate and the solutions allowed to evaporate to dryness. The residue was dissolved in 2 ml of 3% (v/v) $HClO_4$ followed by

addition of 2.5 ml of an internal standard Co solution (1000 $\mu\text{g/ml}$). The solutions were diluted to 25 ml with deionized water. Reagent blanks were prepared in a similar manner.

Multi-element solutions containing 0.1 to 50 $\mu\text{g/ml}$ of standard were prepared from appropriate spectrographic standards and each solution contained 100 $\mu\text{g/ml}$ of Co as an internal standard.

5.4 Results

In view of the stability of the ICP source it was considered possible that standard calibrations would not vary significantly from day to day provided an internal standard was used to correct for variation in plate sensitivity. By investigating standards on a number of plates it was found that the calibration drifted and therefore the precision of a determination is significantly better when derived from the same plate compared to using a fixed calibration derived from the mean of all calibrations. It is therefore necessary to expose a range of standards for calibration on each plate.

Since a range of standards were recorded on each plate, it was not necessary to use an internal standard for calibration although it must remain to provide fiducial lines for microdensitometry. It is an advantage to avoid the use of an internal standard, since in multi-element standards at high concentrations, the probability of line coincidence with the internal standard line is increased. For example Cr at high

concentration interferes with the Co line at 266.353 nm so that intensity ratios for all elements used with this Co line will be reduced in the standards at high concentrations, thereby affecting the accuracy of the analysis.

Despite the low background of the ICP source some interferences are experienced from OH and Ar bands e.g interferences were observed at 309.271 nm and 318.128 nm for Al and Ca respectively. This causes curvature at the low concentration end of the standards' calibration and causes deterioration of the detection limits. However, alternative lines are available e.g 317.937 nm for Ca.

Table 5.3 shows the emission lines selected for 25 elements determined together with the detection limits in boron, the upper concentration limit that can be determined without dilution of the solutions and the average reagent blank found. Limits of detection were calculated using the expression:

$$\text{LOD} = 3 \times (\text{RSD}) \times I_b / I_a \times C$$

where I_b and I_a are the mean background and analyte intensities respectively, RSD is the relative standard deviation of the background and C is the concentration of the analyte ($\mu\text{g/ml}$). Since the boron matrix is removed the sensitivity of the method can be adjusted by increasing the sample size provided that the limits of detection are not dependent on the reagent blank.

TABLE 5.3
PERFORMANCE OF METHOD

Element	Wavelength nm	L.O.D µg/ml	L.O.D in Boron ppm	Upper Conc limit ppm	Reagent blank for method ppm
Al	309.271	0.5	5	1000	10
Ca	317.933	0.2	2	500	20
Cu	327.396	0.1	1	500	5
Ni	305.083	0.5	5	1000	<5
Mo	313.259	0.5	5	1000	<5
Mg	285.213	0.1	1	500	<1
Fe	259.940	0.1	1	500	15
Cr	283.563	0.1	1	500	<1
La	330.310	0.1	1	500	<1
Mn	294.920	0.1	1	500	<1
Ti	323.452	0.05	0.5	100	<0.5
V	309.311	0.05	0.5	100	<0.5
Zn	334.502	0.1	1	500	<1
Sa	294.364	0.5	5	200	<5
Sr	421.552	0.03	0.3	100	<0.3
Y	371.030	0.1	1	200	<1
Zr	339.198	0.1	1	500	<0.5
Nb	313.079	0.1	1	200	<0.5
Ru	267.876	0.3	3	500	<3
In	303.936	1	10	1000	<10
Cd	228.802	10	100	2000	<10
Gd	335.047	0.05	0.5	200	0.5
Ba	455.403	0.05	0.5	200	0.5
Dy	353.170	0.1	1	100	<1
Pb	283.306	1	10	2000	<10

Table 5.4 shows the standard deviation of the concentrations of the elements in five solid portions of the control sample and from the analysis of five aliquots taken from a bulk solution of the same material. Duplicate exposures were made in all cases and from these the precision of the ICP/AES method for the analysis of a sample solution was calculated. If the precision of the ICP determination, derived from the duplicate exposure of all solutions is compared to the precision obtained from replication of the solution aliquots of the sample, it can be seen that the precision deteriorates significantly for Al, Ca and Mo but not for the other elements. In the case of Al and Ca this may be due to variations in the level of contamination, and this is supported by observation that the variation in reagent blank for these two elements are generally higher than for other elements. For Mo it may be attributed to differences in the chemical processing of the sample solution aliquots. Similarly, if precisions are compared between solid sample portions and solution aliquots there is significant deterioration in precision in determining Fe and Mn. This can be attributed to variations in the amount of these elements that can be dissolved, or that the distribution of these elements in the sample is not uniform.

The overall precision with which impurities can be determined in a solution ranged from 3% to 8% RSD, which is typical of a technique which uses photographic detection. The precision of the method ranged from 10% to 15% RSD, but for elements such as Ca, Al and Fe, at low concentrations contamination causes a deterioration of this precision. Since the



TABLE 5.4

PRECISION OF ICP-SPECTROGRAPHIC DETERMINATION

Element	Mean Concentration ppm	Standard Deviation		
		ICP Determination ppm (a)	Solution Aliquots ppm (b)	Solid Sample ppm (c)
Al	280	8	28	22
Ca	270	16	40	56
Cu	29	3.1	3.7	6.0
Ni	36	3.4	1.5	5.5
Mo	165	7.7	16	33
Mg	110	9.2	10.0	19
Cr	41	3.8	5.0	2.1
La	6.0	0.6	0.5	0.2
Fe	1100	13	10	97
Mn	680	8	6	41

- (a) From duplicate exposures measured on 5 aliquots of the same solution.
- (b) From duplicate exposures measured on 5 aliquots of solution taken from a bulk solution.
- (c) From duplicate exposures measured on 5 portions of solid sample taken through the whole procedure.

precision within sample solutions is significantly better than that between solid samples, it is recommended that the better performance can be obtained by single exposures of sample solutions, allowing more sample replicates to be analysed on one plate.

The accuracy of the method was tested in two ways. In the first simulated boron sample solutions, with known additions of impurity at the 10 to 20 ppm level in pure H_3BO_3 , were prepared and analysed. As shown in Table 5.5 apart from Mn at low concentration there is no significant loss of impurities. In the second, results obtained from the analysis of the boron control sample R23 were compared with results obtained from other methods such as epithermal neutron activation (ENAA) and flame atomic absorption spectroscopy (FAA). As shown in Table 5.6 good agreement is found between all three methods, except that Fe determination by FAA is low compared to other methods. It is also noticeable that good agreement is found for the determination of Mn by all three methods, and it appears that at this high concentration there is not a significant loss of Mn.

5.5 Discussion

Although the method was developed for the determination of impurities in elemental boron, it is also applicable to the analysis of any boron compound that can be dissolved. The stability of boron to acid attack depends on its purity and its physical form, and in some cases heating in HNO_3/HF at $190^\circ C$ in PTFE pressure vessels is necessary. Boron carbide is even more

TABLE 5.5

ANALYSIS OF SIMULATED SAMPLES

Element	Expected Concentration ppm	Mean Concentration ppm	Recovery %
Al	20.0	19.0 ± 4.0	95 ± 20
	10.0	8.2 ± 1.5	82 ± 15
Ca	20.0	17.0 ± 3.3	85 ± 16
	10.0	8.8 ± 1.2	88 ± 12
Cu	20.0	21.0 ± 3.6	105 ± 20
	10.0	11.1 ± 1.5	110 ± 15
Ni	20.0	20.1 ± 2.0	100 ± 10
	10.0	10.2 ± 0.8	100 ± 8
Mo	20.0	20.0 ± 1.5	100 ± 8
	10.0	9.5 ± 2.0	95 ± 20
Mg	20.0	18.5 ± 1.2	93 ± 6
	10.0	8.3 ± 1.2	83 ± 12
Cr	20.0	17.5 ± 2.9	88 ± 15
	10.0	9.0 ± 1.1	90 ± 11
La	20.0	22.2 ± 6.0	105 ± 30
	10.0	13.0 ± 3.3	110 ± 15
Fe	20.0	19.1 ± 1.6	95 ± 8
	10.0	11.0 ± 1.3	110 ± 13
Mn	20.0	16.5 ± 1.6	83 ± 8
	10.0	8.0 ± 1.2	80 ± 6

Errors quoted as the 95% Confidence Limits derived from 4 complete replicate analyses.

TABLE 5.6

COMPARATIVE ANALYSIS OF BORON SAMPLE R23

Element	ICP/AES ppm	FAA ppm	ENAA ppm
Al	280 ± 60	310 ± 30	-
Ca	270 ± 50	230 ± 30	-
Cu	29 ± 3	28 ± 3	-
Ni	36 ± 5	32 ± 5	31 ± 3
Mo	165 ± 30	180 ± 30	170 ± 20
Mg	110 ± 15	130 ± 20	-
Cr	41 ± 3	38 ± 3	47 ± 7
La	6.0 ± 1.8	-	5 ± 1
Fe	1100 ± 140	860 ± 50	1045 ± 50
Mn	680 ± 40	650 ± 100	660 ± 20

ICP/AES - Inductively coupled plasma atomic emission spectroscopy

FAA - Flame atomic absorption spectroscopy

ENAA - Epithermal neutron activation analysis

Errors quoted as 95% confidence limits derived from 3 replicate analyses.

resistant and in this case dissolution is achieved in a sealed silica Carius tube using HClO_4 at 300°C for up to 72 hours. The size of apparatus available limits the amount of sample that can be dissolved to 0.2g which, at the concentration of solution required, allows only 2 ml of solution for analysis. Commercial nebulisers for ICP require about five times that volume of solution for the exposure times used in this method. To overcome this problem a recirculating nebuliser was designed which will be fully described in Chapter 8.

Although the method was developed to provide low limits of detection in pure materials, the results for the control sample show that higher concentrations can be determined satisfactorily. The use of photographic plates, however, limits the upper concentration level that can also be determined in the solution. The range of concentration can be extended by reducing the exposure time, and a second exposure of e.g 12 seconds extends the range by a factor of ten. This was achieved using a rotating step sector which gave an exposure ratio of 100:10 at the slit. The impurity line is measured in the more appropriate portion of the spectrum, whilst the fiducial line is still measured in the 120 second exposure portion.

5.6 Conclusions

ICP/AES, using photographic recording and a computer controlled microdensitometer, has been successfully applied to the analysis of boron. The method proved capable of analysing three samples in triplicate for 25 elements in about three days.

The sensitivity of the method for these elements in boron ranges from 1 to 10 ppm when using a 1.0g sample. For a number of elements, e.g Fe, Ca, Mg, the limit of detection is limited by the reagent blank and the use of high purity reagents and clean working conditions is essential.

The precision of the method for a single determination ranges from 10% to 15% RSD and much of this error arises from the chemical preparation. To obtain the best precision it is therefore important to replicate sample portions rather than replicating exposures of the same portion. The accuracy of the method has been confirmed by the analysis of synthetic samples and also by comparison of results obtained in a boron control sample by at least one other method. The method may be extended to the analysis of other boron compounds provided they can be dissolved satisfactorily.

CHAPTER 6

DEVELOPMENT OF A MICROCOMPUTER CONTROLLED SCANNING MONOCHROMATOR ICP SYSTEM

The development of the ICP-Spectrograph system showed that ICP/AES has considerable capability for trace multi-element analysis of boron. However, there are two alternative approaches for measuring and recording spectral data. These are:

(i) simultaneously using a polychromator and photo-electric recording:

and (ii) sequentially using a scanning monochromator and photo-electric recording.

Although (i) is the more rapid and economical in terms of analyte solution it was not used in this study as it lacks flexibility in the choice of analytical wavelengths available. In cases where serious line coincidences are encountered, problems leading to reduced sensitivity, accuracy and precision can occur. More appropriately with a scanning monochromator system, i.e. (ii), spectral lines of interest are recorded and measured by fast slewing to a wavelength close to the line of interest and then slowly step scanning over the line, thereby recording the integrated data points at each step to create a profile of the peak and its background. Several factors, e.g optical and mechanical performance can influence the accuracy and precision with which the instrument can identify and measure

correctly spectral lines. Commercial scanning systems have been developed over the past few years but generally they have been aimed at applications involving relatively small numbers of materials which give simple emission spectra. In such applications the resultant spectra can be handled by low cost spectrometers of inferior optical performance but such systems lack the versatility and performance required here. Consequently in order to investigate the potential of sequential ICP/AES, a system was constructed and its performance evaluated.

6.1 Instrumentation

A schematic layout of the microcomputer controlled scanning ICP system is shown in Fig. 6.1 and a photograph of the hardware constructed is shown in Fig. 6.2.

The inductively coupled plasma used for this work was a Plasma-Therm system, Model HFP 2500D with a crystal controlled generator operating at 27.12 MHz and maximum output of 2.5 kW. The nebuliser was a Plasma-Therm Model TN-1 pneumatic cross-flow type. Light from the plasma was focussed as a 1:1 image on to the entrance slit of a 1 metre focal length Spex 1802 spectrometer (Fig. 4.4) with a 2400 grooves/mm holographic grating. The spectrometer was modified to include a thermostatted radiator set at 28°C. A refractor plate mounted inside the spectrometer, close to the entrance slit and operated manually by a micrometer, was included to allow precise wavelength alignment on specific peaks for single element determinations. Instrumental conditions used are given in Table 6.1.

FIG. 6.1

COMPUTER CONTROLLED SCANNING MONOCHROMATOR SYSTEM

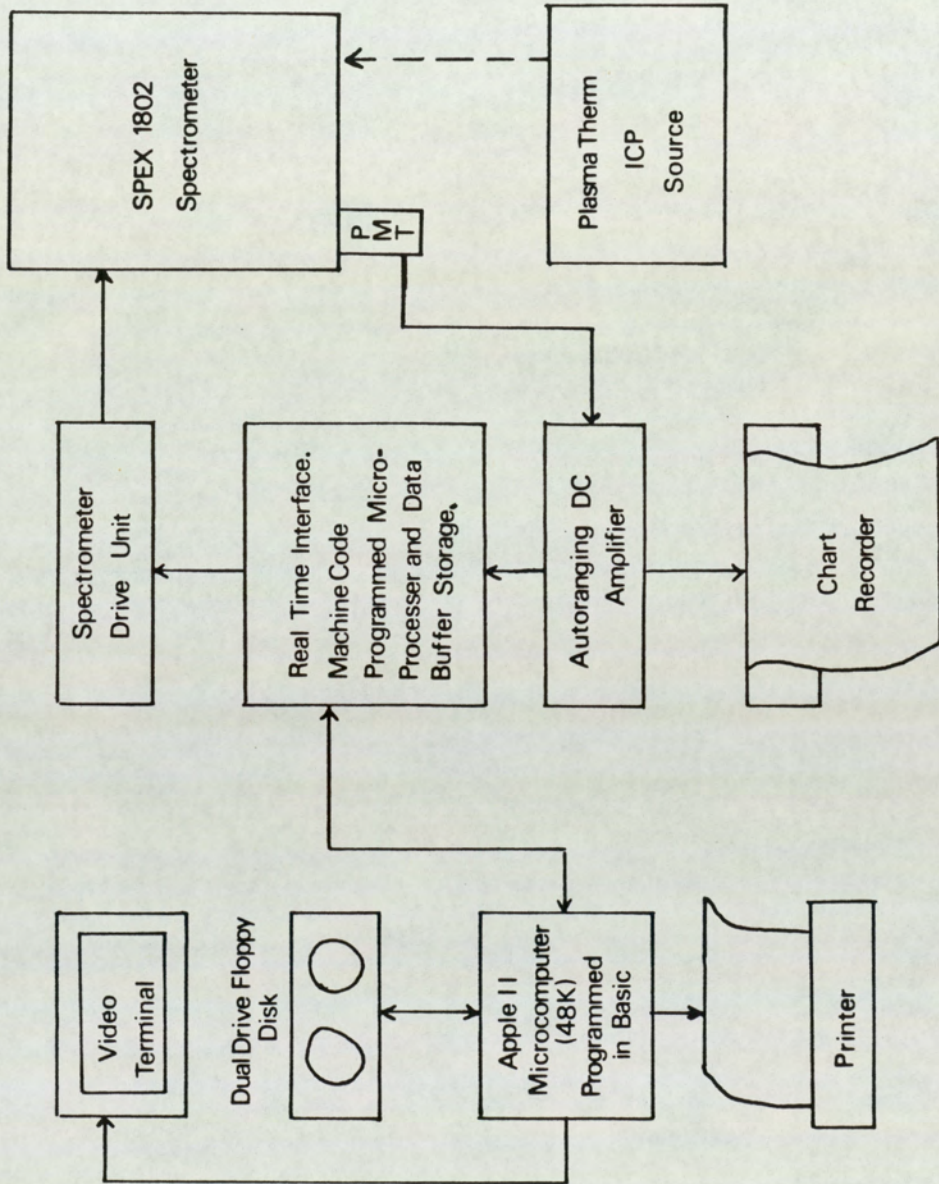


FIG. 6.2

ICP/SCANNING MONOCHROMATOR SYSTEM



- (A) ICP Source.
- (B) R.F. Generator.
- (C) Spectrometer.
- (D) Apple II Computer System.
- (E) Autoranging Amplifier.
- (F) Linkman Interface.
- (G) Spectrometer Drive Unit.

TABLE 6.1

CONDITIONS FOR SCANNING MONOCHROMATOR SYSTEM

PLASMA

Type	Plasma Therm Model HFP 2500D
Frequency	27.12 MHz
Torch type	Demountable Fassel
Forward power	1.5 kW
Reflected power	<5 W
Coolant gas flow	15 l/min
Auxiliary gas flow	1.4 l/min
Injector gas flow	0.7 l/min at 12 psi
Observation height above work coil	18 - 22 mm
Nebuliser	Pneumatic cross flow Plasma-Therm Model TN-1

OPTICAL

Spectrometer	1 metre Spex 1802
Grating	2400 grooves/mm Holographic
Wavelength range	190 to 900 nm
Entrance slit width	20 μ m
Exit slit width	20 μ m
Slit height	2 mm

DETECTION

Type	Photomultiplier
kV)	(EMI-9802 operating at 1.67

AMPLIFIER

Type	J S Systems autoranging amplifier (range 10^6 DC).
------	---

COMPUTER SYSTEM

Type	Apple II (48K) operating in DOS 3.3
Language	Applesoft extended BASIC
Interface	J S Systems real time Linkman with 16K Mostek-Zilog 280 CPU

SAMPLE CHANGER

Model	Plasma Therm auto sampler
Sample capacity	20 x 100 ml bottles
Control	Automatic control via Linkman interface.

It was considered essential to acquire and process raw spectral data simultaneously. This was achieved by including a real-time interface which incorporated a data buffer storage (10 K) for temporarily storing raw data. For optimum control speed this was programmed in machine-code. On transferring control programs from the disk storage this interface controls all spectrometer functions independently of the computer, thereby permitting the computer to accept temporarily stored data from the interface for processing.

6.2 Software Development

The original software supplied with the computer system did not function in real-time and hence sequential data acquisition and processing was unacceptably tedious and time consuming. Since it was originally written for processing X-ray diffraction data it was not totally appropriate for the analysis of ICP spectral data where the number of lines is considerably greater. Therefore new software specific to ICP/AES was written by the author.

6.2.1 Procedure

When the operating disks are loaded into the drive units the software is automatically loaded and run. A menu is displayed showing the various system functions available. The five main procedures are:

- (i) Activating the Linkman interface:

- (ii) Establishing the experimental parameters in the Analysis File;

- (iii) Aligning the spectrometer wavelengths;

- (iv) Conducting an analysis;

- (v) Displaying operating prompts.

Procedure (i) establishes communication between the computer and the interface; procedures (ii), (iii) and (iv) are used in analysis and are described more fully below.

On selecting option (ii) the operator is requested to enter analysis identification followed by a list of wavelengths for all the elements to be determined. An Analysis File containing all the slew, scan and integration parameters required for the analysis is created and stored.

In order to obtain correct wavelength measurement the spectrometer is calibrated using the 324.754 nm and 327.396 nm Cu lines (1 µg/ml). These lines are scanned automatically and the wavelength difference between the measured and expected line positions is recorded and is used to correct the position of the analyte lines during subsequent analysis.

On selecting option (iv) the operator is requested to enter the relevant Analysis File name. Standards must be run before analytical samples so that the calibration is established.

6.2.2 Spectral Line Identification and Measurement

Spectral lines are scanned in three stages:

- (i) the line is approached to within 2 nm of the expected position at a speed of 150 nm/min;
- (ii) in the range 2 to 0.075 nm of the expected position the line is approached at a speed of 5 nm/min;
- and (iii) the line is step-scanned over 0.15 nm at 0.001 nm intervals, each step taking 0.1 sec.

Of the 150 data points so obtained only 80 points centred at the middle of the scan range are taken for processing. The above parameters have been derived for optimum accuracy and reproducibility of locating spectral lines using this instrument. They may be different from those of other instruments.

Since there are over 100,000 emission lines within the spectral range 220 to 460 nm, frequently more than one emission line will lie within the step-scanned range, i.e 0.08 nm, used. It is therefore necessary to search for all lines within the recorded spectrum and to identify the line of interest. The approach adopted is based on the smoothing and differentiation procedure of Savitsky and Golay (32). The processed data on tabulated wavelengths, peak-heights and background corrected

peak-heights are printed for all identified lines after each spectrum is scanned. Corrected peak-heights for standards are stored for further processing. When all standards have been examined standard calibrations, fitted to quadratics, are established. Samples are analysed by interpolation from these calibration curves.

6.2.3 Determination of Single Wavelengths

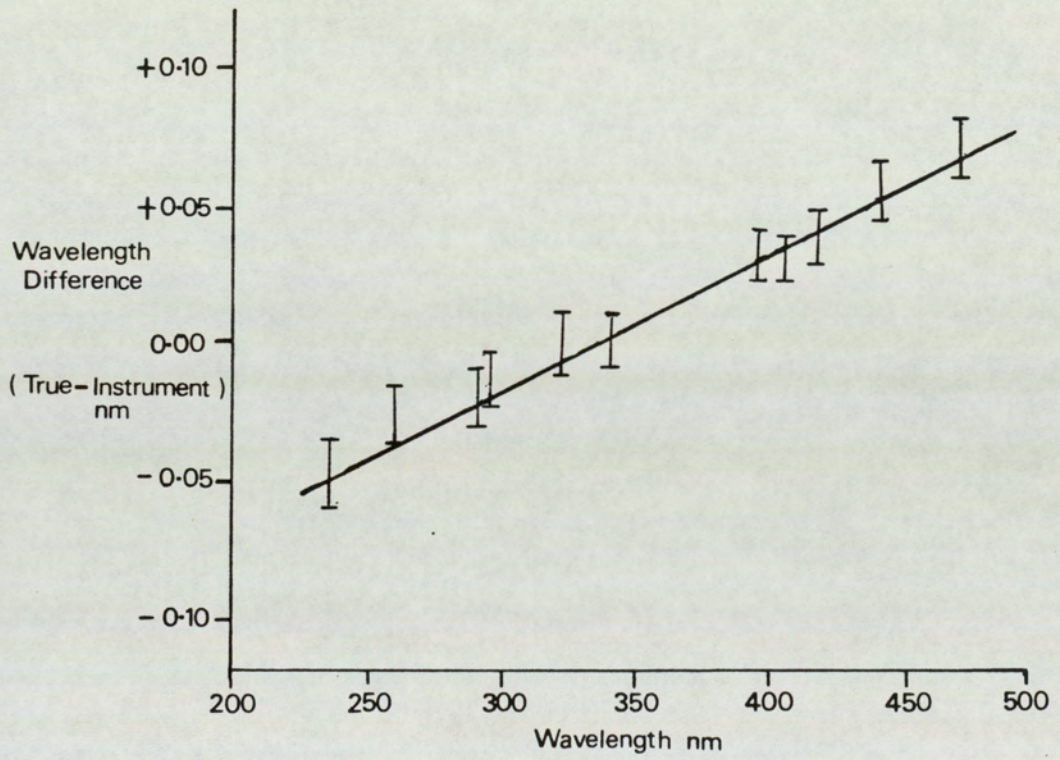
In cases where a single element is to be determined an improvement in precision of spectral intensity measurement (typically <1% RSD) can be achieved by taking longer integration times (>5 sec) with the monochromator aligned on the peak-height wavelength position of the sought element.

6.2.4 Spectrometer Wavelength Calibration

In order to retain accuracy of spectral line identification, wavelength calibration is carried out at monthly intervals. A standard solution of Al, Ga and Ba (each at 100 µg/ml concentration) is introduced into the plasma and eleven spectral lines between 250 nm and 490 nm examined. A linear wavelength difference plot is constructed which can then be used for correcting apparent wavelengths for other lines. Such data are stored in the Analysis File. A typical example of the calibration is shown in Fig. 6.3.

FIG. 6.3

WAVELENGTH CALIBRATION



Error bars give the range in Wavelength Difference
obtained from 5 replicate spectral scans.

6.3 Assessment of Instrumental Performance

Several parameters e.g optical performance, mechanical performance, sensitivity, precision and accuracy, were examined in order to evaluate the overall ability of the system to identify correctly and quantify emission lines.

The dispersion and practical resolution were evaluated by recording the spectrum of a Ti solution (10 µg/ml) over the range 322.700 to 322.950 nm.

Mechanical errors associated with the wavelength drive mechanisms of analytical instruments can influence the way in which the various systems can locate accurately and reproducibly spectral lines. This was examined by conducting replicate analyses for ten elements in solution. At each wavelength six measurements were performed from which the mean value and standard deviation about the mean were derived.

Precision was examined by conducting five replicate analyses of multi-element solutions prepared from BDH 'SPECTROSOL' grade standards.

To demonstrate the accuracy of the system the boron control sample R23 was analysed for trace elements. The chemical treatment used was described in Section 5.3.

Limits of detection (LOD) for fifteen elements were calculated as described in Section 5.4.

6.4 Results and Discussion

Unequivocal identification of emission lines solely by wavelength or position in the spectrum requires that the optical quality of the spectrometer and the mechanical performance of the scanning system should be the best achievable thereby minimising the possibility of mis-identification. The resolution and dispersion of the scanning system permit lines 0.02 nm apart to be resolved satisfactorily. Line mis-identification arises primarily from two causes. In the first case the expected line is absent and a second line is incorrectly taken for measurement. If the difference between the wavelength of the observed line and the expected wavelength is significant in comparison with the precision of the wavelength setting, the second line will be rejected. As shown in Table 6.2 the standard deviation of wavelength position obtained from replicate multi-element spectral scans was generally less than 0.015 nm. Thus the peak search range was taken as ± 0.04 nm which is equal to a value corresponding with the 99% confidence limits. In the second case both expected and interfering lines are observed. In this case the second line is automatically rejected if it is outside the range defined above. If both are within the range, the one furthest away from the expected position is rejected. Poor mechanical performance arises mainly from the "free-play" in the split sine-bar carriage located on the lead screw of the spectrometer

TABLE 6.2

MECHANICAL PERFORMANCE

Element	True Wavelength (nm)	Mean Difference from the true wavelength (nm) ^(a)	Standard Deviation (nm)
Mn	257.610	- 0.015	0.009
Fe	259.940	- 0.001	0.006
Cr	283.563	+ 0.009	0.014
Mg	285.210	+ 0.008	0.004
Ni	305.082	- 0.014	0.006
V	309.311	+ 0.003	0.007
Ca	317.933	- 0.004	0.007
Cu	327.396	+ 0.021	0.013
La	333.749	+ 0.005	0.007
Ti	338.376	- 0.001	0.007

(a) Difference = True wavelength - measured wavelength

Five replicate analyses were conducted.

drive mechanism which explains the commonly observed feature of overshooting of spectral lines with subsequent loss of wavelength accuracy. This problem was overcome by reducing the approach speed in the vicinity of the spectral line but this has the disadvantage of increasing the analysis time. This limitation of operational speed is apparent in the Spex 1700, 1800 and 1269 series of spectrometers which use the sine bar and lead screw configurations as shown in Fig. 6.4. To make better use of the good optical performance of the spectrometer, a modification to the software was made enabling spectral lines within peak search scans to be selected as the true line of interest. This rejects any interfering line provided it is resolved from the line of interest. Although this requires greater operator involvement it has advantages when complex spectra are examined. Whilst the elapsed time for analysis is not of great significance the disproportionately large amount of operator time is a disadvantage. This problem was overcome by using a commercial automated sample changer.

Table 6.3 shows that detection limits range between 0.001 to 0.1 $\mu\text{g/ml}$ and are comparable with those published elsewhere (38). As shown in Table 6.4 the precision of photo-electric recording is 1 to 2% RSD, and, as shown in Table 6.5 when applied to a boron control sample the technique is free from bias.

One major advantage of photo-electric recording is that a linear calibration exists over a wide range of concentration (10^6) thereby permitting major, minor and trace elements to be

FIG. 6.4

SPEX 1802 WAVELENGTH DRIVE MECHANISM

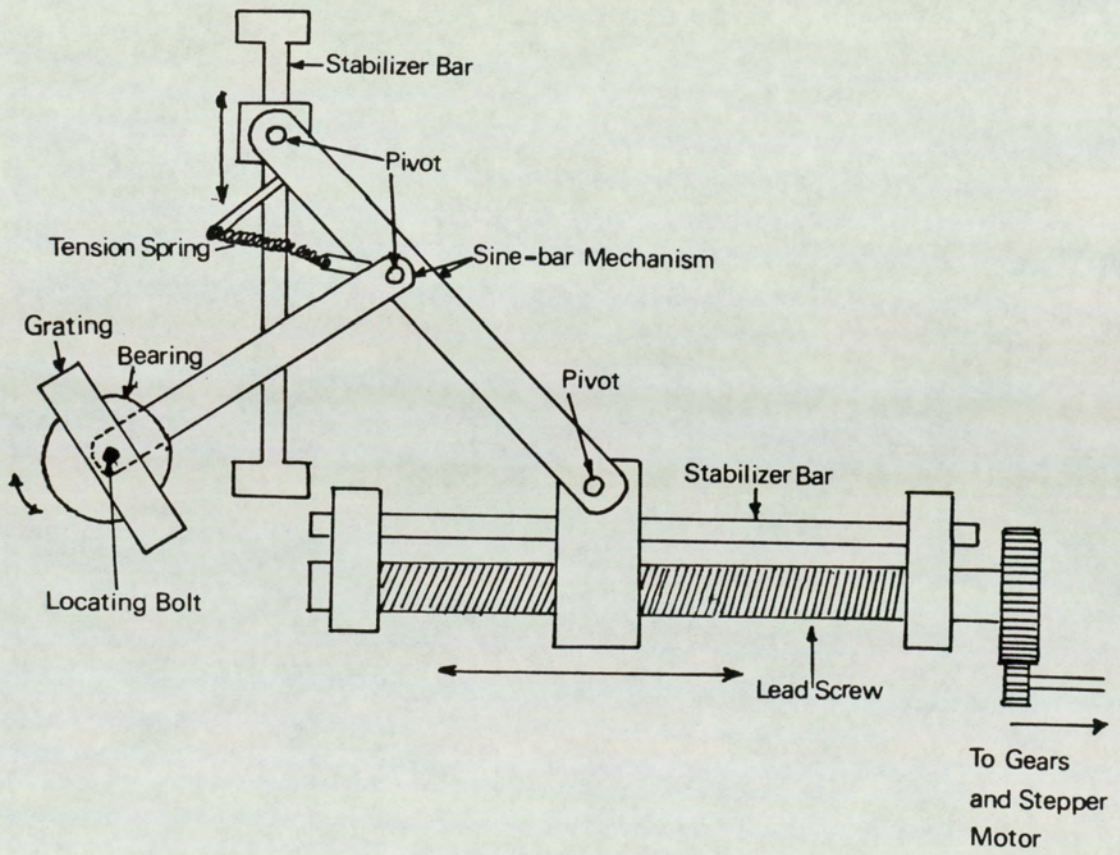


TABLE 6.3

DETECTION LIMITS

Element	Wavelength nm	Limits of Detection $\mu\text{g/ml}$	
		Observed	Tabulated(38)
Zn	213.856	0.010	0.002
Co	221.647	0.050	0.010
Mg	257.610	0.0039	0.0014
Fe	259.940	0.0059	0.0062
Cr	283.563	0.0066	0.0071
Mg	285.210	0.0013	0.0016
Ni	305.082	0.034	-
V	309.311	0.0025	0.0050
Ca	317.933	0.0102	0.010
Cu	327.396	0.0041	0.0097
La	333.749	0.027	0.010
Ti	338.376	0.0019	0.0081
Al	396.122	0.080	0.028
Ga	403.284	0.113	0.111
Ga	417.231	0.052	0.066
Ba	455.477	0.0015	0.0013
Ba	493.409	0.0034	0.0029

TABLE 6.4

PRECISION FOR FIVE REPLICATE
ANALYSES

Element	Expected Concentration $\mu\text{g/ml}$	Precision % RSD
Mn	1.0	1.5
	2.0	0.7
Fe	1.0	0.8
	2.0	0.7
Cr	1.0	1.7
	2.0	1.5
Mg	1.0	0.6
	2.0	0.3
Ni	1.0	1.0
	2.0	1.0
V	0.5	1.9
	5.0	0.4
Cu	1.0	0.7
	2.0	1.7
La	1.0	1.3
	2.0	2.4
Ti	1.0	0.9
	2.0	0.3

TABLE 6.5

ANALYSIS OF BORON SAMPLE R23

Element	Concentration ppm	
	Reference Value	Sequential ICP/AES
Ca	270 ± 58	256 ± 29
Cu	28 ± 4	30 ± 3
Ni	33 ± 8	34 ± 2
Mo	172 ± 45	165 ± 20
Mg	120 ± 24	110 ± 15
Cr	42 ± 8	44 ± 3
La	6 ± 2	5.6 ± 0.8
Fe	1000 ± 140	960 ± 120
Mn	660 ± 110	660 ± 28
Cd	<5	<5
Pb	<2	<2

Errors quoted as 95% confidence limits derived from 3 replicate analyses.

measured sequentially in the same solution without pre-treatment although each additional element requires a further volume of sample. Where this is a limitation it can be overcome by the use of a recirculating nebuliser which will be described in Chapter 8.

6.5 Conclusions

A sequential scanning monochromator system was constructed which is capable of accurate trace multi-element analysis on solutions with a precision of 1 to 2% RSD. Its high sensitivity (typically LOD <0.01 µg/ml) and large dynamic range (10^6) provide a considerable analytical capability. Optical performance, in terms of line resolution and identification, is considerably better than most commercial systems, and this, combined with its flexibility, provides a versatile tool for a range of analytical problems. The system has been used extensively during the last two years for routine boron analysis.

The mechanical performance limits the speed of operation of the system. Although this cannot be readily improved it is not a major disadvantage within the present requirements.

CHAPTER 7

COMPARISON OF SPECTROGRAPHIC AND SCANNING

MONOCHROMATOR SYSTEMS

During the last three decades, photo-electric recording in emission spectroscopy has eclipsed photographic recording to the extent that very few laboratories use the latter and many ICP-Scanning monochromator systems employing the former mode of detection are available commercially. When the number of elements being sought is not large and also when spectral line interferences are not significant, this approach is probably the more suitable. However, when analysing for trace elements in boron, where the number of elements being sought is large and the concentration of impurity elements can vary between 1 and 1000 ppm, then this approach may have its limitations. In this event, resort is made to photographic recording in which the whole emission spectrum is recorded permanently and can be examined in detail subsequently. In order to determine the more appropriate method of specific analyses, the relative performances of the two systems were assessed in terms of detection limits, precision, accuracy, sample economy, optical dispersion, optical resolution and wavelength reproducibility.

7.1 Experimental

The spectrographic and scanning monochromator systems and operating conditions have been described in Chapters 5 and 6 respectively.

Dispersion and practical resolution were compared by recording the Ti spectra of a 10 $\mu\text{g/ml}$ solution. With the scanning monochromator only that part of the spectrum in the range 322.700 to 322.950 nm was recorded, whereas for the spectrographic recording the whole spectrum was recorded but only the same wavelength region scanned using the microdensitometer.

Errors associated with mechanical operation, which can affect final accuracy and precision, were evaluated using replicate analyses for ten elements in solution. At each wavelength six measurements were performed, from which the mean and standard deviations about the mean were derived.

Using the same spectral data, limits of detection (LOD) (calculated as described in Section 5.4) and the precision of replicate determinations were derived for each system. The quantities of sample consumed and the times for analyses were also recorded. The accuracy was tested by comparing the results obtained from the analysis of boron sample R23, as given in Chapters 5 and 6, with expected values averaged from determinations made by other methods.

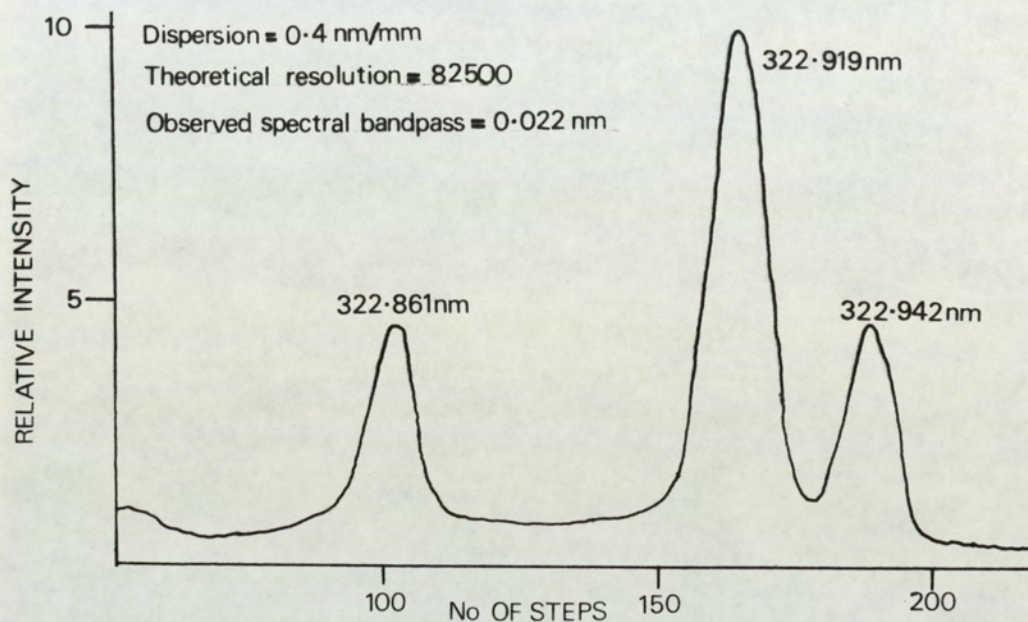
7.2 Results and Discussion

As shown in Fig. 7.1(a) and 7.1(b), the resolutions and dispersions of the two systems are similar; lines 0.02 nm apart can be resolved satisfactorily by both instruments and the

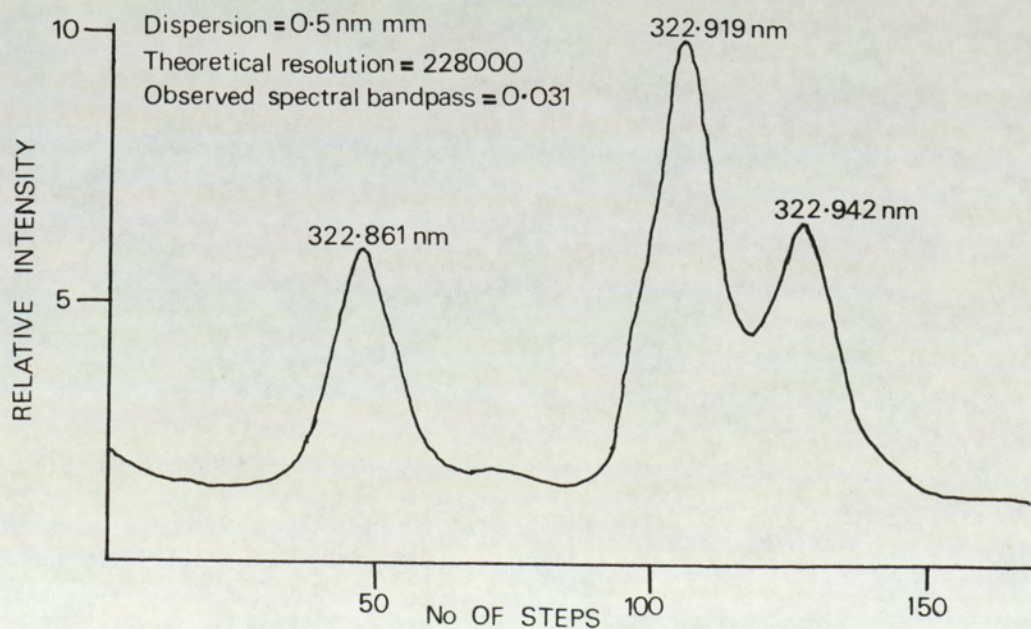
FIG. 7.1

SPECTRAL SCANS OF A TITANIUM SOLUTION (10 μ g/ml)

(a) RECORDED WITH THE SCANNING MONOCHROMATOR



(b) RECORDED WITH THE SPECTROGRAPH
AND MICRODENSITOMETER



line half-widths correspond to the best resolution given by Boumans (39). As discussed in Section 6.4 the primary cause of incorrect identification of a spectral line arises when other more prominent lines appear within the wavelength limits that define the criteria for rejection. Table 7.1 shows that the microdensitometer locates lines more precisely than the scanning monochromator system, and as the criteria for line rejection are based on wavelength reproducibility, the former is therefore the more suitable for correct identification of lines, especially in complex spectra.

Spectrographic determination of trace elements requires a single 2 min exposure which permits all lines in the wavelength range 200 to 480 nm to be recorded permanently. Subsequent computer controlled microdensitometer examination requires little manual involvement. Hence, the total time for the spectrographic system relates mainly to spectra acquisition. In contrast, the scanning monochromator requires an additional volume of sample solution and, in the absence of a completely automated sample changing system, the analyst's time is increased for every additional element to be determined. Sample economy can be improved significantly by using a recirculating nebuliser and this is described in Chapter 8.

Table 7.2 shows clearly that photo-electric detection is more sensitive than photographic detection, often by at least an order of magnitude. However, both methods are capable of detecting impurities at the sub- $\mu\text{g/ml}$ level.

TABLE 7.1

Element	True Wavelength (nm)	Mean Difference from true wavelength (nm)		Standard Deviation (nm)	
		Micro densitometry	Scanning Mono-chromator	Micro densitometry	Scanning Mono-chromator
Mn	257.610	+ 0.005	- 0.015	0.002	0.009
Fe	259.940	- 0.001	0.000	0.001	0.006
Cr	283.563	- 0.005	0.009	0.002	0.014
Mg	285.210	- 0.009	+ 0.008	0.002	0.004
Ni	305.082	0.000	- 0.014	0.001	0.006
V	309.311	- 0.004	+ 0.003	0.002	0.007
Ca	317.933	- 0.001	- 0.004	0.002	0.007
Cu	327.396	- 0.001	+ 0.021	0.002	0.013
La	338.376	+ 0.002	- 0.001	0.002	0.007

(a) Difference = True wavelength-measured wavelength

TABLE 7.2

COMPARISON OF SENSITIVITIES

Element	Wavelength nm	Limits of Detection $\mu\text{g/ml}$	
		Photographic Detection	Photoelectric Detection
Mn	257.610	0.041	0.0039
Fe	259.940	0.091	0.0059
Cr	283.563	0.095	0.0066
Mg	285.213	0.011	0.0013
Ni	305.082	0.28	0.034
V	309.311	0.053	0.0025
Ca	317.933	0.164	0.0102
Cu	327.396	0.094	0.0041
La	333.749	0.31	0.027
Ti	338.376	0.069	0.0019

As shown in Table 7.3 the precision of photo-electric recording is in the range 1 to 2% RSD and is better than that of photographic recording, for which it is in the range 5 to 10% RSD.

The results given in Table 7.4 indicate that, within experimental error, both techniques are free from bias. Although the spectrographic recording system is better suited for interpreting complex spectra, once the major constituents have been identified spectrographically and the optimum spectral line identified, the scanning monochromator system can then be used to give better precision. Also, owing to the better sensitivity of photo-electric detection the scanning monochromator gives lower detection limits. The poorer sensitivity for the spectrographic determination of Cd arises from the inferior sensitivity of the photographic plate at this wavelength (228.802 nm).

7.3 Conclusions

Although during the last three decades photographic recording of emission spectra has been superseded largely by scanning and direct reading methods, there are instances, especially in trace multi-element analysis, where there are advantages in using the former. The main advantage is that all spectral data in the range 200 to 480 nm can be recorded permanently in a single exposure that can be interpreted later using computer controlled microdensitometry. Hence the method still provides an economical means of analysis. However, photo-electric detection has superior sensitivity and precision. Consequently, to obtain overall best results both systems should be used as clearly their performances are complementary.

TABLE 7.3

COMPARISON OF PRECISION

Element	Expected Concentration µg/ml	Precision (A)	
		Spectrographic Analysis	Spectrophotometric Analysis
Mn	1.0	5.8	1.5
	2.0	6.4	0.7
Fe	1.0	6.1	0.8
	2.0	10.1	0.7
Cr	1.0	4.5	1.7
	2.0	10.1	1.5
Mg	1.0	5.1	0.6
	2.0	7.2	0.3
Ni	1.0	11.7	1.0
	2.0	12.6	1.0
V	1.0	5.5	1.9
	2.0	10.1	0.4
Ca	1.0	3.1	0.6
	2.0	10.5	0.5
Cu	1.0	10.6	0.7
	2.0	10.0	1.7
La	1.0	8.2	1.3
	2.0	10.4	2.4
Ti	1.0	2.8	0.9
	2.0	10.7	0.3

(A) Precision = (Standard deviation/mean) x 100 where the standard deviation is based on 5 determinations.

TABLE 7.4

ANALYSIS OF BORON SAMPLE R23

Element	Expected Value ppm	Spectrographic Analysis ppm	Spectrophotometric Analysis ppm
Al	295	280 ± 60	289 ± 18
Ca	250	270 ± 50	256 ± 29
Cu	29	29 ± 3	30 ± 3
Ni	33	36 ± 5	34 ± 2
Mo	161	165 ± 30	165 ± 20
Mg	110	110 ± 15	110 ± 15
Cr	44	41 ± 3	44 ± 3
La	5.5	6.0 ± 1.8	5.6 ± 0.8
Fe	1070	1100 ± 140	960 ± 120
Mn	670	680 ± 40	660 ± 28
Cd	<5	<100	<5
Pb	<2	<10	<2

Errors quoted as 95% confidence limits based on three determinations.

CHAPTER 8

DEVELOPMENT OF A RECIRCULATING PNEUMATIC NEBULISER FOR SMALL SAMPLE VOLUMES

As described in Chapter 3 the most common method of introducing sample solutions into an ICP source is to generate a fine aerosol by pneumatic nebulisation. With conventional nebulisers, <2% of the solution actually enters the source, the remainder, which consists of coarse spray is trapped in the spray chamber and allowed to drain to waste. This poor efficiency in sample transfer is normally of little importance since the amount of solution available is unlimited. However, there are occasions when the volume is limited by the amount of sample available or by the amount that can be dissolved. Furthermore, with the application of sequential multi-element analysis using the scanning monochromator system, there is a need to nebulise a sample for long uninterrupted periods of time. Obviously a considerable gain in efficiency in sample use can be achieved by recovering the bulk of the solution which normally drains to waste and recycling to the nebuliser.

The use of pneumatic nebulisers where the waste solution is recovered is well known (40, 41) and was used extensively in flame photometry up to 30 years ago, when their use declined, probably because the inconvenience of changing samples became more important as rapid monochromator and photo-electric detection systems took over from photographic

recording. Many of the systems used metal components, most required a considerable volume of solution, 10 to 20 ml, and all required a high gas flow which is not suitable with ICP. Novak (42) constructed a recirculating fixed cross-flow nebuliser for use in ICP/AES on the Rauterberg and Knippenberg design (43) but this also required an inhibitive large volume of solution and its construction would require the service of a highly skilled glassblower. Since no reference to a system using commercially available nebulisers using small volumes of sample for ICP/AES was identified at the outset of this work, a recirculating nebuliser suitable for use with an ICP source was developed.

8.1 Design Requirements

A number of factors are important in designing nebuliser spray chambers. Nebulisers for ICP sources are made to fine tolerances because of the limited volume of gas available for nebulisation and it was expected that consistent performance would be most easily achieved by using a commercial nebuliser such as the Meinhard glass concentric nebuliser. For the analysis of boron carbide the maximum volume of sample available was 2 ml and to operate on this volume both the hold up of sample in the spray chamber and the drainage time should be small. The spray chamber design should also allow for a rapid and effective flushing to eliminate memory effects from a previous sample. Most ICP sources are adversely affected by the ingress of air and it is necessary to prevent air entering the spray chamber during sample changeover and to provide an uninterrupted flow of argon to the plasma to maintain stability. Finally the precision and

sensitivity of the system should not be significantly worse than a conventional nebuliser spray chamber, and the system should be easy to operate routinely.

8.2 Prototype Recirculation Nebuliser

Figs. 8.1 and 8.2 show schematically the design of the prototype recirculating nebuliser. Rapid return of waste solution to the nebuliser inlet is aided by moving the nebuliser and spray chamber vertically. The Meinhard concentric nebuliser operates efficiently in this position, and is small enough to be readily accommodated within the spray chamber. The nebuliser sprays into a central inner tube which traps the bulk of the coarse spray and the fine spray passes through a hole at the top of this tube to the plasma. Rapid drainage is assisted by trapping most of the coarse spray inside the central tube, by angling the bottom edge of this tube and by coating all the interior surfaces with a silicone film. Efficient cleaning of the system between sample nebulisation is achieved by filling the spray chamber completely with deionised water with argon passing through the nebuliser during the earlier stages of filling.

Fig. 8.2 shows the purpose of the two sets of valve systems. One system, consisting of a drain valve and water inlet valve is used for rapid flushing and flooding of the spray chamber. The second system is used for controlling the argon by-pass system which allows the ICP source to be sustained during sample changeover.

FIG. 8.1

PROTOTYPE RECIRCULATING NEBULISER

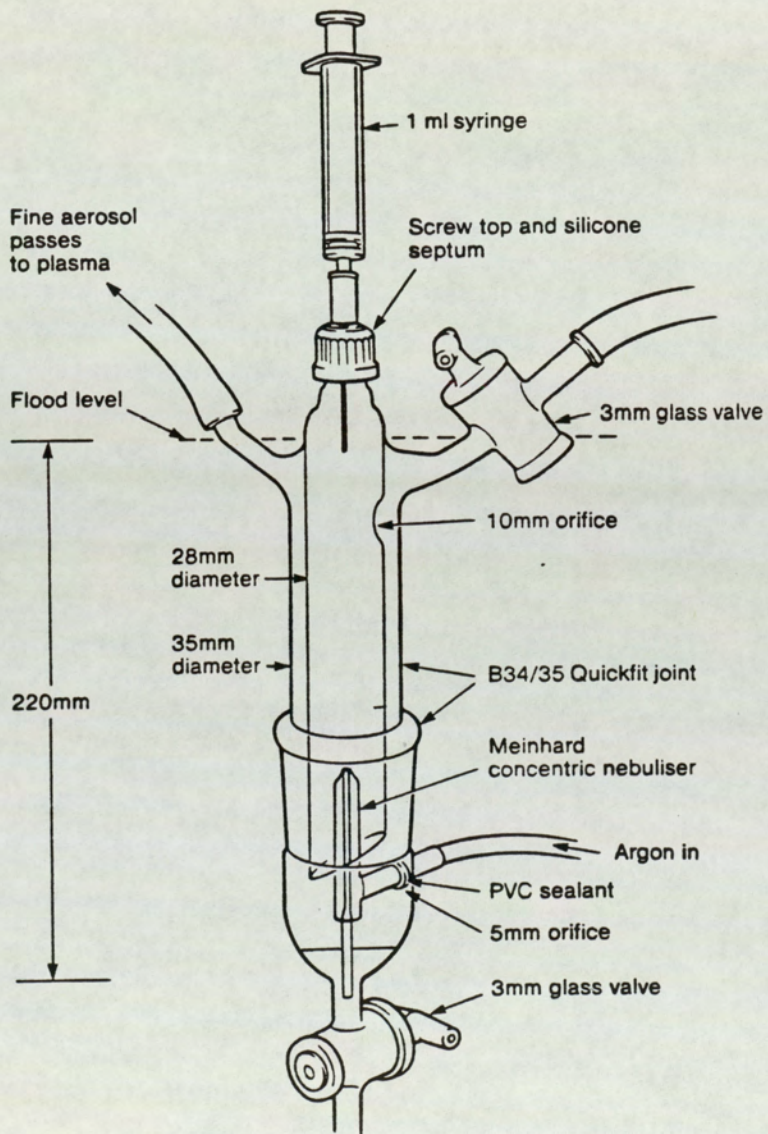
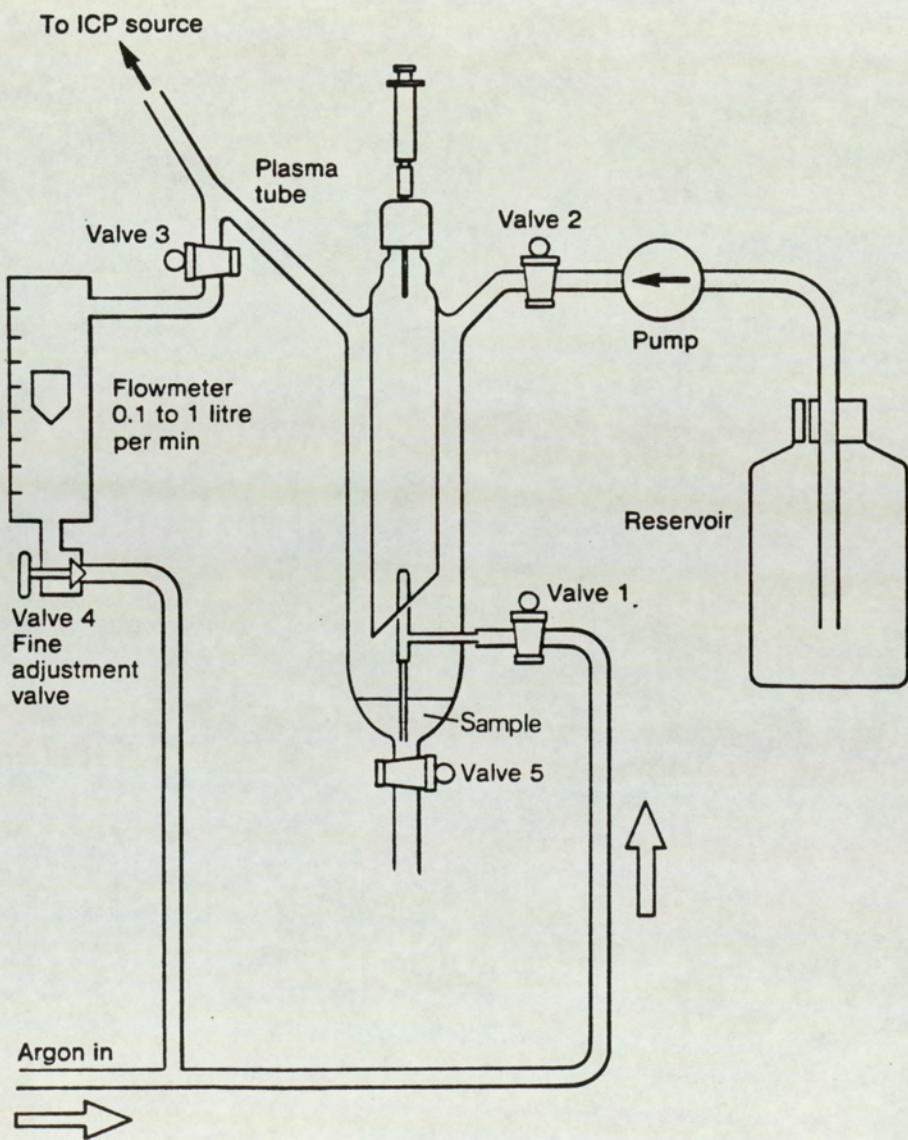


FIG. 8.2

SCHEMATIC REPRESENTATION SHOWING VALVE AND ARGON BY-PASS SYSTEMS



8.2.1. Performances

The scanning monochromator system described in Chapter 6 was used to evaluate the nebuliser. With the exception of nebuliser conditions, all other ICP source and spectrometer conditions were as described previously. For comparative purposes a conventional nebuliser was required and this was provided by removing the Meinhard concentric nebuliser (Model TR-30-A3) from the recirculating system and fitting it to a Scott-type spray chamber.

The nebulising characteristics of the recirculating and conventional nebulisers were compared by measuring the sensitivity, the limit of detection and short term precision of each of the three elements, Zr, Ti and Cu. As shown in Table 8.1 no significant difference between the two systems was observed. Thus the quantity and size of spray reaching the plasma from either nebuliser system is not sufficiently different to affect the performance of the ICP source.

Using a recirculating nebuliser the efficiency with which memory effects are overcome is important. This was tested by monitoring the level of sample present after each flushing and flooding cycle. This was carried out by recording the response of the 327.926 nm Zr emission from 1 ml of a 100 µg/ml solution. After a flooding and flushing cycle, the response from a blank solution was also recorded. This was repeated until a blank level reading was re-attained. The results show a decontamination factor of 5×10^3 , i.e the actual Zr content of

TABLE 8.1

A COMPARISON OF DETECTION LIMITS AND STABILITY ACHIEVED
BY A CONVENTIONAL AND RECIRCULATING NEBULISERS

Element	Wavelength nm	Detection Limit µg/ml		Short Term Precision* (mean conc 0.125 µg/ml)	
		A	B	A	B
Zr	343.823	0.02	0.02	0.0026	0.0020
Ti	338.376	0.01	0.02	0.0078	0.0077
Cu	327.396	0.003	0.004	0.0026	0.0034

A = using the recirculating nebuliser

B = using a conventional nebuliser.

* Short term precision is defined as the standard deviation of 50 0.1 sec integrations.

the 1 ml blank solution recorded after the first wash was 0.02 $\mu\text{g/ml}$. Thus in most practical cases, two washing and flooding cycles would overcome memory effects.

The short term precision described above does not take into consideration the error associated with sample change-over. This is particularly so in the recirculating system where injection of sample and efficiency in drainage can significantly contribute to precision. The precision of the nebuliser systems were compared by making ten replicate determinations of a 2.5 $\mu\text{g/ml}$ Zr solution. The standard deviations obtained were 0.06 $\mu\text{g/ml}$ and 0.05 $\mu\text{g/ml}$ for the recirculating and conventional nebulisers respectively which are not significantly different.

8.2.2 Appraisal of the Prototype Recirculating Nebuliser

The prototype nebuliser operates successfully for up to ten minutes with a volume as small as 1 ml. Its performance in terms of precision and sensitivity, is not significantly different from a conventional system. The working procedure devised has reduced the memory effects to insignificant levels. The prototype system found increasing use with both ICP systems. However, its use was cumbersome and involved a large number of manual procedures in the sample change-over process. Hence, an automated version which used a microprocessor and a system of electronic valves was constructed.

8.3 Development of a Microprocessor Controlled Version

The system is shown in Fig. 8.3 and consists of a nebuliser control unit and the nebulising unit. A schematic representation of the nebulising unit is given in Figure 8.4. Essentially the nebuliser, spray chamber and argon by-pass system remain unchanged from those of the prototype as the initial design proved adequate for nebulising small volumes, e.g 1 to 2 ml. Modifications include four solenoid valves, a water pump and three optical sensors. Solenoid valves were constructed from PTFE thereby minimising contamination of sample or de-ionized water. Similarly optical sensors rather than conductance devices were used to monitor fluid levels. A standard Lucas 10SJ 12V water pump was used to provide a flowrate of 1 l/min for flushing and flooding the spray chamber.

LED (light emitting diode) sensors, manufactured by Hewlett Packard, were fitted with a photo-transistor and a lens which was taken from a prefocussed light bulb. By fitting the lens a near parallel beam of light is obtained rather than the divergent beam normally associated with LEDs. The light beam passes into the glass spray chamber. When the chamber is empty the light is diffused, and very little falls on to the photo-transistor, but when the tube is filled, the fluid acts as a magnifier and sufficient light reaches the photo-transistor to be detected. Both the maximum fill and drain sensors operate on this principle. The froth sensor, positioned around the middle of the spray chamber, senses the froth produced by the argon

FIG. 8.3

MICROPROCESSOR CONTROLLED RECIRCULATING NEBULISER

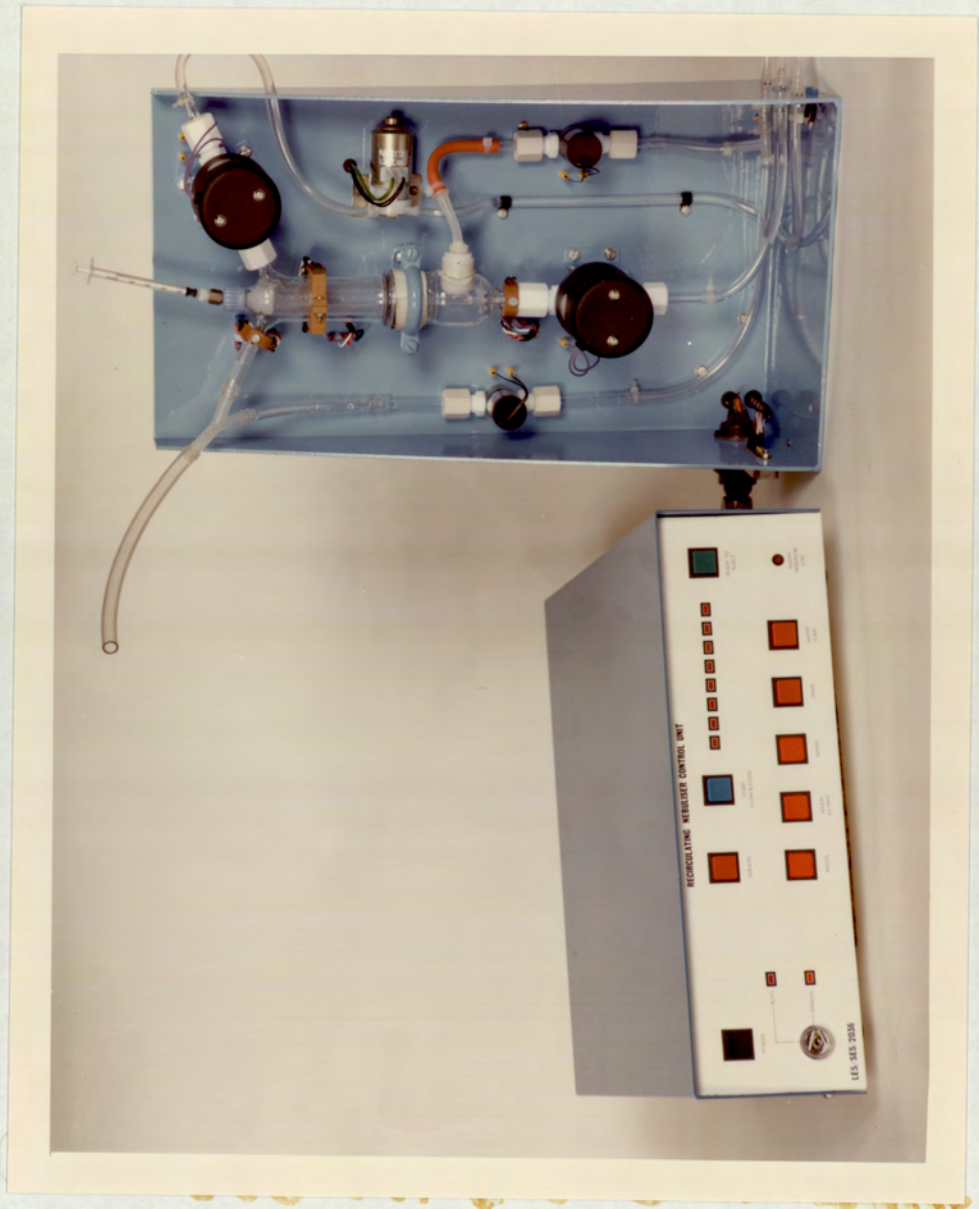
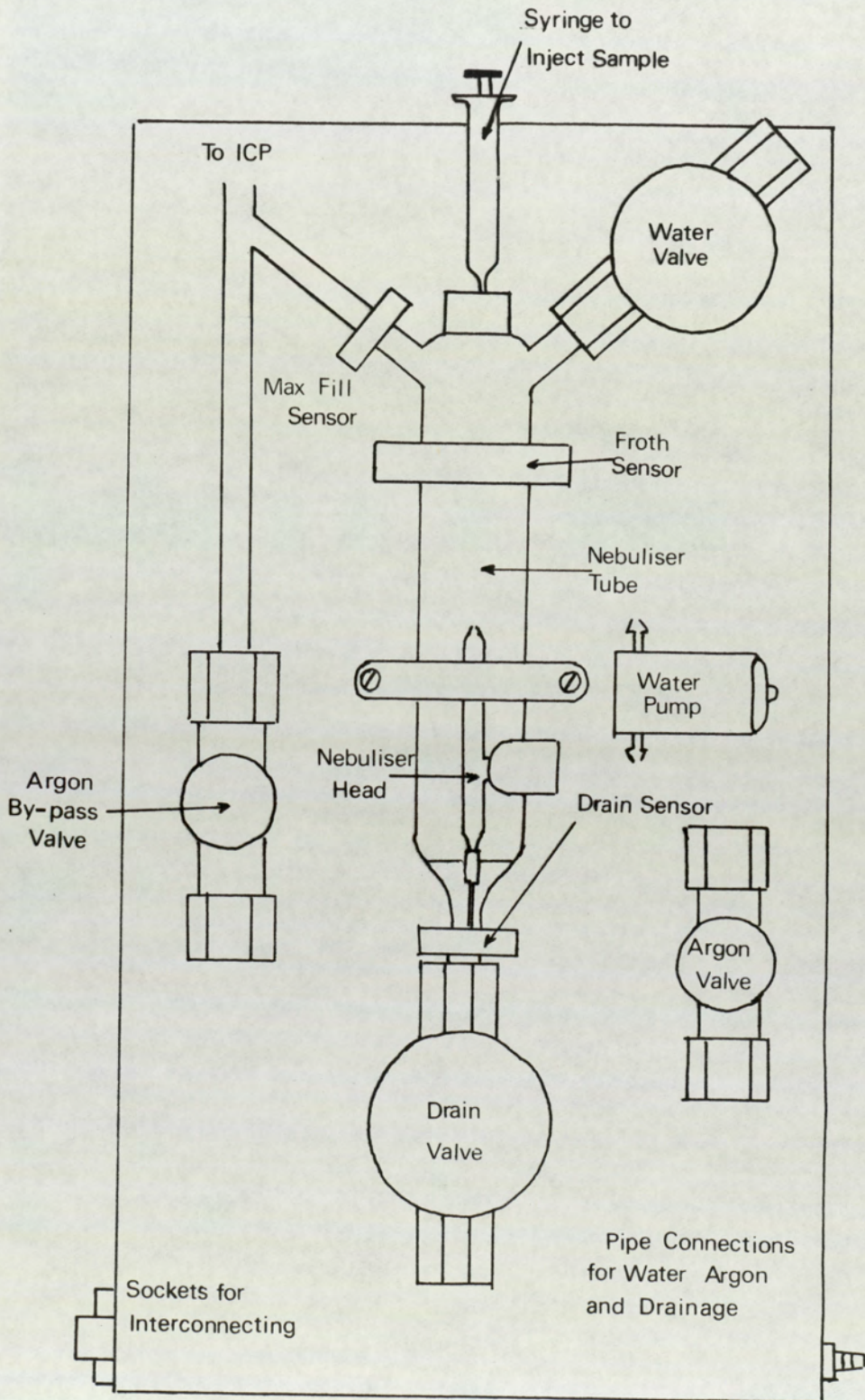


FIG. 8.4

SCHEMATIC DIAGRAM OF NEBULISING UNIT



stream as it rises up during the flush and flood sequence and then signals the microprocessor to shut off the argon supply to the nebuliser. The froth sensor uses a similar photo-transistor and circuitry as the drain sensor. Since an LED could not be used because of the wider separation of the light source and photo-transistor an infra-red emitting diode was used. The maximum fill sensor is positioned around the output arm of the spray chamber and signals when the tube has completely filled with water during the flush and flood sequence.

The nebuliser unit is connected to the control unit by two multi-core cables, enabling remote operation. The control unit contains the power supplies, microprocessor module, sensor interface circuitry and the valve pump interface circuitry. Push button controls are located on the front of the panel of the control system. Included is a key switch which enables the unit to operate in automatic or manual mode. In automatic mode, the control unit responds to two push buttons; one sets the system in a sample-nebulising mode and the other initiates the flush and flood cycle for sample change-over leaving the system in a status ready to inject the next sample. The status of the auto-flushing cycle is displayed on a series of eight LEDs. In manual mode the operator has complete control over valves and pump by the push button switches. The CDP microprocessor is programmed in hexadecimal.

Microprocessor control of the sample change-over process permits a change-over period of about 3 min. As a result of automating this process the system can be used in routine analyses. By replacing the sample introduction syringe with a thin glass tube coupled to a peristaltic pump and autosampler, and linking the nebuliser control unit with the ICP computer system interface, a totally automated system can be obtained.

8.4 Nebulisation Characteristics of the Recirculating Nebuliser

Initially the recirculating nebuliser was used for spectrographic analysis which readily permitted internal standardisation of the sample solutions and hence provided correction for any variation in the nebuliser efficiency. Subsequently, the system was then used extensively for sequential ICP analysis using the scanning monochromator system and generally without internal standardisation. In this situation good short and long term stabilities are essential. The short term stability, or noise, is more directly an aspect of the Meinhard concentric nebuliser performance rather than of the design of spray chamber, and has not been found to vary significantly between the recirculating and conventional configurations. Both variation in temperature and solvent evaporation can cause signal drift i.e gradual change in the signal intensity with time. Variation in solution temperature will result in a change in sample viscosity and hence a change in nebulisation efficiency. Gradual evaporation of water from the sample solution into the argon gas stream results in sample concentration. In both cases an increase in the emission signal

will be observed. Some dilution of the solution to be nebulised occurs from incomplete drainage of the nebuliser spray chamber after flooding. It therefore was necessary to define the practical limitations of the recirculating nebuliser when used with a scanning monochromator without the benefit of an internal standard.

8.4.1 Results and Discussion

A standard solution containing known concentrations of six elements was introduced into the plasma by first using the recirculating nebuliser and then the conventional system. The limits of detection were calculated as before. The results, given in Table 8.2, show no significant difference between the two systems.

The precision of the ICP is also largely determined by the performance of the nebuliser. However, in the case of the recirculating nebuliser some water remains within the spray chamber after washing and draining and this will dilute the sample solution. In a carefully designed system the volume of retained water is about 0.1 ml, causing a 5% dilution of the sample solution. Variation in this volume will be reflected in the precision obtained from replicate determinations on a number of sample portions. The results, given in Table 8.3, indicate that the precision obtained was not significantly worse than that obtained using a conventional nebuliser. In this case, since both sample and standards are similarly diluted, the accuracy of determination is not effected by this dilution.

TABLE 8.2
COMPARISON OF DETECTION LIMITS

Element	Wavelength nm	Detection Limit ng/ml	
		Conventional	Recirculating
Mg	279.553	0.16	0.12
Cu	324.754	2.3	2.0
Zr	343.823	3.3	2.4
Y	371.030	1.5	1.3
Ca	393.366	0.13	0.11
La	408.672	4.5	5.2

TABLE 8.3
COMPARISON OF PRECISION FOR FIVE REPLICATE
ANALYSES ON A STANDARD MULTI-ELEMENT SOLUTION

Element	Expected Concentration µg/ml	Observed Concentration µg/ml		Relative Standard Deviation %	
		A	B	A	B
Mg	2.00	2.03	2.06	1.7	3.1
Cu	5.00	4.93	5.09	2.6	3.3
Zr	5.00	5.08	5.26	2.3	2.8
Y	5.00	4.99	4.96	2.6	2.3
Ca	2.00	1.94	1.95	3.4	1.6
La	50.00	48.79	49.63	3.2	2.2

A = Conventional Nebuliser

B = Recirculating Nebuliser

As found with the prototype system a decontamination factor of 5×10^3 was observed for successive flush and flood cycles. In many cases where samples of similar concentrations are being analysed a single washing cycle is sufficient and rarely are two or more cycles necessary to eliminate cross-contamination completely.

Although experience has indicated that the recirculating nebuliser provides a stable emission signal, it may be susceptible to some cumulative effects which are not present in conventional nebulisers. Carpenter (44) has found that there is a steady increase in signal with time. This could arise from differences in the operating parameters. Two possible factors which explain this difference are changes in temperature or the humidity of the argon. In view of the large surface area provided during nebulisation, the use of dry argon could cause significant evaporation of the sample solution with a consequent increase in concentration of the sample with time. Increasing the temperature of the solution not only increases the rate of evaporation but also affects the rate of nebulisation because of reduced viscosity. The extent of these effects was studied by nebulising solutions with dry and humidified argon at both ambient temperature (20°C) and at 35°C. The temperature of 35°C represents that which the spray chamber might attain if it were placed within the plasma enclosure. After 20 min nebulisation the remaining sample solution was analysed using a conventional nebuliser. The temperature of the solution was monitored continuously during the nebulisation period with a thermistor sealed into the base of the spray chamber.

To assess the stability of the system at ambient temperature a 2 ml portion of a 10 $\mu\text{g}/\text{ml}$ Cu solution was injected into the nebuliser and both the emission signal at 324.756 nm and the solution temperature were recorded over a period of 20 min. The results of the mean of three runs using dry argon are shown in Figs. 8.5a and 8.5b. The initial drop in signal is consistent with the expected dilution of the sample with 0.1 ml of de-ionized water remaining in the chamber after washing. Subsequently no drift in signal is observed; the relative standard deviation of the observed signal being 1.5%. The drop in solution temperature can be attributed to cooling of the system by adiabatic expansion of argon at the nebuliser. Cooling of the solution by evaporation could cause a similar effect, but the analysis of the remaining solution, shown in Table 8.4, shows the expected dilution of sample, rather than a concentration of sample that would be expected if significant evaporation was occurring. Thus it does not appear necessary to use wet argon when the spray chamber remains at ambient temperature.

Stability at an elevated temperature was investigated by repeating the experiment with the spray chamber heated externally, to about 35°C, using an infra-red lamp. Sample solutions were stored and injected at 22°C, and in this case both dry argon and argon saturated with water were used.

As shown in Figs. 8.6a and 8.6b at 35°C there is a substantial reduction in signal when argon saturated with water vapour is used. This behaviour is also observed with conventional nebulisation. Both curves in Fig. 8.6a are similar

FIG. 8.5

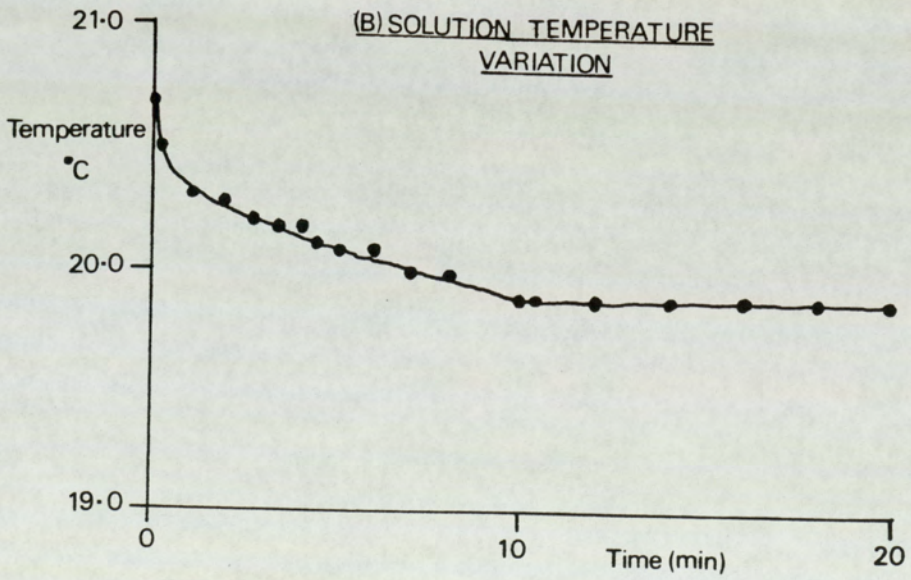
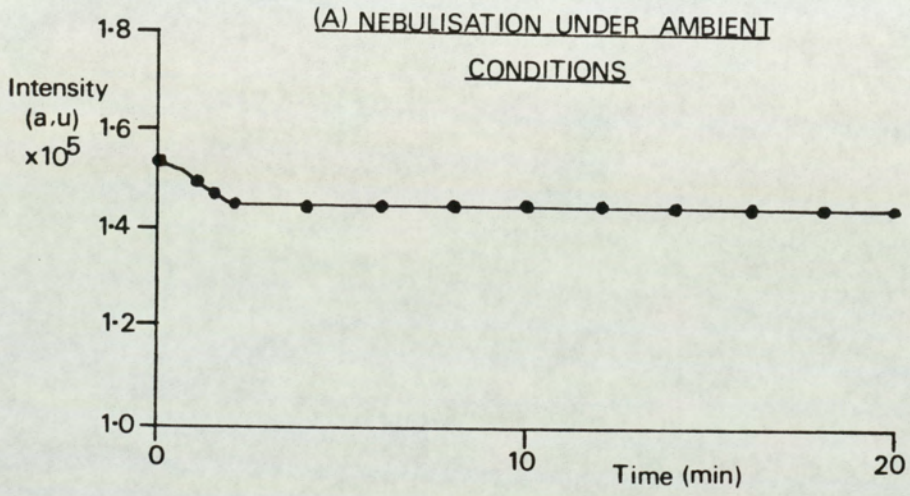
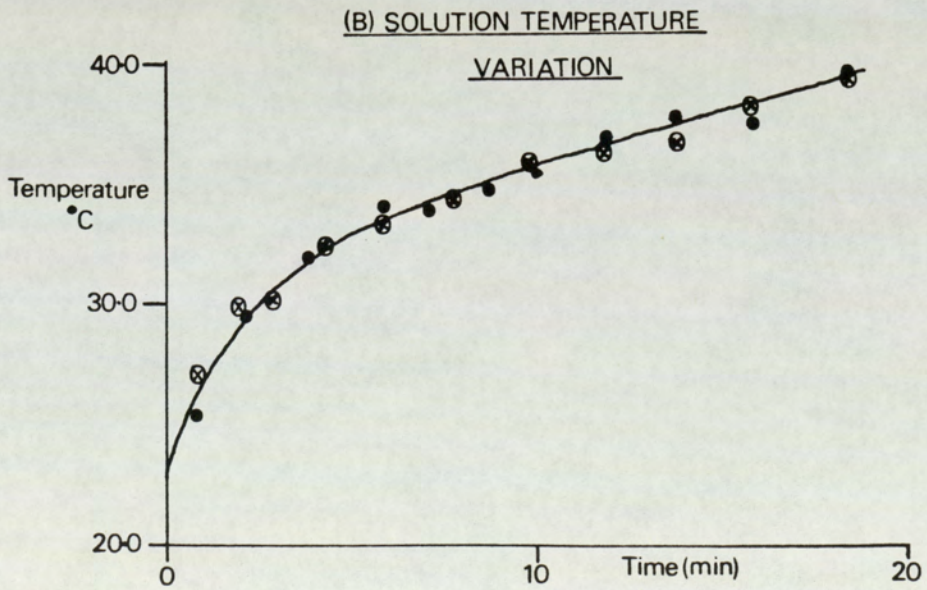
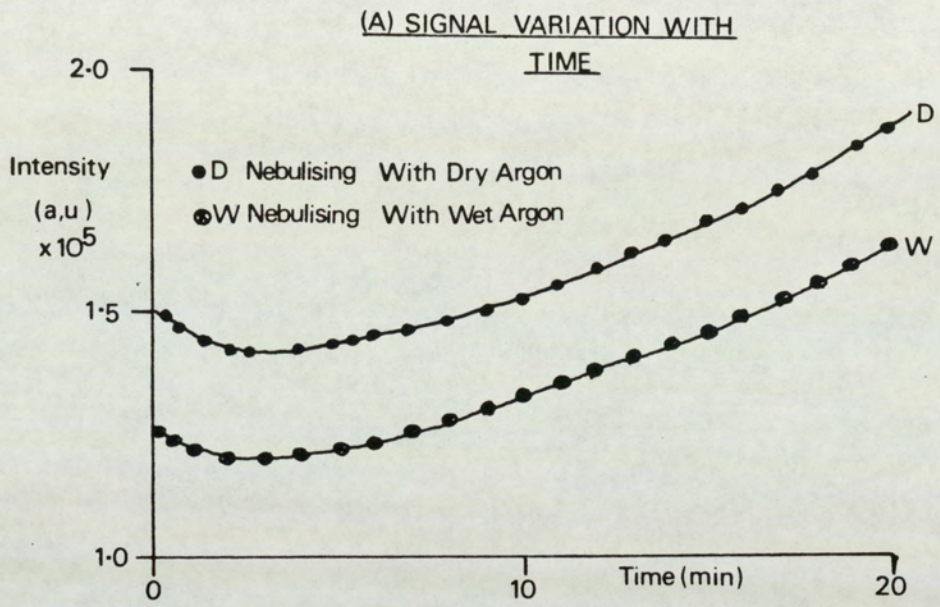


TABLE 8.4

CONCENTRATION OF Cu IN A SAMPLE SOLUTION
AFTER EACH NEBULISATION

Nebulisation Conditions	Nebulisation Time min	Number of Replicates n	Mean Observed Concentration $\mu\text{g/ml}$	Standard Deviation $\mu\text{g/ml}$
22°C and Dry Argon	2	5	9.5	0.3
22°C and Dry Argon	20	3	9.4	0.4
35°C and Dry Argon	20	3	9.8	0.7
35°C and Wet Argon	20	3	9.6	0.8

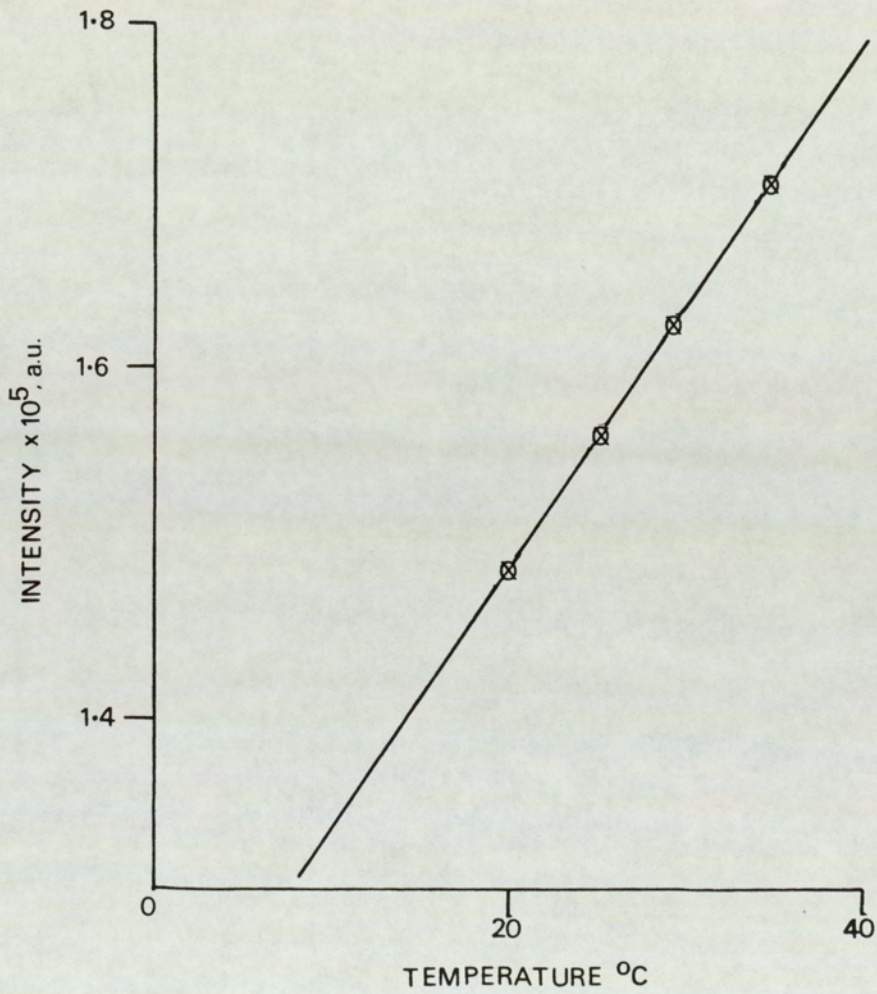
FIG. 8.6



showing an initial decrease in signal intensity due to dilution followed by steady increases. The close similarity between the curves for dry and wet argon suggests that this is not due to concentration by evaporation. This is confirmed by the analysis of the remaining solution, given in Table 8.4, which shows that the concentration of Cu in the recovered solution is not significantly different from that obtained for nebulisation at ambient temperature. The solution temperature rises during the experiment from heating during contact with the walls of the spray chamber. This decreases its viscosity which in turn affects the nebulisation characteristics and the emission signal. The effect of solution temperature on the performance of the Meinhard nebuliser, when used in the conventional mode, was studied by heating a sample solution. This was achieved by passing the uptake tubing through a thermostatted water bath. Over the 20 to 40 min range it was found that the emission signal for copper increased by $\sim 1.5\%$ for every $^{\circ}\text{C}$ rise in solution temperature (Fig. 8.7). This is a greater increase than that expected with the recirculating nebuliser, but it does demonstrate the importance of solution temperature in relation to nebuliser performance. The discrepancy can be attributed to the difficulty in defining adequately the temperature conditions that exist within the recirculating nebuliser while these conditions are changing rapidly. Nevertheless these experiments indicate that the temperature of the solution being nebulised is the major factor in obtaining stable emission signal intensities when using the recirculating nebuliser and that some care should be taken to protect the spray chamber from external sources of heat. If this is done this system will give stable signals over a long period of time.

FIG. 8.7

CHANGE IN NEBULISATION EFFICIENCY
WITH TEMPERATURE



The absence of any significant concentration of solution by evaporation in the system described can probably be ascribed to the type of nebuliser used and the design of spray chamber. Any explanation is confined almost completely to the fine spray consumed in the plasma, and negligible for the coarse spray trapped and returned to the nebuliser. It is suggested, therefore, that an important factor in any design of spray chamber for recirculating nebulisers is that the coarse spray, which does not reach the plasma, should be separated as rapidly as possible from surfaces over which there is a high argon flow. Further the nebuliser chosen should have a low flow of argon, which in the present case is 0.6 l/min.

8.5 Conclusions

The recirculating nebuliser has been improved by using a microprocessor control which permits easier use and provides a consistent system for washing and sample changover. These developments allow sequential ICP multi-element analyses on a series of small samples to be carried out with little operator involvement.

A number of constraints in the design and application of the system have been recognised. The spray chamber must be designed such that liquid hold-up after drainage is minimised. If this is reduced to 0.1 ml the dilution effect on a solution is sufficiently reproducible that the precision and accuracy are the same as those achieved with conventional nebulisation. It is also necessary to protect the spray chamber from external heat

sources since a temperature rise will significantly increase the observed signal. This can be attributed to an increase in the efficiency of the nebulisation process and not to a concentration of solution by evaporation. It has therefore been demonstrated that the recirculating nebuliser can be used with a sequential scanning monochromator for multi-element analysis, without any significant deterioration in performance over conventional nebulisation, and with as little as 1 ml of sample solution.

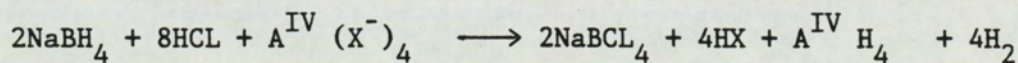
CHAPTER 9

HYDRIDE GENERATION FOR SENSITIVE DETERMINATION OF SELECTIVE ELEMENTS IN BORON CARBIDE

The principal benefits of vapour phase sample injection are:

- (i) The avoidance of the use of a nebuliser, which is a major cause of problems, and which sets a limit to the salt content of the sample solution.
- (ii) The potential for 100% efficiency of injection.
- (iii) The injection of a homogeneous medium into the plasma, which demands a lower power input to achieve complete atomisation of the sample.

The elements Ge, Sn, Pb, As, Sb, Bi, Se and Te form volatile hydrides which are generated from aqueous solutions by sodium tetrahydroborate (NaBH_4) reduction i.e



where A is the analyte and X is the anion, which are introduced to the ICP source via the injector argon flow. Reported limits of detection (typically at ng/ml levels) are generally superior to those obtained by pneumatic nebulisation (45, 46).

Consequently hydride generation was investigated as a means of improved sensitivity of hydride forming elements in boron compounds.

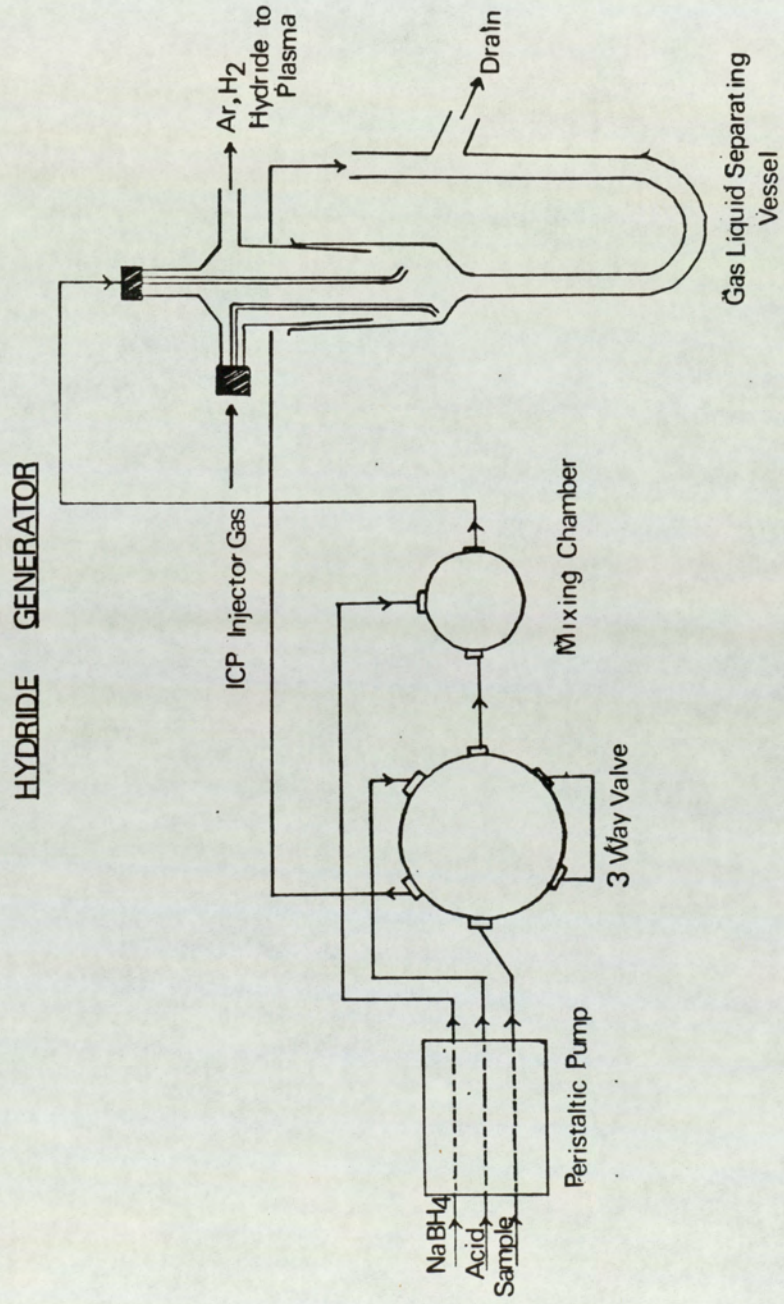
9.1 Instrumentation

The ICP scanning monochromator and instrumental conditions used were described in Chapter 6. The hydride generator used was a Plasma Therm Model PSA No. 10.002. Filtered 1% NaBH_4 solution stabilized in 0.1M NaOH and prepared from BDH 'ANALAR' grade reagents were used. The hydride generator (Fig. 9.1) incorporates a peristaltic pump which continually supplies NaBH_4 solution and the acid blank solution to the mixing chamber where they react. The sample solution and blank must be of the same acid concentration in order to minimise fluctuations in hydrogen formation and hence instabilities in the ICP source. An injector gas flow of 1.2 l/min argon (at 2 psi) was found to give optimum sensitivity. On introduction of the acidified sample solution a 3-way valve is switched to supply NaBH_4 and the sample solution to the mixing chamber where the analyte is reduced to its hydride. The contents of the mixing chamber are then pumped to a separation vessel where the gaseous fraction separates from the liquid. The ICP injector gas flow carries the gaseous hydride and hydrogen to the plasma where they are atomized and excited. Emission was measured by the ICP-Scanning monochromator system.

9.2 Experimental

Several parameters must be optimised, however, to achieve maximum sensitivity, e.g the acid selected, its concentration, and the analyte oxidation state. For each element several acid media were examined. Most elements selected for

FIG.9.1



this analysis were obtained as BDH 'SPECTROSOL' grade aqueous standards in the required oxidation state. Te, P and S however, were in higher oxidation states and required reduction. A procedure exists (47) for the reduction of As(V), Sb(V) and Se(VI) to their corresponding lower oxidation states by the action of a halide ion and heat. This method was applied to Te, P and S.

Initially one standard of each element was made up in several different acid media (0.1M HCl, 5M HCl and 1% tartaric acid - all BDH 'ANALAR' grade) and a detection limit (calculated as described in Section 5.4) for each obtained. From these the acid conditions which gave the lowest detection limit for each element were determined. A range of standards was then prepared for each element in the appropriate acid medium and these were used for calibration.

Solutions of boron carbide sample BC1 were prepared as described in Section 5.2. The Carius tube reaction mixtures were then taken up in either HCL or tartaric acid solutions to cover all the elements of interest.

9.3 Results and Discussion

Table 9.1 gives the optimum conditions for each element, the detection limits obtained using these conditions, and for comparison the limits of detection obtained using pneumatic nebulisation. As found elsewhere (48) PbH_4 could not be generated readily and consequently no improvement in sensitivity

TABLE 9.1

OPTIMUM CONDITIONS FOR HYDRIDE GENERATION
AND COMPARISON OF DETECTION LIMITS

Element	Wavelength nm	Oxidation State	Acid Conditions	Analyte conc.	LOD *by HG µg/ml	LOD # by PN µg/ml
Se	196.026	IV	5M HCL	1	<0.005	<0.08
Te	214.281	IV	"	0.1	<0.002	<0.04
As	193.696	III	"	1	<0.002	<0.05
Sb	206.833	III	"	1	<0.002	<0.03
Bi	223.061	III	"	1	<0.002	<0.03
Hg	253.652	II	"	0.1	<0.0005	<0.06
Pb	220.353	II	"	10	<4	<0.04
Ge	265.118	IV	1% Tartaric	1	<0.0001	<0.05
Sn	283.990	IV	"	1	<0.003	<0.03
P	213.618	III	-	-	-	<0.4
S	216.890	IV	-	-	-	-

* Limits of detection obtained using hydride generation

Limits of detection obtained using pneumatic nebulisation.

over pneumatic nebulisation was achieved. PH_3 and H_2S are formed from the lower oxidation states (III and IV resp.) of these elements only. Sample solutions after Carius tube dissolution contain P and S in higher oxidation states as phosphates (P(V)) and sulphates (S(VI)) which, under the reaction conditions used, cannot be reduced to form hydrides. Chemical methods involving halide ions and heat were used to reduce these higher oxidation states but were not successful and therefore P and S could not be determined by hydride generation into the ICP. Te, as a spectroscopic standard, was obtained as telluric acid Te(VI) which was not suitable for hydride generation. However, this could be readily reduced to Te(IV), which does form a hydride, by treatment with 5M HCL. 1% tartaric acid gave the best sensitivity for Sn and Ge while 5M HCl was the most suitable medium for the generation of Hg and the hydrides of Se, As, Sb, Bi and Te.

Results for the analysis of boron carbide sample BC1 using the conditions given above are shown in Table 9.2. The figures are consistent with limits of detection obtained by neutron activation and spark source mass spectroscopy. In the case of Sn, Ge, Bi and Hg an improvement in detection limits was achieved.

9.4 Conclusions

Hydride generation, as a sample introduction technique for ICP/AES provides a method for determining very low levels (<1 ppm) of certain elements which are not particularly sensitive

TABLE 9.2

RESULTS FROM ANALYSIS ON BORON
CARBIDE SAMPLE BC1

Element	Concentration (ppm)		
	HG + ICP/AES	SSMS	ENAA
Sn	<0.2	<1	<2
Ge	0.5	1	5
Bi	0.01	1	ND*
Hg	0.5	3	5
As	1	0.1	0.01
Se	2	0.5	0.5
Sb	0.5	1	0.01
Te	0.5	1	0.1

* ND = Not determined by ENAA.

by pneumatic nebulisation. In general ng/ml detection limits are achievable. This improved sensitivity is due both to the removal of the matrix water from the plasma and to greater sample transport to the plasma by gaseous sample introduction. The analyte oxidation state and acid conditions are important factors in the formation of the gaseous analyte hydride. P and S are commonly found in oxidation states (V) and (VI) respectively which are not suitable for hydride generation. Chemical pretreatments have been investigated in order to reduce these elements to the required oxidation states but none was found to be successful. No suitable acid conditions were found for the reduction of Pb. Although electrochemical reductions may provide a possible approach to reducing Pb, such steps would considerably increase the analysis time and hence were not considered further.

Application of the technique has been demonstrated for the determination of Sn, Ge, Bi, Hg, As, Se, Sb and Te in high purity boron carbide and it is envisaged that the method will find routine use for the determination of these elements.

CHAPTER 10

A COMPARISON OF ICP/AES AND OTHER

MULTI-ELEMENT TECHNIQUES

Although this study has shown that ICP/AES has considerable capability for multi-element analysis of boron materials the technique has some limitations. Although 50 elements were determined to ppm levels often it is desirable to determine as many 70 elements. Clearly in these cases the requirements cannot be met using ICP/AES alone. Other multi-element techniques such as neutron activation analysis (NAA) and spark source mass spectrometry (SSMS) are used for such analyses. The performances of each of these techniques were compared. Assessment was made by comparing results obtained from the analysis of boron carbide control samples.

10.1 Inductively Coupled Plasma Atomic Emission Spectroscopy

Both ICP-Spectrograph and ICP-Scanning monochromator systems, described in Chapters 6 to 9, were used to determine as many trace elements as possible in the boron carbide control materials BC1, BC2 and BC3. Analytical results are given in Tables 10.1 to 10.3.

TABLE 10.1
ICP/AES RESULTS FOR BC1

Element	Result ppm	Element	Result ppm	Element	Result ppm
Na	ND	Rb	ND	Eu s	<1
Mg m	4.5 ± 0.5	Sr s	<0.2	Gd s	<0.5
Al m	8.4 ± 0.4	Y s	<0.01	Tb s	<1
Si	ND	Zr s	<5	Dy m	<0.5
P	ND	Nb s	<5	Ho s	<1
S	ND	Mo s	<5	Er s	<0.5
Cl	ND	Ru s	ND	Tm s	<1
K	ND	Rh	ND	Yb s	<0.1
Ca s	12 ± 1	Pd s	<0.2	Lu s	<0.5
Sc m	<0.01	Ag	ND	Hf	ND
Ti m	7 ± 1	Cd	<0.1	Ta m	<0.1
V m	10 ± 1	In	<1	W m	<20
Cr m	18 ± 1	Sn hg	<0.5	Re	ND
Mn m	0.9 ± 0.6	Sb hg	<0.5	Os	ND
Fe m	60 ± 10	Te hg	<0.5	Ir m	<1
Co m	9 ± 1	I	ND	Pt m	<2
Ni m	8 ± 5	Cs	ND	Au m	<0.5
Cu s	<0.5	Ba s	<0.1	Hg hg	<0.5
Zn m	18 ± 14	La s	<1	Tl	ND
Ga s	<5	Ce s	<5	Pb m	<2
Ge hg	<0.5	Pr s	<5	Bi hg	<0.5
As hg	<1	Nd s	<1	Th	ND
Se hg	<2	Sm s	<1	U	ND
Br	ND				

s = Spectrographic result
m = Photometric result
hg = Hydride generation result
ND = Not determined

TABLE 10.2

ICP/AES RESULTS FOR BC2

Element	Result ppm	Element	Result ppm	Element	Result ppm
Na	ND	Rb	ND	Eu s	<1
Mg m	26 ± 3	Sr s	5 ± 2	Gd s	<0.5
Al m	135 ± 10	Y s	<0.01	Tb s	<1
Si	ND	Zr s	<5	Dy m	<0.5
P	ND	Nb s	<5	Ho s	<1
S	ND	Mo s	<5	Er s	<0.5
Cl	ND	Ru	ND	Tm s	<1
K	ND	Rh	ND	Yb s	<0.1
Ca s	430 ± 40	Pd s	<0.2	Lu s	<0.5
Sc m	0.05 ± 0.02	Ag	ND	Hf	ND
Ti m	340 ± 40	Cd	<0.1	Ta m	<0.1
V m	<5	In	<1	W m	<20
Cr m	12 ± 8	Sn hg	<0.5	Re	ND
Mn m	11 ± 1	Sb hg	<0.5	Os	ND
Fe m	740 ± 60	Te hg	<0.5	Ir m	<1
Co m	ND	I	ND	Pt m	<2
Ni m	4 ± 0.5	Cs	ND	Au m	<0.5
Cu s	30 ± 10	Ba s	19 ± 2	Hg hg	<0.5
Zn m	<2	La s	<1	Tl	ND
Ga s	<5	Ce s	<5	Pb m	<2
Ge hg	<0.1	Pr s	<5	Bi hg	<0.5
As hg	<1	Nd s	<1	Th	ND
Se hg	<2	Sm s	<1	U	ND
Br	ND				

s = Spectrographic result
m = Photometric result
hg = Hydride generation result
ND = Not determined.

TABLE 10.3

ICP/AES RESULTS FOR BC3

Element	Result ppm	Element	Result ppm	Element	Result ppm
Na	ND	Rb	ND	Eu s	<1
Mg	25 ± 3	Sr s	3 ± 2	Sd s	<0.5
Al	140 ± 7	Y s	<0.01	Tb s	<1
Si	ND	Zr s	<5	Dy m	<0.5
P	ND	Nb s	<5	Ho s	<1
S	ND	Mo s	<5	Er s	<0.5
Cl	ND	Ru	ND	Tm s	<1
K	ND	Rh	ND	Yb s	<0.1
Ca s	180 ± 20	Pd s	<0.2	Lu s	<0.5
Sc m	0.05 ± 0.02	Ag	ND	Hf	ND
Ti m	630 ± 70	Cd	<0.1	Ta m	<0.1
V m	5	In	<1	W m	<20
Cr m	25 ± 15	Sn hg	<0.5	Re	ND
Mn m	10 ± 5	Sb hg	<0.5	Os	ND
Fe m	390 ± 15	Te hg	<0.5	Ir m	<1
Co m	ND	I	ND	Pt m	<2
Ni m	3 ± 1	Cs	ND	Au m	<0.5
Cu s	40 ± 20	Ba s	10 ± 3	Hg hg	<0.5
Zn m	2	La s	<1	Tl	ND
Ga s	5	Ce s	<5	Pb m	<2
Ge hg	0.5	Pr s	<5	Bi hg	<0.5
As hg	5 ± 2	Nd s	<1	Th	ND
Se hg	2	Sm s	<1	U	ND
Br	ND				

s = Spectrographic result
m = Photometric result
hg = Hydride generation result
ND = Not determined.

10.2 Spark Source Mass Spectrometry

Spark source mass spectrometry (SSMS) has been used extensively for multi-element trace survey analysis for many years (49). In this study an AEI Type MS702 spark source mass spectrometer employing photographic recording was used. The mass spectra were evaluated visually using a comparator.

As boron carbide is non-conducting, high purity graphite (Ringsdorff-Werke GHBN) is added in a 1:1 ratio as an electrode support material. Electrodes were prepared by pressing (400,000 psi) 100 mg quantities of the powdered sample in a PTFE die. Spectra were recorded on Ilford Q2 photographic plates over a mass range of 7 to 260 amu. Thirteen exposures of each sample were made ranging from 10^{-4} to 100 nc, in increments of a factor of 3. Table 10.4 lists normal operating conditions used. Results for boron carbide materials BC1, BC2 and BC3 are given in Tables 10.5 to 10.7.

10.3 Neutron Activation Analysis

In recent years development of high resolution gamma spectrometry and data processing have considerably extended the role of neutron activation analysis as a versatile, non-destructive method which is sensitive, selective and precise and consequently the technique has been used extensively for trace element analysis. A detailed description of the technique is given elsewhere (50).

TABLE 10.4

NORMAL OPERATING CONDITIONS USED

Spark frequency	500 kHz
Spark voltage	30 kV
Pulse length	200 μ s
Pulse repetition rate	100 Hz
Magnet current	260 mA
Magnet range. Effective	
Mass range at 260 mA	7 to 250 amu
Accelerating voltage	20 kV
Analyser pressure	10^{-5} Pa
Source pressure	10^{-4} Pa
Exposure range	0.0001 to 300 nc
Photographic Plate	Ilford Q2
Developer	Ilford Phenisol (25%)
Developing Time	3 min at 20°C
Fixer	Iford Ilfofix
Fixing Time	30 min at 20°C

TABLE 10.5

SSMS RESULTS FOR BC1

Element	Result ppm	Element	Result ppm	Element	Result ppm
Na	<300	Rb	<0.5	Eu	<1
Mg	<700	Sr	0.4	Gd	<2
Al	30	Y	<0.5	Tb	<0.5
Si	300	Zr	<1	Dy	<2
P	4	Nb	<0.5	Ho	<0.5
S	40	Mo	5	Er	<2
Cl	50	Ru	<1	Tm	<0.5
K	50	Rh	<0.5	Yb	<2
Ca	20	Pd	<1	Lu	<1
Sc	<2	Ag	<1	Hf	<2
Ti	7	Cd	<1	Ta	<200
V	20	In	<0.5	W	<20
Cr	20	Sn	<1	Re	<1
Mn	6	Sb	<1	Os	<2
Fe	70	Te	<1	Ir	<1
Co	7	I	<0.5	Pt	<2
Ni	30	Cs	<0.5	Au	<1
Cu	3	Ba	2	Hg	<3
Zn	50	La	<0.5	Tl	<1
Ga	<0.4	Ce	<0.5	Pb	<1
Ge	<1	Pr	<0.5	Bi	<1
As	<0.1	Nd	<2	Th	<0.1
Se	<0.5	Sm	<2	U	<1
Br	0.6				

Expected accuracy on positives is within a factor of 3.

TABLE 10.6

SSMS RESULTS FOR BC2

Element	Result ppm	Element	Result ppm	Element	Result ppm
Na	<200	Rb	0.1	Eu	<0.5
Mg	<600	Sr	5	Gd	<1
Al	80	Y	0.1	Tb	<0.1
Si	900	Zr	0.5	Dy	<0.5
P	30	Nb	0.3	Ho	<0.2
S	100	Mo	1	Er	<0.5
Cl	100	Ru	<0.5	Tm	<0.2
K	40	Rh	<0.1	Yb	<0.5
Ca	400	Pd	<0.5	Lu	<0.2
Sc	<0.05	Ag	<0.2	Hf	<0.5
Ti	200	Cd	<0.5	Ta	<20
V	1	In	<0.1	W	0.6
Cr	6	Sn	1	Re	<0.5
Mn	8	Sb	0.5	Os	<0.5
Fe	600	Te	<0.5	Ir	<0.5
Co	0.5	I	<0.1	Pt	<0.5
Ni	2	Cs	<0.1	Au	<0.2
Cu	30	Ba	20	Hg	<1
Zn	5	La	0.1	Tl	<0.5
Ga	<0.1	Ce	0.5	Pb	4
Ge	<0.2	Pr	<0.1	Bi	<0.2
As	2	Nd	<0.5	Th	<0.2
Se	0.1	Sm	<0.5	U	<0.2
Br	0.5				

Expected accuracy on positives is within a factor of 3.

TABLE 10.7

SSMS RESULTS FOR BC3

Element	Result ppm	Element	Result ppm	Element	Result ppm
Na	<800	Rb	0.1	Eu	<0.5
Mg	<2000	Sr	10	Gd	<1
Al	300	Y	0.1	Tb	<0.2
Si	3000	Zr	2	Dy	<0.5
P	100	Nb	0.3	Ho	<0.2
S	40	Mo	4	Er	<0.5
Cl	500	Ru	<0.5	Tm	<0.5
K	10	Rh	<0.5	Yb	<0.2
Ca	500	Pd	<10	Lu	<0.2
Sc	0.5	Ag	<0.2	Hf	<20
Ti	2000	Cd	<0.5	Ta	<6
V	6	In	<0.1	W	2
Cr	70	Sn	4	Re	<0.5
Mn	60	Sb	2	Os	<0.5
Fe	700	Te	<1	Ir	<0.5
Co	0.7	I	<0.1	Pt	<0.5
Ni	9	Cs	<0.5	Au	<0.2
Cu	100	Ba	20	Hg	<1
Zn	1	La	0.2	Tl	<0.5
Ga	0.2	Ce	0.2	Pb	4
Ge	0.2	Pr	<0.2	Bi	<0.2
As	8	Nd	<0.5	Th	<0.5
Se	0.2	Sm	<1	U	<0.5
Br	0.5				

Expected accuracy on positives is within a factor of 3.

The Herald water moderated and cooled swimming pool type reactor was used. This provided an epithermal flux of 10^{12} n/sec/cm² at a maximum power of 5MW. The experimental method used is fully described elsewhere (51). The results obtained for BC1, BC2 and BC3 are given in Tables 10.8 to 10.10.

10.4 Comparison of Results

The aspects of performance which have been considered for comparing the relative merits of each technique are: element coverage, sensitivity, precision and accuracy, analytical speed, the operator effort required to complete the full analysis of a single material, the quantity of sample required.

In total some 50 elements were determined using ICP/AES methods and excluding those elements positively identified, for 33 elements detection limits ≤ 1 ppm were obtained. For positively identified elements the scanning monochromator has a precision of $< 5\%$ RSD and when the results are compared with those obtained using the other techniques, agreement is good. ICP methodology necessitates sample dissolution which requires 0.5 g of material and can take up to two days particularly when more refractory boron materials are to be examined. A further 3 days are required to complete the necessary instrumental procedures on both ICP/AES systems. Thus the effort required for complete analyses is relatively high in comparison to the other techniques. However, the technique does give the best detection limits for some elements, e.g. Ca, Ba, Sr, Sc, Y, Mg.

TABLE 10.8

ENNA RESULTS FOR BC1

Element	Result ppm	Element	Result ppm	Element	Result ppm
Na	20 ± 18	Rb	<0.5	Eu	<0.1
Mg	ND	Sr	<0.5	Gd	<0.1
Al	ND	Y	<250	Tb	<0.01
Si	ND	Zr	<0.2	Dy	<5
P	ND	Nb	<20	Ho	<0.01
S	ND	Mo	2.5 ± 0.3	Er	<0.2
Cl	<200	Ru	<1	Tm	<0.2
K	<10	Rh	<0.1	Yb	<0.2
Ca	ND	Pd	<0.05	Lu	<0.2
Sc	<0.1	Ag	<1	Hf	<0.5
Ti	12 ± 1	Cd	<0.2	Ta	<0.1
V	11 ± 3	In	<0.5	W	0.14 ± 0.03
Cr	18 ± 4	Sn	<5	Re	<0.02
Mn	0.8 ± 0.1	Sb	<0.01	Os	<0.05
Fe	65 ± 31	Te	<0.5	Ir	<0.01
Co	0.5 ± 0.1	I	<0.02	Pt	<0.5
Ni	8 ± 1	Cs	<0.1	Au	<0.005
Cu	<2	Ba	<1	Hg	<5
Zn	15 ± 1	La	<0.02	Tl	ND
Ga	<0.005	Ce	<0.5	Pb	ND
Ge	<0.5	Pr	<0.5	Bi	ND
As	<0.01	Nd	<0.5	Th	<0.01
Se	<0.5	Sm	<0.2	U	<0.01
Br	0.1 ± 0.03				

Errors quoted as 95% confidence limits based on 3 replicate determinations.

ND = Not determined.

TABLE 10.9
ENAA RESULTS FOR BC2

Element	Result ppm	Element	Result ppm	Element	Result ppm
Na	85 ± 18	Rb	0.5	Eu	0.1
Mg	ND	Sr	5 ± 0.5	Gd	0.2
Al	ND	Y	100	Tb	0.01
Si	ND	Zr	0.8 ± 0.2	Dy	5
P	ND	Nb	<20	Ho	<0.01
S	ND	Mo	2 ± 0.2	Er	<0.2
Cl	60 ± 10	Ru	<1	Tm	<0.2
K	15 ± 5	Rh	<0.4	Yb	<0.2
Ca	ND	Pd	<0.05	Lu	<0.2
Sc	2 ± 0.2	Ag	<1	Hf	<0.5
Ti	387 ± 10	Cd	<0.2	Ta	0.2 ± 0.1
V	2 ± 0.5	In	<0.5	W	0.4 ± 0.1
Cr	19 ± 5	Sn	<5	Re	<0.005
Mn	10 ± 2	Sb	0.4 ± 0.1	Os	<0.05
Fe	750 ± 60	Te	<0.5	Ir	<0.01
Co	1 ± 0.2	I	<0.1	Pt	<0.5
Ni	4 ± 0.4	Cs	<0.1	Au	<0.005
Cu	31 ± 3	Ba	15 ± 2	Hg	<5
Zn	3 ± 1	La	0.2 ± 0.02	Tl	ND
Ga	<0.1	Ce	<0.5	Pb	ND
Ge	<1	Pr	<0.5	Bi	ND
As	1 ± 0.1	Nd	<1	Th	0.07 ± 0.05
Se	<0.5	Sm	<0.5	U	0.1 ± 0.01
Br	1 ± 0.5				

Errors quoted as 95% confidence limits based on 3 replicate determinations.

ND = Not determined.

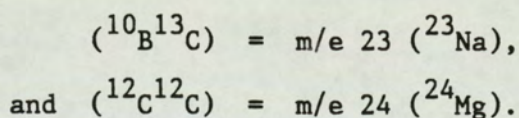
TABLE 10.10
ENAA RESULTS FOR BC2

Element	Result ppm	Element	Result ppm	Element	Result ppm
Na	52 ± 10	Rb	<0.5	Eu	<0.1
Mg	ND	Sr	<5	Gd	<0.2
Al	ND	Y	<100	Tb	<0.01
Si	ND	Zr	3 ± 1.5	Dy	<5
P	ND	Nb	<30	Ho	<0.01
S	ND	Mo	6.9 ± 0.5	Er	<0.2
Cl	<50	Ru	<1	Tm	<0.2
K	<10	Rh	<0.4	Yb	<0.2
Ca	ND	Pd	<0.05	Lu	<0.2
Sc	<2	Ag	<1	Hf	0.2 ± 0.1
Ti	970 ± 50	Cd	<0.2	Ta	0.1 ± 0.1
V	5 ± 2	In	<0.5	W	4.2 ± 0.7
Cr	40 ± 10	Sn	3.4 ± 0.8	Re	<0.01
Mn	10 ± 2	Sb	3.0 ± 0.2	Os	<0.05
Fe	355 ± 40	Te	<0.5	Ir	<0.01
Co	<2	I	<0.1	Pt	<0.5
Ni	3.9 ± 0.6	Cs	<0.2	Au	<0.005
Cu	55 ± 10	Ba	8.7 ± 1.2	Hg	<4
Zn	<3	La	0.3 ± 0.1	Tl	ND
Ga	<0.1	Ce	<0.5	Pb	ND
Ge	<1	Pr	<0.5	Bi	ND
As	7.3 ± 0.8	Nd	<1	Th	0.2 ± 0.1
Se	<0.5	Sm	<0.5	U	0.4 ± 0.2
Br	1.5 ± 0.2				

Errors quoted as 95% confidence limits based on 3 replicate determinations.

ND = Not determined.

In general, SSMS gives results for 70 elements and is the only technique offering such a wide range of element coverage. Excluding positively identified elements, detection limits <1 ppm were recorded for 40 elements. Due to the poor precision of the technique, for positively identified elements a factor of x3 must be applied to the result. Consequently, the technique is limited to a qualitative role. For elements such as Na and Mg the limits of detection can be as high as 100 to 500 ppm in boron carbide due to matrix interference such as:



However, the technique is the most rapid with all trace elements being determined in a single working day. Although during micro-spark sampling only about 50 μg are consumed during the analysis, which gives rise to poor precision, 100 mg of material is required for preparing electrodes.

Sixty elements were determined by ENAA. Excluding positively identified elements, 47 elements were reported as having ≤ 1 ppm detection limits although poor detection limits of Mg, Y, Nb, Ca, and Al were recorded. Also detection limits for Bi, Tl, and Pb in boron compounds are typically >1000 ppm, hence, these elements are not determined by activation analysis. A precision of 5 to 15% RSD was achieved and no positively identified elements were reported to have a concentration significantly different to those obtained by other methods. The relatively long irradiation and counting periods (in total 2 weeks) associated with activation analysis can become a limitation but as most of the data acquisition and processing

procedures are automated, the degree of operator effort is comparatively small. The method is non-destructive and requires a sample of about 200 mg.

Table 10.11 summarizes the relative performances of each technique and indicates that if ~70 elements are to be determined in boron materials no single technique can fulfil the requirements. If analysis was required for a material which was of a higher purity than those analysed in this work, then possibly the detection limits and element coverage of SSMS could be sufficient. However, analytical data obtained for the materials used in this study showed that the total impurities ranged between 2 to 3000 ppm, and therefore the analyses included quantitative determination of trace elements by ENAA and ICP/AES. Although ENAA offers the best approach on both analytical and economic grounds there still remains a number of elements, e.g Mg, Y, Nb, Ca, Al, Bi, Pb, Sr and Ba for which ENAA does not have the required sensitivity but for which quantitative determination is required. These are provided by ICP/AES. In general, good agreement of quantitative data obtained by ICP/AES and ENAA was obtained. For these reasons only a combination of all three techniques can provide the required information. Although the required analytical data is provided by these techniques the analyses involve lengthy counting periods, are labour intensive, and in the case of ICP work sample dissolution is necessary. For these reasons it is worthwhile examining the potential of other multi-element techniques. Two techniques which were considered are wavelength dispersive X-ray fluorescence and ICP-Mass spectrometry

TABLE 10.11

GENERAL APPRAISAL OF MULTI-ELEMENT TECHNIQUES
CURRENTLY USED FOR BORON ANALYSIS

Technique	Element Coverage	Sensitivity (a)	Qualitative or Quantitative	Analytical Speed (b)	Operator Effort (c)
ICP/AES	55	33	Quantitative	7 - 14 days	7 - 14 days
ENAA	60	47	Quantitative	7 - 14 days	2 - 4 days
SSMS	70	40	Qualitative	1 day	1 day

- (a) The number of elements, excluding those positively identified, which were reported as having detection limits <1 ppm.
- (b) The analytical speed relates to the total time require to complete a full characterisation of a single material.
- (c) The operator effort relates to the actual time spent by the analyst on a single material.

10.5 Wavelength Dispersive X-ray Fluorescence

Wavelength dispersive X-ray fluorescence (WDXRF) has been applied to the determination of trace elements in boron materials (1) but poor detection limits (typically 10 to 50 ppm) were obtained. However, this poor sensitivity could be attributed to limitations imposed by the WDXRF equipment used and may not be representative of modern instruments. The operational stability of modern WDXRF instrumentation and the elimination of time consuming wet chemical treatment is important in relation to the total time for analysis. As instrument time on a modern WDXRF instrument was available at the Department of Geological Sciences at the University of Aston in Birmingham, a limited assessment of the technique was made.

10.5.1 Experimental

A Philips Model 1400 WDXRF system was used. The instrument parameters used are summarized in Tables 10.12 and 10.13. A thorough treatise on the theoretical aspects of WDXRF instrumentation and analysis is given elsewhere (52, 53).

Preliminary measurements were made using powdered samples (5 μm) of boron carbide materials BC1, BC2 and BC3. The powders were sprinkled over Mylar film and integrations at the fluorescent peak and background positions (given in Table 10.13) for Fe, Mn, Cr, Ti, Ca, Cu and Zn were recorded. Good linear correlations between known concentrations and background corrected intensities were observed for all the elements.

TABLE 10.12

CRYSTALS USED IN THE PHILIPS 1400

Crystal	2d Spacing nm	Identification No.
LiF 220	0.2848	1
LiF 200	0.4028	2
Ge	0.6532	3
P.E.	0.8742	4
T.L.A.P	2.575	5

TABLE 10.13

INSTRUMENTAL CONDITIONS

Element Line	(A) COL	(B) DET	(C) XTL	(D) Bandpass UPL LNL	(E) Exciter KV MA	(F) Angle°	(G) Background +OFFS° -OFFS°
Al K α	F	P	4	80 29	50 55	145.045	1.50 1.50
Ca K α	C	P	2	72 30	50 55	113.205	2.00 2.00
Ti K α	F	P	2	70 10	50 55	86.120	1.10 1.10
Mn K α	F	P	1	67 20	50 55	95.160	0.60 0.60
Fe K α	F	P	2	68 17	50 55	57.480	1.50 1.50
Cr K α	F	P	1	66 14	50 55	107.100	1.64 1.64
Cu K α	F	PS	2	68 20	60 45	44.990	0.50 0.50
Zn K α	F	PS	2	70 24	60 45	41.755	0.40 0.00
Sr K α	F	S	1	72 20	70 40	35.800	0.50 0.50
Ba K α	F	S	1	64 28	70 40	15.510	0.00 0.18
U L α	F	S	2	64 22	70 40	26.130	0.00 0.30
La L α	F	P	2	64 38	50 55	82.890	1.00 1.00
Pb L β	F	S	2	66 18	70 40	28.255	0.30 0.30
Mo K α	F	PS	2	75 25	70 40	20.245	0.20 0.20

Key:

(A)Collimator:coarse/fine

(B)Detector:proportional/
scintillator

(C)Crystal type:See Table 11.1

(D)Spectral bandpass

(E)Voltage and current settings
for Rh exciter tube.

(F)Crystal angles used.

(G)Background positions.

Figs. 10.1a and 10.1b give the plots obtained for Ca and Fe as typical examples. Detection limits were calculated as described in Section 5.4 and in general ranged from 0.5 to 2 ppm. These preliminary results were sufficiently encouraging to warrant further, more detailed assessment.

Improved sample presentation to the X-ray beam was made using pressed discs. These were made by pressing boron carbide powders using polybutylmethacrylate (CRANCO, ICI product No H190.155) as binder. CRANCO is available in a sufficiently pure form as a 20% solution in xylene. The depth to which 95% of the incident X-rays are absorbed (critical depth) for boron carbide/CRANCO material was calculated to be approximately 0.2 mm (at $\lambda = 2.5\text{\AA}$) and so to obtain optimum sensitivity and sample economy a disc containing some 0.5 g of material is required. However, in order to produce a sufficiently mechanically rigid disc a thickness of 3 mm was preferred requiring 5 g of material.

Discs were prepared by weighing 8.50 g portions of boron carbide and 7.50 g CRANCO solution into polythene dishes. After thorough mixing, the solvent was evaporated by heating under an infra-red lamp. The residue was broken up and frozen to enable efficient grinding with a pestle. 5.0 g portions of sample were transferred to a die press, heated to 300°C and then pressed at 6000 psi.

FIG. 10.1a

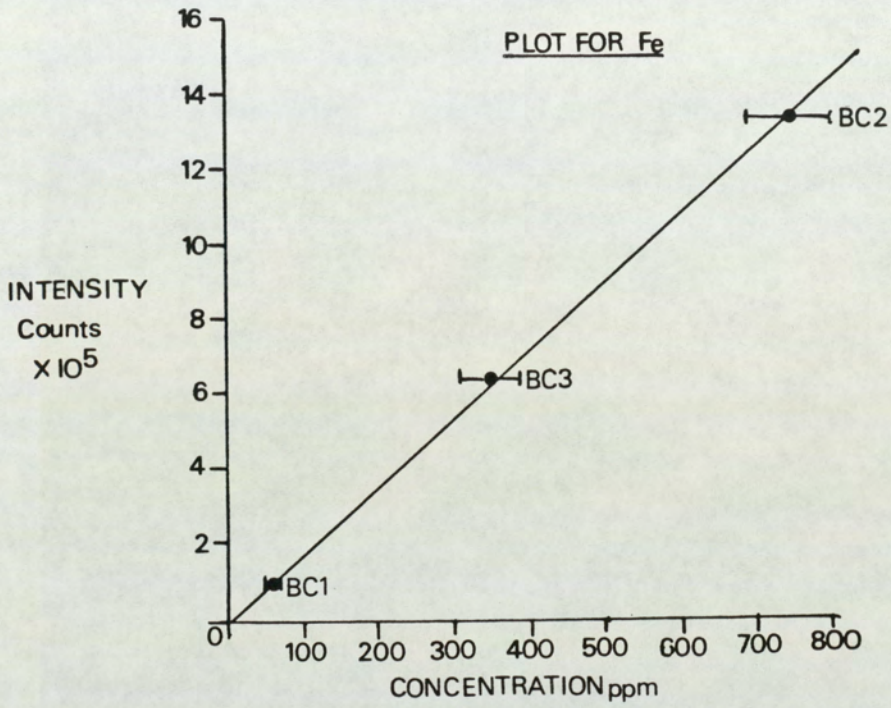
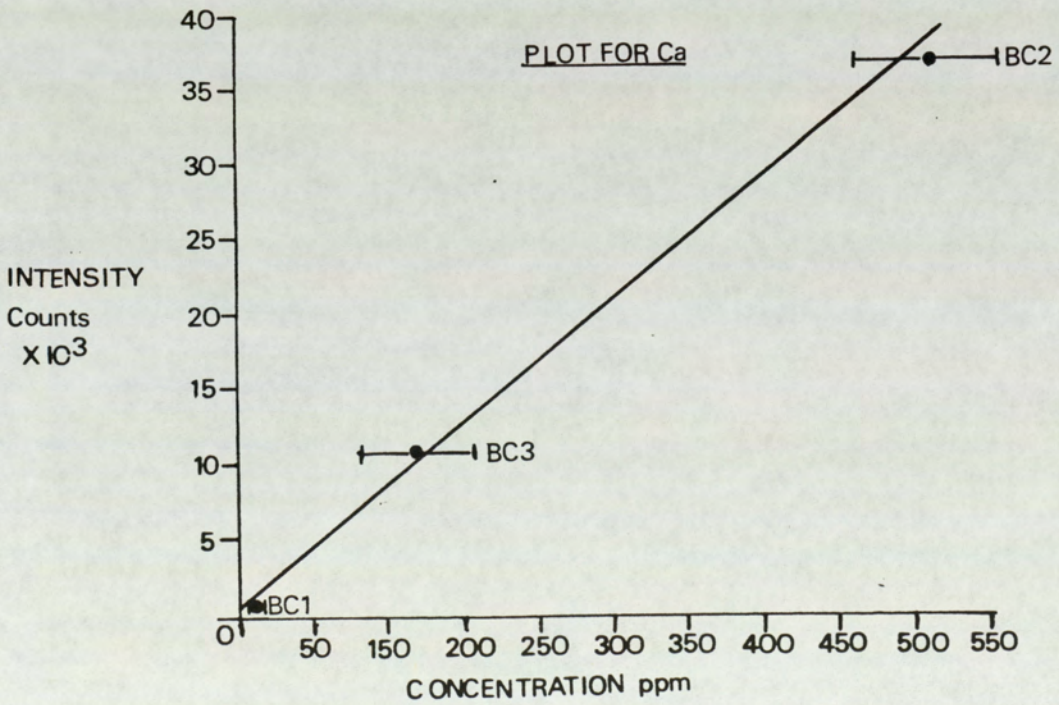


FIG. 10.1b



Error bars give the 95% C.L. on the expected concentrations.

Ti, Ca, Al, Fe and Si are found in various boron carbide materials at a suitable range of concentrations for the WDXRF technique and so sample discs of BC1, BC2, BC4, BC5 and BC6 provided a method of calibration for these elements.

For other elements which are not present in these materials, or are present but only at consistently low levels, synthetic standards were prepared. Two methods of preparing synthetic standards were used. Method (1) involves preparation using standard aqueous solutions while Method (2) involves addition of elemental oxides. Boron carbide sample BC6 was used for preparing standard discs as it was the only material available in sufficient quantity and previous analysis showed the material to be relatively pure.

In Method (1), μl volumes of standard solutions (BDH 1000 $\mu\text{g}/\text{ml}$ 'SPECTROSOL' grade) were pipetted on to 10.00 g portions of BC6. The water and acid were vaporized from the sample, CRANCO solution added and discs prepared as described previously.

In Method (2) a stock standard of the elements was prepared by weighing suitable quantities of the elemental oxides (Johnson and Matthey 'SPECPURE' grade) into 100 g of BC6. The standard was slurried in carbon tetrachloride and milled for several hours. The solvent was evaporated and the final powder used to prepare a range of standards by weighted dilution. Using both methods, multi-element standards containing 2 to 50 ppm of commonly determined elements were prepared.

Absorption and enhancement interferences are two types of interelement effects which are found in XRF work. Absorption of the incident X-rays by impurity elements can bring about considerable changes in the fluorescence radiation of an analyte. The degree at which this attenuation occurs depends on the mass fraction and mass absorption coefficient of the impurity. In order to determine the level of impurity contamination necessary to cause serious absorption interference, a set of 10 ppm standards containing 0.05 to 5% Pb were prepared. Enhancement interference occurs when radiation from an impurity element is of a wavelength corresponding to the adsorption edge wavelength of second analyte and results in a spuriously high signal. In the boron carbide materials commonly examined the most abundant impurity element is Si which can have a concentration as high as 2000 ppm. Si has a strong enhancement effect on Al measurements. To assess enhancement effects a second set of 10 ppm standards was prepared to which 0.1 to 5% Si was added.

10.5.2 Results and Discussion

Using discs of BC1, BC2, BC4, BC5 and BC6 linear calibrations were obtained for Fe, Ca, Ti, Al, and Si. Typical examples are given in Fig. 10.2. Table 10.14 compares the results interpolated from these calibrations for BC3 with results obtained by other techniques. Within experimental error the results show no bias.

CALIBRATION USING CONTROL
MATERIALS

FIG. 10.2a.

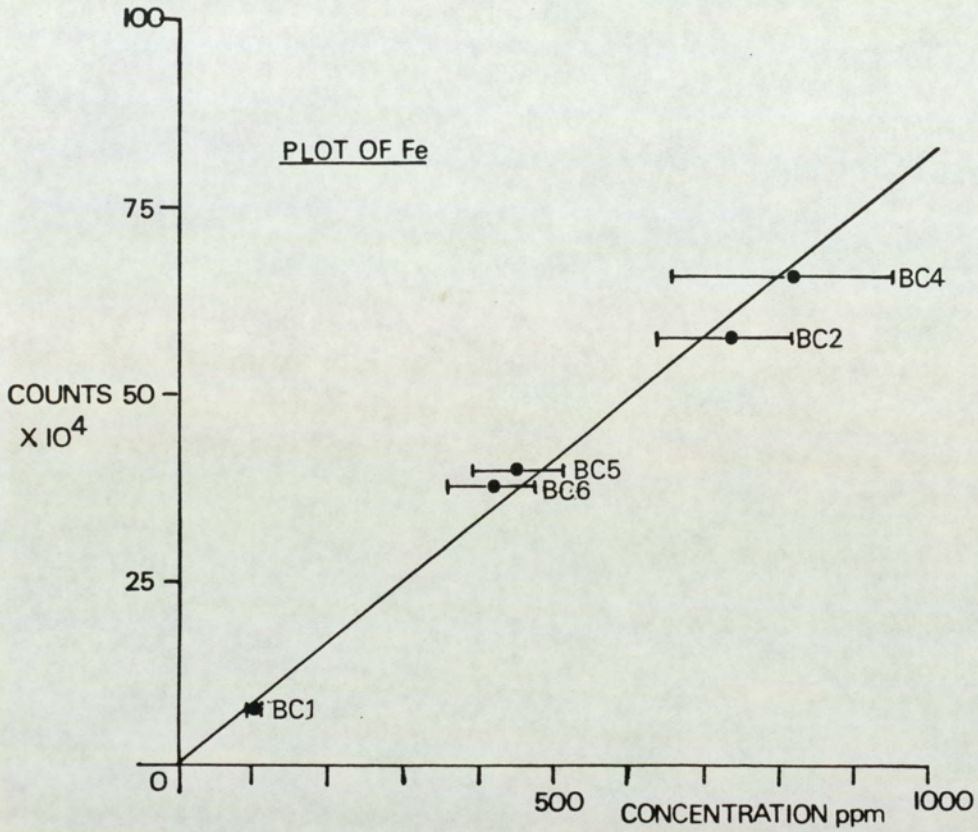
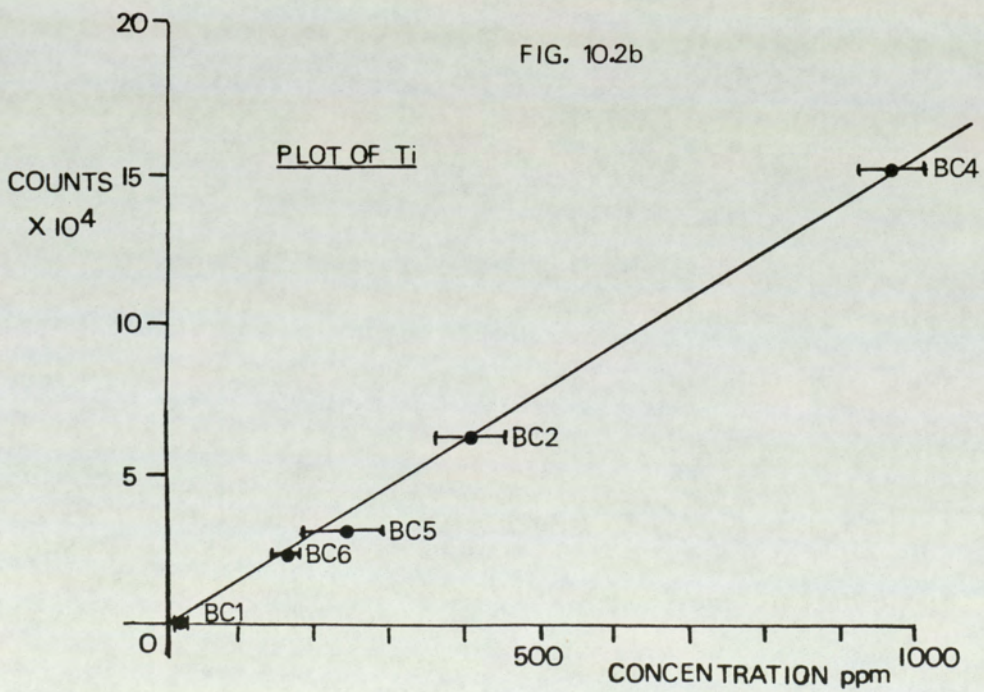


FIG. 10.2b



Error bars give the 95% C.L. on the expected concentration.

TABLE 10.14

COMPARISON OF XRF RESULTS AND RESULTS OBTAINED
BY OTHER METHODS : USING BORON CARBIDE CONTROL
MATERIALS AS STANDARDS

Sample	Element	XRF # Result ppm	Expected * Concentration ppm
BC3	Fe	355 ± 4	355 ± 40
	Ti	1000 ± 7	970 ± 50
	Ca	140 ± 1	115 ± 40
	Si	1740 ± 60	1730 ± 60
	Al	150 ± 6	140 ± 7

* Results based on data obtained by ENAA, SSMS and ICP/AES

Results based on the mean and 95% C.L from five determinations.

Standards prepared by both Method (1) and Method (2) gave good linear correlation and good agreement with each other indicating that either method could be used. Fig. 10.3 gives, as a typical example, the plot obtained for Pb using both suites of synthetic standards. Using these calibrations, concentrations of elements were interpolated for the control materials BC1, BC2 and BC3. Table 10.15 summarises the results which, with the only exception of a high Cu result for BC1, show good agreement. At present no satisfactory explanation can be given for the high Cu result but it is likely to have been caused by contamination of the sample during preparation of the disc.

Method precision was evaluated by conducting element determinations on five portions of BC3. The standard deviations recorded are given in Table 10.16 and range from 0.6 to 1.9% RSD.

In order to determine the level of contamination necessary to cause a 10% signal deterioration, the signals recorded for each element in a series of 10 ppm standards containing various levels of Pb were plotted against the Pb content. Fig. 10.4 shows that a Pb content of $>0.1\%$ is required to cause significant signal deterioration.

The level of Si contamination necessary to cause a significant (10%) enhancement was determined by measuring the Al signal from a set of 10 ppm standards containing 0 to 5% Si. Fig. 10.5 indicates that Si levels below 5% do not cause significant interference.

FIG. 10.3

CALIBRATION PLOT FOR Pb USING
SYNTHETIC STANDARDS

- x - standards prepared by solution additions
- - standards prepared by element oxide additions.

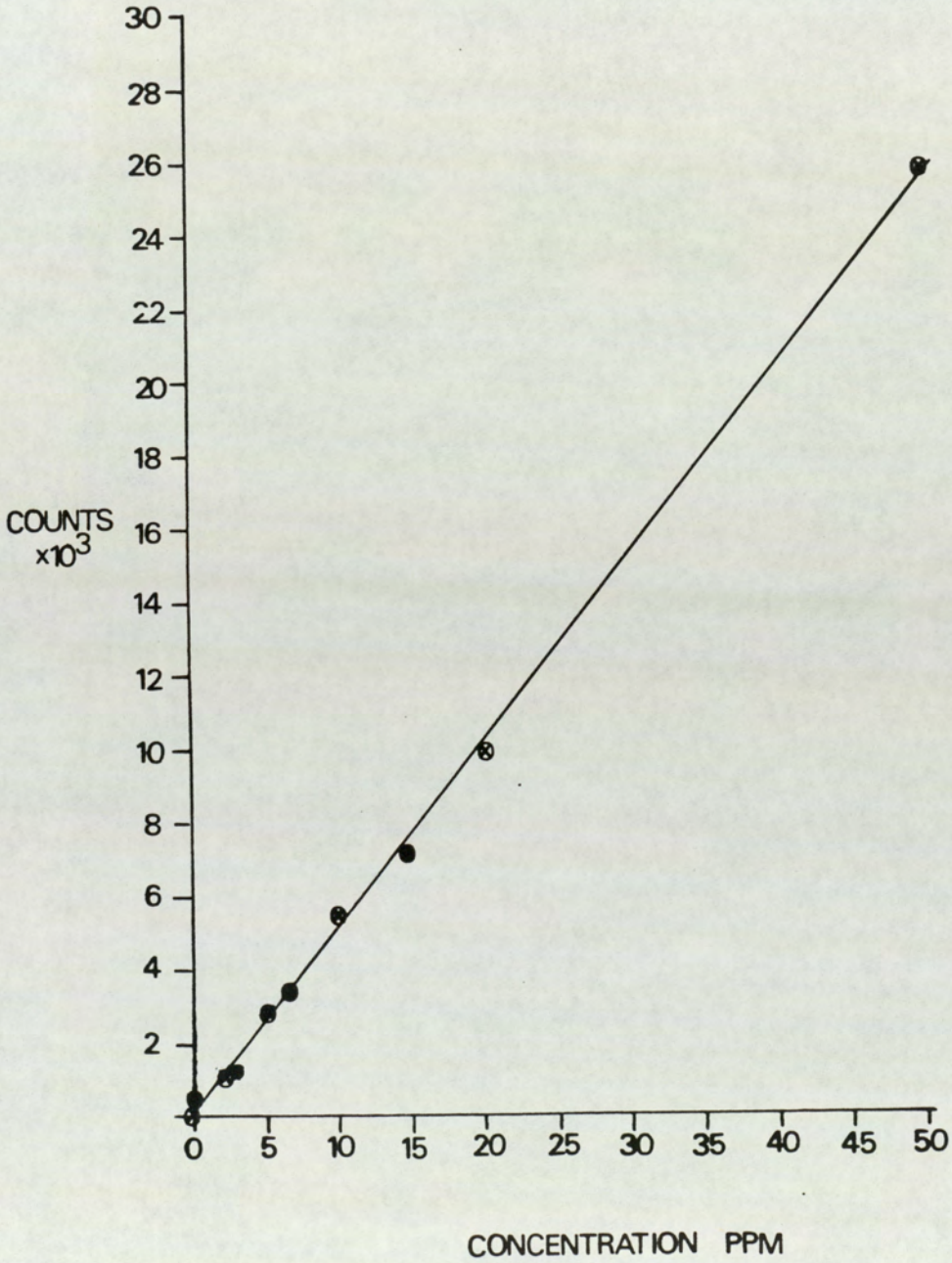


TABLE 10.15

COMPARISON OF XRF RESULTS WITH RESULTS POOLED FROM DATA
OBTAINED BY ENAA, SSMS AND ICP/AES: USING SYNTHETIC STANDARDS

Element	Concentration PPM							
	BC1		BC2		BC3			
	XRF	Expected	XRF	Expected	XRF	Expected	XRF	Expected
Zn	15 ± 2	15 ± 2	4 ± 1	3 ± 1	2.6 ± 0.1	<5	<5	<5
Sr	<0.5	<0.5	6 ± 1	5 ± 0.5	3 ± 1	<5	<5	<5
Mo	3 ± 2	3 ± 0.5	3 ± 1	2 ± 0.2	5 ± 2	7 ± 0.5	7 ± 0.5	7 ± 0.5
Ba	<1	<1	16 ± 7	15 ± 2	7 ± 3	9 ± 1	9 ± 1	9 ± 1
U	<1	<1	<1	<0.1	<1	<1	<1	<1
La	<0.5	<0.02	<0.5	0.2 ± 0.02	<0.5	0.3 ± 0.1	0.3 ± 0.1	0.3 ± 0.1
Pb	<1	<1	2.0 ± 1.5	<2	3 ± 2	<2	<2	<2
Cu	13 ± 1	<0.5	34 ± 5	31 ± 3	58 ± 1	55 ± 10	55 ± 10	55 ± 10
Mn	<1	1 ± 0.5	7 ± 1	10 ± 2	9 ± 2	10 ± 2	10 ± 2	10 ± 2
Cr	17 ± 2	18 ± 1	15 ± 4	12 ± 8	25 ± 1	25 ± 15	25 ± 15	25 ± 15

Errors quoted as 95% confidence limits on 3 determinations.

TABLE 10.16

PRECISION ON FIVE REPLICATE
DETERMINATIONS OF BC3

Element	Mean Result ppm	Standard Deviation	Relative Standard Deviation
Fe	353	2.9	0.010
Ti	999	5.6	0.006
Ca	150	1.0	0.007
Si	1735	28.4	0.016
Al	152	2.9	0.019

FIG.10.4

Pb ABSORPTION INTERFERENCE

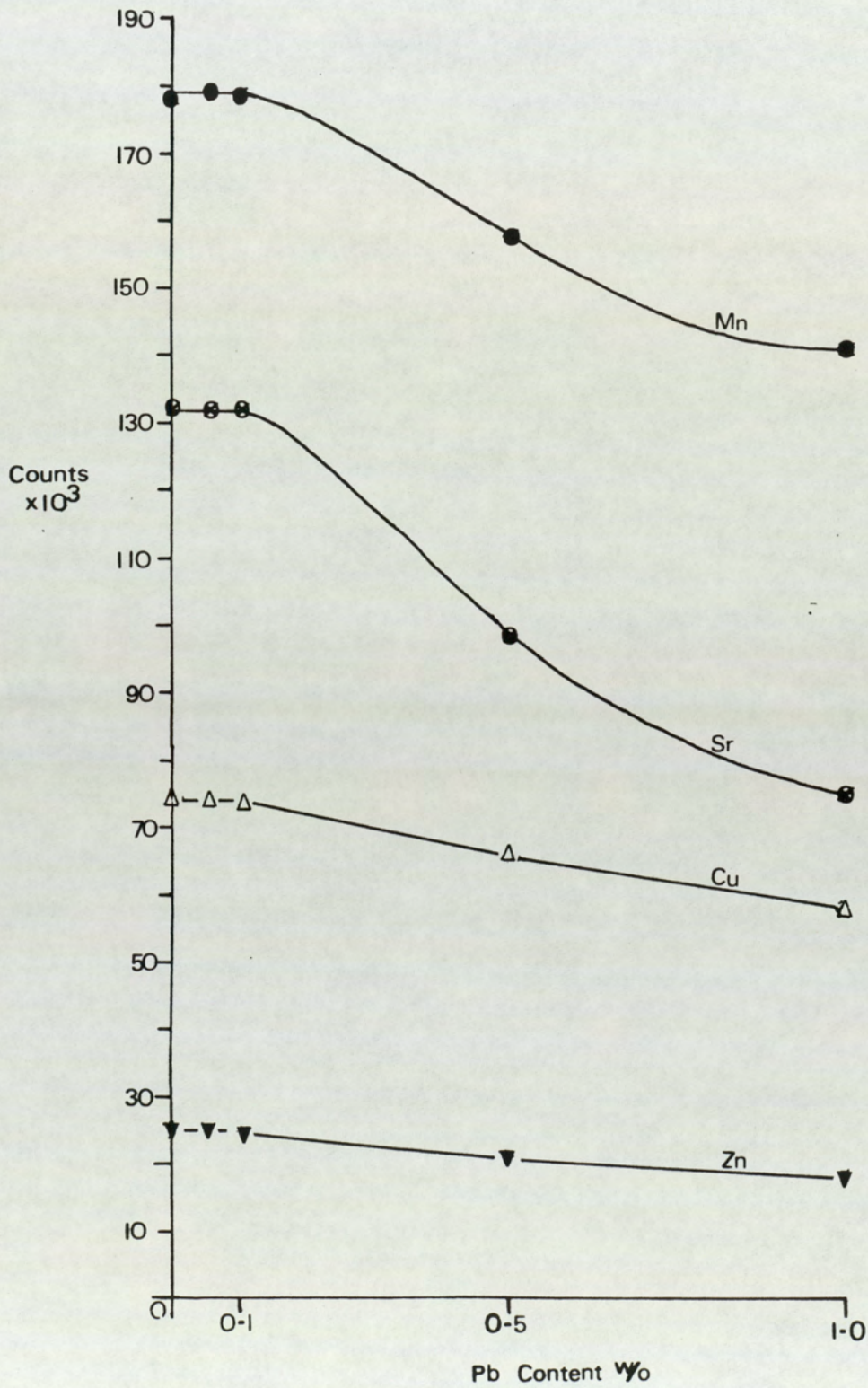
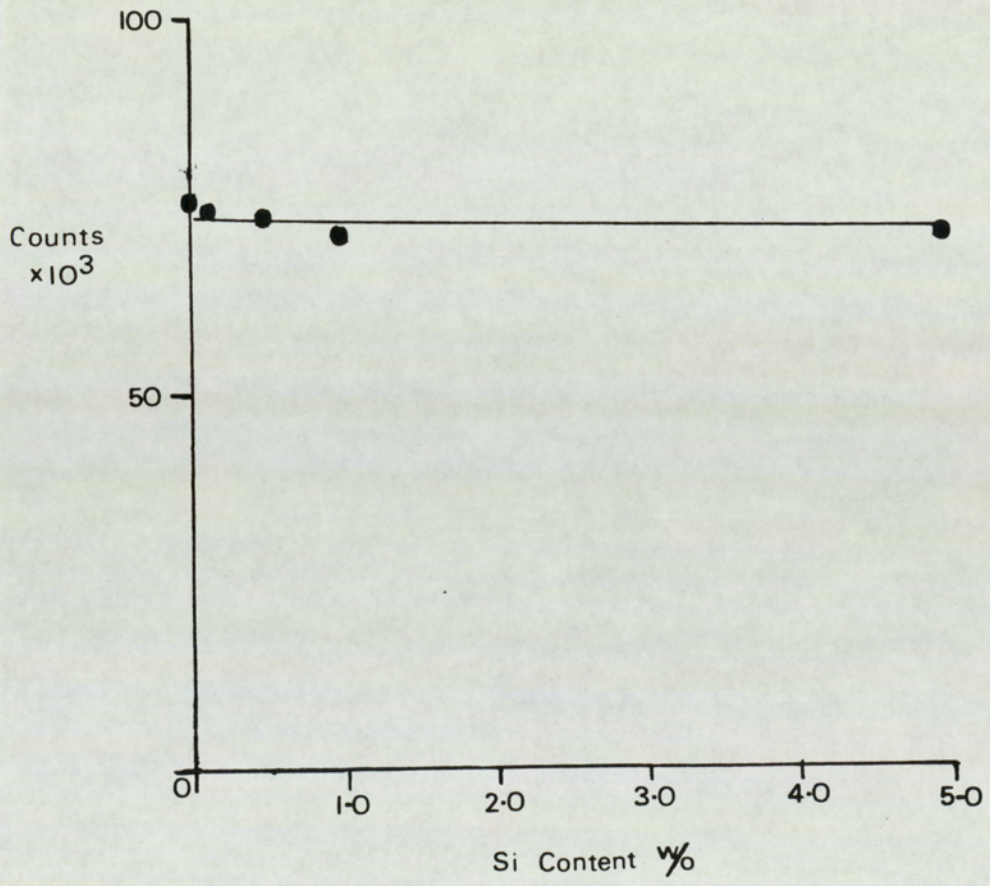


FIG. 10.5

Si ENHANCEMENT ON Al



Limits of detection for the list of elements studied are given in Table 10.17 and are generally at the 1 ppm level.

10.5.3 Conclusions on XRF Method

From this limited study it can be concluded that useful detection limits can be achieved using the described method. Because of the limited availability of the instrument this study was restricted only to 15 elements although the technique has a much wider element coverage. Good accuracy was achieved using control samples and synthetic standards for calibration. WDXRF results compared favourably with those obtained by other methods and a precision of 1 to 2% RSD was achieved for replicate determinations. Although this precision becomes worse (10 to 15% RSD) when the concentration levels to be determined approach the limits of detection, for boron analysis this is not a serious limitation. In relation to the impurity levels found in boron carbide materials that were examined, interelement interferences are negligible. The practical advantage offered by this technique is its simplicity of operation. Analysis need not be carried out by experienced staff and as modern WDXRF instruments are highly automated involvement by operator is mainly concerned with the preparation of sample discs. As standards and control samples can be re-used, and a new disc prepared in an hour the analysis of a single material could easily be completed in a single working day. Clearly the technique has considerable potential for routine boron analysis. However, a major disadvantage is that the method is restricted to cases where 5 g of material are available.

TABLE 10.17

LIMITS OF DETECTION

Element	Line	Limit of Detection ppm
Sr	K α	0.5
Zn	K α	0.5
Pb	L β	1
Cu	K α	0.5
U	L α	1
Mo	K α	1
Ba*	K α	1
Cr*	K α	0.5
Mn*	K α	1
La*	L α	0.5
Si*	K α	1
Fe	K α	0.5
Ti	K α	1
Ca	K α	0.5
Al*	K α	2

* = integration time of 100 sec used,
otherwise 20 sec.

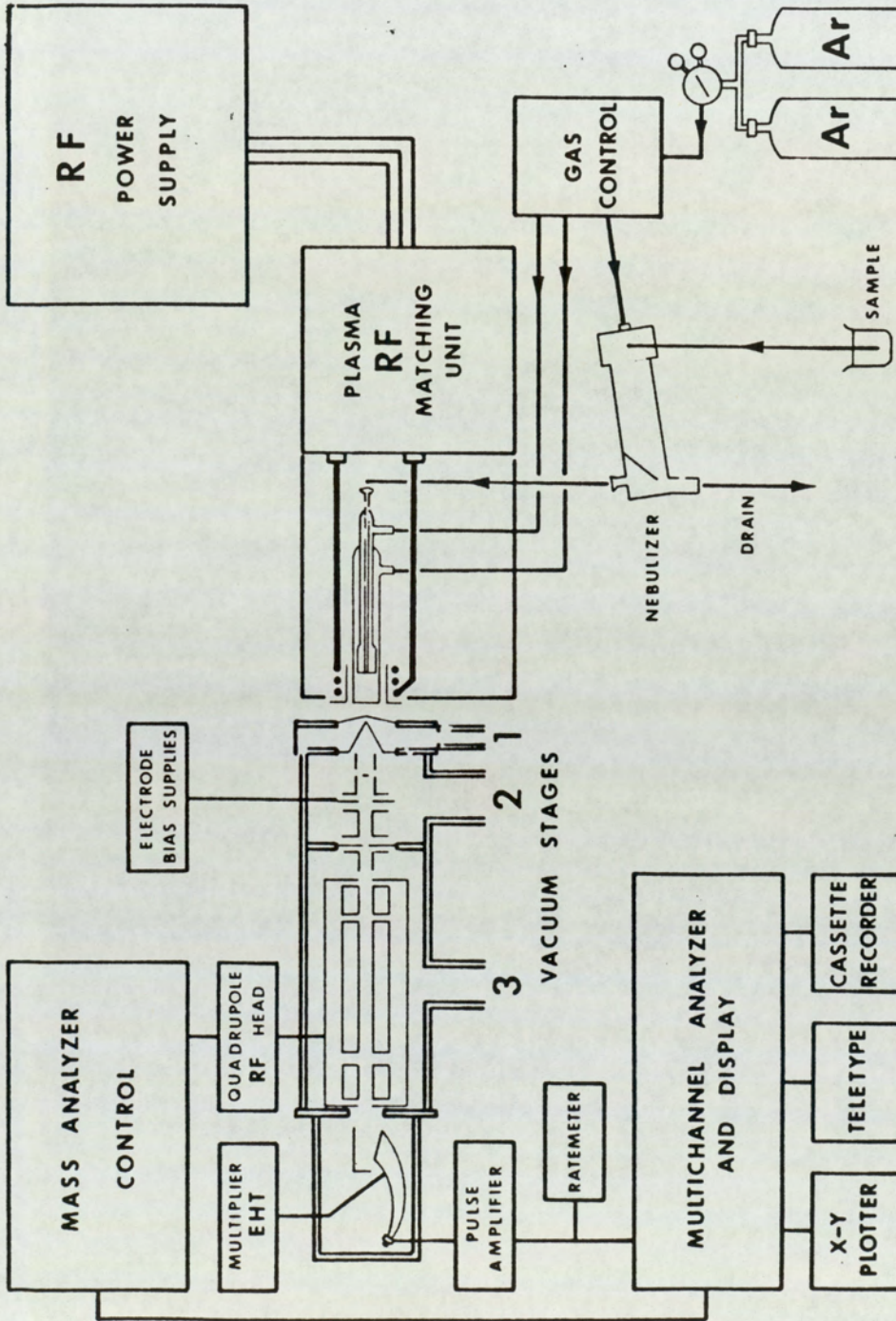
10.6 ICP-Mass Spectrometry

The sensitivity of mass spectrometry for multi-element analysis is exemplified by the performance reported for spark source mass spectrometry. However, as the method of sampling used in SSMS is not precise the technique is limited to a qualitative role. If an ICP is used as an ion source with mass spectrometry then the analytical advantages of both combine to give a technique that is, in theory, sensitive, precise, accurate and has wide element coverage. In 1975 Houk and Fassel (54) and Gray (55) pioneered the coupling of an ICP source to a mass spectrometer. Commercial instruments are now available and applications of the technique are widely reported for various materials (56, 57). Using a demonstration instrument at V.G. Isotopes the technique's performance was assessed. However, as the instrument time available was limited, only tests for sensitivity and element coverage were carried out.

10.6.1 Experimental

A schematic diagram of the instrument is given in Fig. 10.6. Sample solutions are introduced into the plasma using conventional nebulisation. Dissociation, atomisation and ionization take place in the tail-flame of the plasma, and a portion of the ionized gas is introduced into the vacuum system of the mass spectrometer. The quadrupole mass spectrometer acts as a filter, transmitting only ions with a pre-selected mass:charge ratio. Ions are detected with a single channel electron multiplier. The quadrupole control is set for the

FIG. 10.6



ICP MS SYSTEM SCHEMATIC

first mass range required and its scan synchronized with each sweep of the Multi-channel Analyser (MCA) so that ions with a particular mass:charge ratio are always recorded in the same channel or group of channels. A complete mass spectrum is integrated and recorded in 1 min. Data recorded in the MCA are transferred to an IBM microcomputer for graphical display and manipulation of spectra. Operating conditions used are given in Table 10.18.

Multi-element standard solutions were prepared by dissolving 0.60 g of H_3BO_3 (Johnson and Matthey 'SPECPURE' grade) in 50 ml de-ionized water, adding 100 μ l volumes of various standard element solutions (BDH 'SPECTROSOL' grade at 1000 μ g/ml), 2 ml of $HClO_4$ ('ARISTAR' grade) and making up to volume using de-ionized water. 1 ppm In was added to provide for internal standardisation. Boron carbide sample (0.1 g) solutions were prepared as described in Section 5.5. 1 ppm In was added to each solution before diluting to 100 ml. Qualitative spectral scans were performed for each solution.

10.6.2 Results and Discussion

Fig. 10.7 shows a typical mass spectrum obtained when spraying a solution containing 0.6% H_3BO_3 and 2% $HClO_4$. The major spectral background peaks are formed from the plasma support gas, its impurities, nitrogen and oxygen from entrained air and B and Cl the nebulised solution. As can be seen in Fig. 10.8, apart from these interferences the boron sample spectra contain predominantly peaks corresponding to the single charged ionic species of each isotope.

TABLE 10.18

ICP/MS INSTRUMENTAL CONDITIONS

ICP

Torch	Fassel Demountable Type
Coolant Gas Flow	12 l/min
Auxiliary Gas Flow	1.0 l/min
Injector Gas Flow	0.5 l/min at 20 psi
Nebuliser	Perkin Elmer Fixed Cross-flow
Sampling Height	10 mm Above Work Coil

MASS SPECTROMETER

Vacuum Stage 1	1.5 mb
" " 2	2.0×10^{-4} mb
" " 3	3.0×10^{-6} mb
Mass Range	5 to 250 amu
Dwell Time	250 μ s
No. of Sweeps	120

FIG. 10.7

ICP/MS SPECTRUM OF A BLANK SOLUTION:

0.6% H_2BO_3 AND 2% $HClO_4$

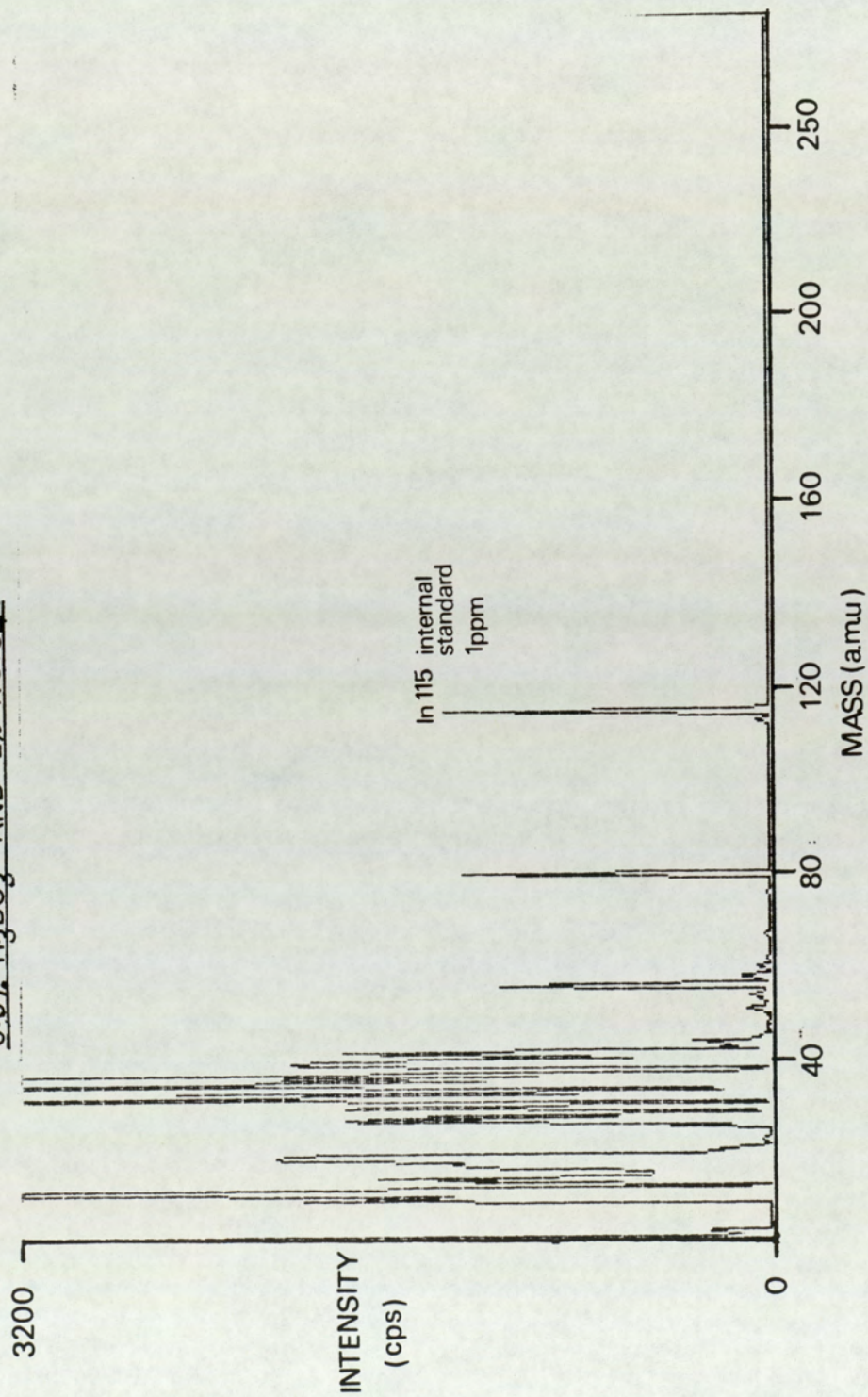
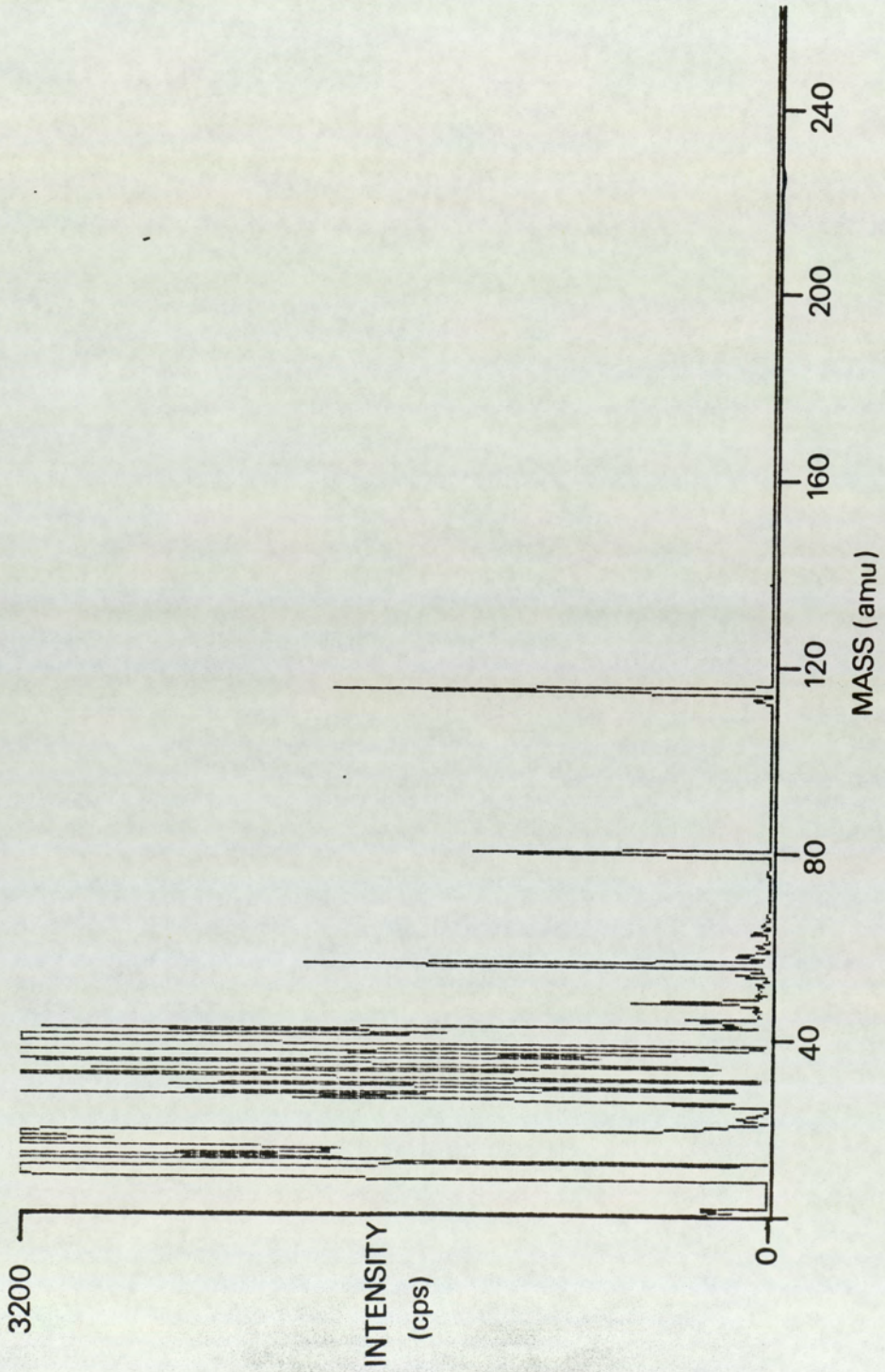


FIG. 10.8

ICP/MS SPECTRUM OF BC3



Peak integration data were used to compile the detection limits given in Table 10.19. In general, 57 elements free from spectral interferences had detection limits ≤ 1 ppm. Although only semi-quantitative analysis was performed on the control samples BC2 and BC3 the results, given in Table 10.20 and 10.21, show good agreement with results from other techniques.

10.6.3 Conclusions on ICP-Mass Spectrometry

This limited investigation demonstrates the technique's potential capability for multi-element trace analysis. Most elements are detected as single charged monoatomic ions. Detection limits for trace elements in boron are typically between 0.1 and 1 ppm over a wide mass range from Na to U. Salt condensation over the sampling aperture is not a problem if solutions containing <1% salt content are used. However, in relation to the total analysis of boron carbide, there is no improvement in the time taken to complete the analysis. Although the instrument acquires and processes data rapidly and a single qualitative scan can be completed in less than 3 min, the lengthy sample treatment for boron carbide dissolution (2 to 3 days) is necessary.

TABLE 10.19

ICP/MS DETECTION LIMITS FOR TRACE
ELEMENTS IN BORON

Element	LOD ppm	Element	LOD ppm	Element	LOD ppm
Na	<0.5	Rb	<0.5	Eu	<0.5
Mg	<1	Sr	<0.5	Gd	<0.5
Al	ND	Y	<0.5	Tb	<0.5
Si	ND	Zr	<1	Dy	<1
P	ND	Nb	<0.5	Ho	<0.5
S	ND	Mo	<0.5	Sr	<1
Cl	ND	Ru	<0.5	Tm	<1
K	ND	Rh	<0.5	Yb	<1
Ca	ND	Pd	<0.5	Lu	<0.5
Sc	<0.5	Ag	<0.5	Hf	<1
Ti	<1	Cd	<1	Ta	<0.5
V	<0.2	In	ND	W	<1
Cr	<1	Sn	<0.5	Re	<0.5
Mn	<1	Sb	<0.5	Os	<0.5
Fe	<1	Te	<1	Ir	<0.5
Co	<0.5	I	ND	Pt	<0.5
Ni	<1	Cs	<0.5	Au	<0.5
Cu	<1	Ba	<1	Hg	<1
Zn	<1	La	<0.5	Tl	<0.5
Ga	<1	Ce	<0.5	Pb	<0.5
Se	<1	Pr	<0.5	Bi	<0.5
As	<1	Nd	<0.5	Th	<0.5
Se	<10	Sm	<0.5	U	<0.5
Br	ND				

ND = Not determined.

TABLE 10.20

ICP/MS SEMI-QUANTITATIVE ANALYSIS RESULTS
FOR BC2

Element	ICP/MS Result ppm	Expected Conc. ppm
Na	50	85 ± 18
Mg	25	26 ± 3
Al	ND	-
Si	ND	-
P	ND	-
S	ND	-
Cl	ND	-
K	ND	-
Ca	ND	-
Sc	<50	<0.05
Ti	320	340 ± 40
V	<50	2 ± 5
Cr	10	12 ± 8
Mn	15	11 ± 1
Fe	570	740 ± 60
Co	<1	1 ± 0.2
Ni	<100	4 ± 0.4
Cu	30	30 ± 10
Zn	<1	<2
Ga	<1	<0.1
Ge	<1	<0.1
As	<1	<1
Se	<1	<2
Br	ND	-
Rb	<0.5	<0.5
Sr	3	5 ± 0.5
Y	<0.5	<0.5
Zr	<1	0.8 ± 0.2
Nb	<0.5	<5
Mo	<5	<3
Ru	<0.5	<0.3
Rh	<0.5	<0.1
Pd	<0.5	<0.5
Ag	<0.5	<0.2
Cd	<1	<0.5

Element	ICP/MS Result ppm	Expected Conc. ppm
In	ND	-
Sn	<1	<0.5
Sb	<0.5	0.4 ± 0.1
Te	<1	<0.3
I	<1	<0.02
Cs	<0.5	<0.1
Ba	10	15 ± 2
La	<0.5	0.2 ± 0.02
Ce	<0.5	<0.5
Pr	<0.5	<0.1
Nd	<1	<0.5
Sm	<0.5	<0.2
Eu	<0.5	<0.1
Gd	<0.5	<0.1
Tb	<0.5	<0.01
Dy	<1	<0.5
Ho	<0.5	<0.01
Er	<1	<0.05
Tm	<1	<0.2
Yb	<1	<0.5
Lu	<0.5	<0.2
Hf	<2	<0.1
Ta	<0.5	0.2 ± 0.1
W	<1	0.4 ± 0.1
Re	<0.5	<0.005
Os	<1	<0.05
Ir	<0.5	<0.01
Pt	<0.5	<0.5
Au	<0.5	<0.005
Hg	<1	<0.5
Tl	<0.5	<0.3
Pb	<1	<2
Bi	<0.5	<0.2
Th	<0.5	0.07 ± 0.05
U	<0.5	0.1 ± 0.01

ND = Not determined.

TABLE 10.21

ICP/MS SEMI-QUANTITATIVE ANALYSIS RESULTS
FOR BC3

Element	ICP/MS Result ppm	Expected Conc. ppm
Na	60	52 ± 10
Mg	25	25 ± 3
Al	ND	-
Si	ND	-
P	ND	-
S	ND	-
Cl	ND	-
K	ND	-
Ca	ND	-
Sc	<50	<0.05
Ti	600	630 ± 70
V	<100	5 ± 2
Cr	15	25 ± 15
Mn	15	10 ± 5
Fe	400	390 ± 15
Co	<1	<0.5
Ni	<100	3 ± 1
Cu	50	40 ± 20
Zn	<3	<5
Ga	<1	<0.5
Ge	<1	<0.5
As	1	5 ± 2
Se	<10	<2
Br	ND	-
Rb	<1	<0.5
Sr	2	5 ± 2
Y	<1	<0.5
Zr	<1	3 ± 1.5
Nb	<1	C1
Mo	4	7 ± 1
Ru	<1	<0.5
Rh	<1	<0.5
Pd	<1	<0.5
Ag	<1	<0.5
Cd	<1	<0.5

Element	ICP/MS Result ppm	Expected Conc. ppm
In	ND	-
Sn	<1	<0.5
Sb	<0.5	<0.5
Te	<1	<0.5
I	<1	
Cs	<0.5	<0.5
Ba	5	8.7 ± 1.2
La	<0.5	0.3 ± 0.1
Ce	<0.5	<0.5
Pr	<0.5	<0.2
Nd	<1	<0.5
Sm	<0.5	<1
Eu	<0.5	<0.5
Gd	<0.5	<1
Tb	<0.5	<0.2
Dy	<1	<0.5
Ho	<0.5	<0.2
Er	<1	<0.5
Tm	<1	<0.5
Yb	<1	<0.5
Lu	<0.5	<0.2
Hf	<2	<1
Ta	<0.5	<6
W	2	4.2 ± 0.7
Re	<0.5	<0.5
Os	<1	<0.5
Ir	<0.5	<0.5
Pt	<2	<0.5
Au	<0.5	<0.2
Hg	<1	<0.5
Tl	<0.5	<0.5
Pb	<1	<1
Bi	<0.5	<0.5
Th	<1	<0.5
U	<1	<0.5

ND = Not determined.

CHAPTER 11

CONCLUSIONS

The primary objective of this work was to explore the potential of ICP/AES for the quantitative trace element impurity analysis of boron materials. Two systems were developed, each offering a different approach to recording and measuring emission spectra. The first was an ICP-Spectrograph (58) which used photographic recording and computer controlled microdensitometry for interpreting spectral data. This provided a suitable approach to quantitative multi-element analysis. Since the entire spectrum was permanently recorded during a single 2 min exposure thus allowing all spectral lines of interest to be measured subsequently using an automated microdensitometer, the main advantages of this system were its wide element coverage and its ability to perform well in situations where complex spectra were to be interpreted. The method provided good sensitivity (LOD 1 to 10 ppm) for some 30 elements, a precision of 10 to 15% RSD, and results for positively identified elements showed no bias. The second instrument developed was a sequential scanning ICP system which was equipped with photo-electric detection. This system provided an excellent capability for accurate multi-element analysis giving a precision of 1 to 2% RSD and detection limits obtained were typically ≤ 1 ppm. Its optical performance in terms of dispersion and resolution was better than most commercial systems. Although poor mechanical performance of the wavelength drive mechanism degraded its analytical speed,

limitations were largely overcome by using a more efficient nebuliser and an autosampler.

A comparative study (59) showed that when both systems are used in a complementary manner the best analytical performance is obtained. Using both systems some 50 elements in boron samples were determined with detection limits generally ≤ 1 ppm.

In situations where sample quantity was limited the poor efficiency of conventional nebulisers was unsatisfactory. Hence, recirculating nebulisers were constructed and tested (60, 61). Whilst their sensitivity and precision were not found to be significantly different from those of a conventional system they provided a X10 fold increase in nebulisation efficiency. Using 1 ml of solution, nebulisation for over 10 min was achievable. An investigation into the likely causes of poor long term stability in closed nebuliser systems showed that this design was free from drift effects. Consequently the nebuliser offered a suitable approach to ICP/AES analysis of small sample volumes.

Hydride generation provided an alternative method of sample introduction and gave detection limits of ≤ 1 ppm for Sn, Ge, Bi, Hg, As, Se, Sb and Te in boron materials. For these elements a X10 fold increase in sensitivity over pneumatic nebulisation was achieved.

Although the primary objective of applying ICP/AES to boron analysis was fulfilled and the developments described in this thesis substantially contribute to this field of analysis, the full analytical requirements for trace elements in boron materials cannot be satisfied solely by ICP/AES. Hence, this work was extended to include an evaluation of other multi-element techniques such as activation analysis and spark source mass spectrometry. Boron carbide control materials were analysed by all techniques. The results showed that only by using all three techniques could the full requirements be met. Alternative multi-element techniques were also considered and preliminary assessments of wavelength dispersive X-ray fluorescence (WDXRF) and ICP-Mass spectrometry (ICP/MS) were carried out. WDXRF has a useful capability and offers an economical approach to routine boron analysis. Good sensitivity (LOD typically ≤ 1 ppm), precision (1 to 15% RSD) and accuracy was obtained for the 15 elements studied. A similar performance for a wider range of elements is expected. Although only a limited assessment of ICP/MS could be carried out within the instrument time available, experimental data showed that wide element coverage (70 elements) and good sensitivity (LOD ≤ 1 ppm) can be obtained. Although the technique, in comparison to ICP/AES, is still in its early stages of development it has considerable potential.

REFERENCES

- (1) Lerner, M. L., The Analysis of Elemental Boron, U.S. Atomic Energy Commission, Division of Technical Information, Library of Congress Catalog No. 74:607964, 1970.
- (2) Condon, E. U., Shortly, G. H., The Theory of Atomic Spectra, Cambridge University Press, 1957.
- (3) Webb, M. S. W., Waddingham, M. L., A Versatile Spectroscopic Method for the Analysis of a Wide Range of Materials, AERE Report 5799, 1968.
- (4) Reed, T. B., Plasma Torches, Intern. Sci. Technol, 1962, 42, 42-48.
- (5) Greenfield, S., Jones, I. L., High Pressure Plasmas as Spectroscopic Emission Sources, Analyst, 1964, 89, 713-720.
- (6) Wendt, R. H., Fassel, V. A., Induction Coupled Plasma Spectroscopic Excitation Source, Anal Chem, 1965, 37, 920-922.
- (7) Greenfield, S., McGeachin, H. McD., Smith, P. B., Plasma Emission Sources in Analytical Spectroscopy. Parts I-III, Talanta Review, 1975, 22, 1-15.
" " 1975, 22, 533-562
" " 1976, 23, 1-14.
- (8) Barnes, R., ICP/AES: A Review, Trends. Anal. Chem., 1981, 1, (2), 51-55.
- (9) Boumans, P. W. J. M., DeBoer, F. J., Wither, A. W., Bosveld, M., Outline of a Method for Spectrographic General Survey Analysis using Liquid Sampling and an ICP, Spectrochimica Acta, 1978, 33B, 535-544.
- (10) Floud, M. A., Fasse, V. A., D'Silva, A. P., Computer Controlled Scanning Monochromator for the Determination of 50 elements in Geochemical and Environmental Samples by ICP/AES, Anal. Chem, 1980, 52, 2168-2173.
- (11) Floyd, M. A., Fasse, V. A., Winge, R. K., Katzenberger, T. M., D'Silva, A. P., ICP/AES: A Computer Controlled Scanning Monochromator System for Rapid Sequential Determination of the Elements, Anal. Chem, 1980, 52, 431-438.
- (12) Linn, H., RF Generators for ICP Applications, ICP. Inf. Newsl., 1976, 2, (2), 51-61.
- (13) The American Radio Relay League Antenna Book, 12th Edition, U.S.A., 1970.
- (14) Meinhard, J. E., The Concentric Glass Nebuliser, ICP. Inf. Newsl, 1976, 2, (5), 163-165.

- (15) Knisely, R. N., Amenson, H., Butler, C. C., Fassel, V. A., An Improved Pneumatic Nebuliser for use at Low Nebulising Gas Flows, *Appl. Spectrosc*, 1974, 28, 285-286.
- (16) Kawaguchi, H., Tanaka, T., Mizuike, A., An Ultrasonic Nebuliser for Microliter Samples in ICP/AES, *Bull. Chem. Soc. Jpn.*, 1982, 55, 3033-3034.
- (17) Taylor, C. E., Floyd, T. L., ICP/AES Analysis of Environmental Samples using Ultrasonic Nebulisation, *Applied Spectrosc*, 1981, 35, (4), 408-413.
- (18) Olsen, S. D., Strasheim, A., Tesser, W. A., Sample Introduction into the ICP, *Spectrochimica Acta*, 1983, 33B, 248.
- (19) Fassel, V. A., Rice, G., Lawrence, K., Winge, R., Grabav, F., Some Front End and Back End Innovations in ICP/AES, *Spectrochimica Acta*, 1983, 33B, 95.
- (20) Wolcott, T. F., Sobel, C. B., Fabrication of a Babington-type Nebuliser for ICP sources, *Applied Spectrosc*, 1982, 36, (6) 685-686.
- (21) Ebdon, L., Cave, M. R., A Study of Pneumatic Nebulisation for ICP/AES, *Analyst*, 1982, 107, 172-178.
- (22) Scott, R. H., Fassel, V. A., Knisely, R. N., Nixon, D. E., ICP/AES Analytical Spectrometry: A Compact Facility for Trace for Trace Analysis of Solutions, *Anal. Chem*, 1974, 46, 76-80.
- (23) Farnandez, F. J., Atomic Absorption Determination of Gaseous Hydrides Utilizing No. BH₄ Reduction, *At. Absorpt. Newsl.* 1973, 12, 93-97.
- (24) Thompson, M., Walton, S. J., Kirkbright, G. F., Simultaneous Determinations of Trace Concentrations of As, Sb, Bi, Se, Te, in Aqueous Solution by Introduction of Gaseous Hydrides into an ICP Source for Emission Spectroscopy. Part I: Preliminary Studies, *Analyst*, 1978, 103, 568-579.
- (25) Cope, M. J. Kirkbright, G. F., Burr, P. M., Use of ICP/AES for the Analysis of Doped Cd, Hg, Te Employing a Graphite Rod Electrothermal Vaporization Device for Sample Introduction, *Analyst*, 1982, 107, 611-616.
- (26) Kirkbright, G. F., Walton, S. J., AES with an ICP and Direct Sample Introduction from a Graphite Rad, *Analyst*, 1982, 107, 276-281.
- (27) Thompson, M., Goulter, J. E., Sieper, F., Laser Ablation for the Introduction of Solid Samples into an ICP for Atomic Emission Spectroscopy, *Analyst*, 1981, 106, 32-39.
- (28) Sawyer, R. A., *Experimental Spectroscopy*, Third Edition, Dover Publications Inc., New York, 1963, 30-191.

- (29) Brode, W. R., Chemical Spectroscopy, Second Edition, John Wiley and Sons Inc, 1952, 32-34.
- (30) Sawyer, R. A., loc. cit, 50-53.
- (31) Bettison, W. A., Bundy, T. K., The Application of Computer Controlled Microdensitometry in Optical Emission Spectroscopy, AWRE Rep. No. 041/78, HMSO, 1978.
- (32) Savitsky, A., Golay, M. T. E., Smoothing and Differentiation of Data by Simplified Least Squares Procedures, Anal. Chem, 1964, 86, (8), 1627-1639.
- (33) Sawyer, R. A., loc. cit, 194.
- (34) Nachtreib, N. H., Principles and Practice of Spectrochemical Analysis, First Edition, McGraw-Hill Book Co. Inc., 1950, 106-121.
- (35) Kodak, Data Book of Applied Photography, Volume 4, Printed by Kodak Limited, 1972.
- (36) Nachtrieb, N. H., loc. cit, 119.
- (37) Zimmer, K., Heltai, Sy., Influence of Photographic and Photometric Effects on Spectrographic Evaluation, Part VI: Investigation of Blackening Curves of Line and Continuous Spectra Effects of Background Density Upon the Shape of Blackening Curve of Line Spectra, Acta, Chim, Acad. Sci. Hung, 1980, 103, 289-299.
- (38) Winge, R. J., Paterson, V. J., Fassel, V. A., ICP/AES: Prominent Lines, Appl. Spectrosc, 1979, 33, (3), 206-218.
- (39) Boumans, P. W. J. M., Line Coincidence Table for ICP/AES, Pergamon Press, Oxford, U. K., 1st Edition, 1980.
- (40) Arrhenius, S., Electrical Conductivity of Hot Salt Vapours, Ann. Phys. Chem, 1891, 42, 18-76.
- (41) Gouy, G., Report on Coloured Flames, Ann. Phys. Chem, 1879, 18, 5-101.
- (42) Novak, T., Fixed Crossflow Nebuliser for Use with ICP and Flames, Anal. Chem, 1980, 52, 576-579.
- (43) Rauterberg, E., Knippenberg, E., The Determination of K by Flame Photometric Methods, Angew, Chem, 1940, 54, 477.
- (44) Carpenter, R.C., Personal Communication.

- (45) Hutton, R. C., Preston, B.,
A Simple Versatile Hydride-generation Configuration for
ICP, *Analyst*, 1983, 103, 1409-1411.
- (46) Castillo, T. R., Lanja, J., Aznarez, J.,
Determination of Ge in Coal Ashes by Hydride Generation and
Flame Atomic Absorption, *Analyst*, 1982, 107, 89.
- (47) Thompson, M., Walsh, J.N., *A Handbook of Inductively Coupled
Plasma Spectrometry*, Blackie, London, First Edition, 1983,
158.
- (48) Rose, D. A., Application of Hydride Generation Techniques to
Real Samples, *Anal. Proc.*, 1983, 20, 436.
- (49) Bacon, J. R., Ure, A. M., Spark Source Mass Spectroscopy:
Recent Developments and Applications, *Analyst*, 1984, 109,
1229-1253.
- (50) Fifield, F. W., Kealey, D., *Principles and Practice of
Analytical Chemistry*, First Edition,
International Textbook Co. Ltd., London, 1975, 327-347.
- (51) Davies, J. A., Jefferies, A. C., Hart P.,
Trace Multi-Element Analysis in Boron Materials by
Epithermal Neutron Activation Analysis, *J Radio. Anal +
Nucl. Chem*, 1986, 98, No. 2.
- (52) Jenkins, R., Gould, R. W., *Quantitative X-ray Spectrometry*,
First Edition, Marcel Dekker Inc. New York, 1981.
- (53) Jenkins, R., De Vries, J. L.,
Practical X-ray Spectrometry, Second Edition,
MacMillan and Co. Ltd., 1970.
- (54) Houk, R. S., Fasse, V. A., Flesch, G. D., Svec, H. J.,
Gray, A. L., and Taylor, C. E.,
ICP as an Ion Source for
Mass Spectrometric Determination of Trace Elements,
Anal. Chem., 1980, 82, 2283-2289.
- (55) Gray, A. L., Mass Spectrometric Analysis of Solutions using
an Atmospheric Pressure Ion Source, *Analyst*, 1975, 100,
289-299.
- (56) Houk, R. S., Thompson, J. J., Trace Element Isotope Analysis
by ICP/MS,
Biomed. Mass Spectrom., 1983, 10, (2), 107-112.
- (57) Van Loon, J. C., Balilcki, R., Nimjee, M. C., Brzezinska, A.,
Douglas, D.,
Determination of Metals and Metal Compounds in Air and
Marine Samples by ICP-AES, ICP-MS and GS-AAS,
Heavy Met. Environ. Int. Conf 4th, Conference Proceedings,
1983, 1, 78-81.

- (58) Hulmston, P., The Application of ICP/AES to the Determination of Impurities in Boron and Boron Compounds, *Anal. Chim. Acta*, 1983, 155, 247-252.
- (59) Hulmston, P., Jefferies, A. C., Davies, J. A., Comparison of Photographic and Photoelectric Detection for Multi-element Analysis by ICP/AES, *Analyst*, 1984, 109, 519-522.
- (60) Hulmston, P., A Pneumatic Recirculating Nebuliser System for Small Sample Volume, *Analyst*, 1983, 108, 166-170.
- (61) Hulmston, P., McKillop, S., Nebulisation Characteristics of a Microprocessor-controlled Recirculating Nebuliser for ICP/AES Analysis of Small Sample Volumes, *Analyst*, 1985, 110, 559-562.